

# Immunology for physicists

Alan S. Perelson

*Theoretical Division, Los Alamos National Laboratory, Los Alamos, New Mexico 87545*

G rard Weisbuch

*Laboratoire de Physique Statistique, l'Ecole Normale Sup rieure, 24 rue Lhomond, F 75231 Paris Cedex 5, France*

The immune system is a complex system of cells and molecules that can provide us with a basic defense against pathogenic organisms. Like the nervous system, the immune system performs pattern recognition tasks, learns, and retains a memory of the antigens that it has fought. The immune system contains more than  $10^7$  different clones of cells that communicate via cell-cell contact and the secretion of molecules. Performing complex tasks such as learning and memory involves cooperation among large numbers of components of the immune system and hence there is interest in using methods and concepts from statistical physics. Furthermore, the immune response develops in time and the description of its time evolution is an interesting problem in dynamical systems. In this paper, the authors provide a brief introduction to the biology of the immune system and discuss a number of immunological problems in which the use of physical concepts and mathematical methods has increased our understanding. [S0034-6861(97)00404-2]

## CONTENTS

I. Introduction	1219	F. The continuous-shape-space approach	1253
A. The physicist's approach: Generic properties	1219	G. Bit-string models of the network	1255
B. Basic facts of immunology	1221	1. Model equations	1255
1. Clonal selection	1223	2. Metadynamics	1256
2. Learning and memory	1223	3. Simulation results	1256
3. The self-nonsel self discrimination problem	1224	V. Automaton Approaches	1258
II. Modeling the Immune Repertoire	1225	A. Modeling B-T interactions	1259
A. How large does the repertoire need to be in order to be complete?	1225	B. A model of autoimmune diseases	1259
B. Self-nonsel self discrimination and the probability of recognition	1226	C. Spin-glass models	1260
C. Predicting the size of epitopes	1227	D. Automata on a 2-dimensional shape space with metadynamics	1260
III. Clonal Models	1229	VI. Discussion	1262
A. Receptor cross-linking and cell activation	1229	Acknowledgments	1263
B. Clonal selection models: B-cell proliferation and differentiation	1231	References	1263
C. Affinity maturation	1233		
IV. Network Models	1236	I. INTRODUCTION	
A. The B model	1237	A. The physicist's approach: Generic properties	
B. The two-clone problem	1237		
C. Network topology	1239	The immune system is our primary defense against pathogenic organisms and cells that have become malignantly transformed. The last decade has seen an explosion in detailed experimental findings about the cells, molecules, and genes that make up the immune system. Although our knowledge is far from complete, as the Human Genome Project progresses we shall almost certainly uncover the remaining genes and molecules that influence the behavior of single lymphocytes. After the genes are sequenced, what will remain is the task of understanding in a quantitative way how the cells of the immune system behave and how they interact with each other to generate the coordinated activity seen during an immune response.	
D. Localized attractors	1241	One goal of modeling in immunology, which we shall focus on here, is to deduce macroscopic properties of the system from the properties and interactions among the elementary components. This goal is similar to the purposes of statistical mechanics. The interactions among the components of the immune system are extremely intricate and they are not fully understood. Further, in contrast to the field of neurophysiology, immu-	
1. Cayley tree	1241		
a. Immunity	1242		
b. Tolerance	1243		
c. Extended localization	1243		
d. Percolation	1243		
2. Number of attractors	1244		
3. Basins of attraction and the window-automaton approximation	1245		
a. From virginity to excitation	1246		
b. Tolerance vs vaccination	1247		
4. More realistic topologies	1248		
a. Loops	1248		
b. Distribution of $J_{ij}$ values	1248		
5. Biological interpretations of the localized attractor model	1249		
E. Antibody/B-cell network models	1250		
1. The AB model	1250		
2. The two-clone case	1250		
3. Chaos	1252		

nology has not described the behavior of single cells quantitatively. There are no equivalents in immunology of the Hodgkin-Huxley (1952) equations, which describe how a nerve impulse travels down an axon (see Cronin, 1987). Yet the “macroscopic behavior” of the immune system, as probed in a specific experiment, can be well characterized. The problem then arises of selecting a simple representation for the elementary interactions that would give rise to the organized behavior observed in the immune system. The adventure of statistical physics is full of equivalent endeavors, starting from the description of thermal properties of gases and solids based, respectively, on the assumption of independent particles composing a perfect gas and the coupling of harmonic oscillators, to the more recent description of neural nets. This kind of approach is especially suited to theoretical immunology because of our ignorance about the detailed mechanisms responsible for the observed behaviors of the immune system. To be more specific, we shall look for generic properties among models of the immune system. As in the case of phase transitions in condensed-matter physics, we are interested in semi-quantitative laws, such as scaling laws, which depend only on the general features of the model, and not on its details.

In Sec. II, we shall describe the theory of clonal selection and provide quantitative estimates of how the ability of the immune system to recognize foreign cells and molecules scales with the size of the system. We shall show, with parameters estimated for the mammalian immune system, that an immune system needs at least  $10^5$  different elements to function. The basic elements of the immune system are a class of white blood cells known as lymphocytes. The size of an organism determines the maximum number of its lymphocytes. Thus mice have of the order of  $10^8$  lymphocytes, while humans have of the order of  $10^{12}$ . Thus system sizes are large but not as large as Avogadro’s number.

Cells are already macroscopic systems far from equilibrium from the point of view of thermodynamics, and there is little hope of starting from a simple Hamiltonian as is often done in statistical mechanics. But basically, the simple system of differential equations described in Sec. IV plays the role of the dynamics of an Ising Hamiltonian with respect to diluted magnetic systems or of the discrete time logistic equation for chaos and turbulence. Although it represents a strong simplification of the interactions present in the system, it is expected to belong to the same class of universality as a “true” model of the immune system and to exhibit the same generic properties. In the case of a dynamic system, the generic properties concern the attractors of the dynamics. Some of the questions that we shall address are: Are the attractors limit points, limit cycles, or chaotic? What is their number? What are their basins of attraction? How do these properties relate to the parameters of the differential system? How can one force transitions among the different dynamical regimes? If our hypotheses about the universality of a model are true, the generic properties, qualitative classification of the attractors, and scal-

ing laws should be evident in the phenomenology of the mammalian immune system.

Besides issues of dynamics, we shall address questions of a probabilistic nature. For example, in Sec. II, we ask how well the immune system performs the task of distinguishing self components from foreign or nonself components. We also address a design question: in order to perform efficient self-nonself discrimination, how large a region on a molecule should the immune system examine? If the immune system looks at very small regions, say one or two amino acids, then with a rather limited set of receptors all foreign molecules could be recognized. However, since self molecules are made from the same building blocks, such a recognition system would also recognize all self molecules. If the immune system looks at a very large region of molecules, then a receptor may need to be so specific that it might be able to recognize only one particular molecule, and with finite resources many foreign molecules may escape detection.

Section III begins our foray into dynamics. We first discuss models based on the physical chemistry of receptor-ligand interactions, which underlie the ability of lymphocytes to detect antigen. We then abstract from the chemistry more phenomenological laws that govern the growth and differentiation (or maturation) of lymphocytes into cells with specialized functions, such as plasma cells that secrete antibody at very high rates. We also look at a phenomenon, known as affinity maturation, by which the immune system can improve the average equilibrium binding constant of antibody for antigen.

The immune system is more than a collection of independently operating lymphocytes. While many chemical signals are involved in setting up communication between these cells, here we focus on one class of models, called idiotypic network models, in which signals are propagated via specific interactions between cell surface receptors and antibody molecules. Thus a lymphocyte that detects a foreign antigen can begin secreting antibody  $A_1$ , which is a molecule that has a very specific structure and that can bind the antigen. Molecules  $A_1$  are proteins, and their novel or “idiosyncratic” parts may be detected by other lymphocytes in the immune system. These “second-level lymphocytes” may respond to seeing  $A_1$  by secreting a complementary or “anti-idiotypic” antibody  $A_2$ . Some molecules in class  $A_2$  may resemble the antigen and hence help encode memory of the encounter, while others may be distinct and excite a third level of response. Section IV deals with different approaches to modeling idiotypic networks and understanding their dynamics.

Quantitative information that can be used to evaluate differential equation models is often lacking in immunology. Given this state of affairs, it is frequently desirable to formulate models in which the variables have a limited number of states, e.g., 1 and 0, cells are activated or not. Automata models of this type are summarized in Sec. V.

We conclude, in Sec. VI, with a general discussion of modeling in immunology.

The field of theoretical immunology has been growing rapidly and we have not attempted to review all the work that has been done. This article is primarily a personal perspective centered on our own contributions to the field with briefer descriptions and references given to the work of others. In immunology, as in other fields, certain approaches dominate thinking. In the 1970s and 1980s explaining immunological phenomena in terms of idiotypic networks was extremely popular. Current thinking has shifted, and detailed molecular explanations now dominate the experimental literature. Modeling the biochemical intricacies involved in the interactions between the cells of the immune system has not kept pace with the rapid rate of discovery of new molecules and genes involved in immune regulation. Thus this review focuses more on the network viewpoint, in which concepts from physics have helped make advances, and less on the newly evolving molecular viewpoint. Previous reviews of ours, which deal with both network and non-network aspects of immunology, include Bell, Perelson, and Pimbley (1978), Perelson (1988, 1989b, 1990, 1992), Perelson and Kauffman (1991), Perelson and Weisbuch (1992b), and De Boer *et al.* (1993a). Other reviews include those of Bruni *et al.* (1979), DeLisi and Hiernaux (1982), Marchuk (1983), Atlan and Cohen (1985), Hoffman, Levy, and Nepom (1986), and Příkrylová, Jílek, and Waniewski (1992).

## B. Basic facts of immunology

The immune system is a complex system of cells and molecules distributed throughout our bodies that provides us with a basic defense against bacteria, viruses, fungi, and other pathogenic agents (referred to as foreign antigens). Analogies have been drawn between the immune system and the nervous system. Like the nervous system, the immune system performs pattern recognition tasks, learns, and retains a memory of the antigens that it has fought. The nervous system is commonly decomposed into sensory and motor parts. An analogous separation into recognition and “effector” functions is made in immunology.

The human immune system is controlled by the action of tens or possibly hundreds of types of regulatory and effector molecules. All the molecules that are important in the immune response have not yet been identified, but they include various cell surface receptors and soluble molecules such as interleukins that can transmit signals between cells. A variety of cell types compose the immune system, the most important being a class of white blood cells known as *lymphocytes*. These cells are created in the bone marrow, along with all of the other blood cells, and are transported throughout the body via the blood stream. They can leave the blood through capillaries, explore tissues for foreign molecules or cells (antigens), and then return to the blood through the lymph, the fluid bathing the cells of the body. Lymphocytes

spend considerable time resident in lymphoid organs, such as the bone marrow, the thymus, the spleen, and lymph nodes.

Lymphocytes are subdivided into two major classes: B cells and T cells. B lymphocytes secrete *antibodies*, one of the major protective molecules in our bodies. T cells function mainly by interacting with other cells and have been subdivided into helper T cells and cytotoxic T cells. Helper T cells, which generally express a cell surface marker called CD4, act through the secretion of lymphokines that promote the growth and differentiation of B cells into an antibody-secreting state. Helper T cells are the cells that are predominantly infected by the human immunodeficiency virus, and their depletion plays a major role in AIDS. Cytotoxic T cells, which generally express a cell surface marker called CD8 (and a related cell, the NK or natural killer cell), are responsible for killing virally infected cells and cells that appear abnormal, such as some tumor cells. Models of the kinetics of T-cell and NK-cell killing have been developed by a number of workers including Chu (1978), Merrill (1982), Perelson and Bell (1982), Macken and Perelson (1984; 1985b), Perelson and Macken (1984), Perelson, Macken, *et al.* (1984), and Merrill and Sathananthan (1986). Such models may have relevance to interaction of the immune system with growing tumors (see Kuznetsov *et al.*, 1994). Sometimes T cells can suppress immune responses, and in some literature the term suppressor T cell is used. The existence of antigen-specific T suppressor cells has been questioned (Möller, 1988; Schwartz, 1989), and such cells and models that incorporate them will not be dealt with here.

The interaction of HIV, the virus that causes AIDS, with T cells is of great current interest. Here we shall not discuss AIDS and only remark that models for the interaction of HIV with T cells have been developed by Hraba and Dolezal (1989, 1994), Merrill (1989), Perelson (1989c, 1994), Hraba, Dolezal, and Celikovskiy (1990), McLean and Kirkwood (1990), Nowak and May (1991, 1992, 1993), Nelson and Perelson (1992, 1995), Perelson, Kirschner, and De Boer (1993), Dolezal and Hraba (1994), Essunger and Perelson (1994), and Kirschner and Perelson (1995). Other papers related to modeling HIV infection and the immune system include those of Nowak, May, and Anderson (1990), Nowak and McLean (1991), Nowak *et al.* (1991), McLean and Nowak (1992), Nowak (1992), McLean (1992), De Boer and Boerlijst (1994), Frost and McLean (1994a, 1994b), Ho *et al.* (1995), Wei *et al.* (1995), and Perelson *et al.* (1996). Modeling in this area is occurring at a rapid pace. This list of references is not complete, but should provide an entry into the literature.

From the point of view of pattern recognition in the immune system, the most important feature of both B cells and T cells is that they have receptor molecules on their surfaces that can recognize antigen. In the case of B cells, the receptor is an immunoglobulin (antibody) molecule (Fig. 1) embedded in the membrane of the cell, while in the case of T cells the receptor is simply called the T-cell receptor (TCR). Recognition in the immune

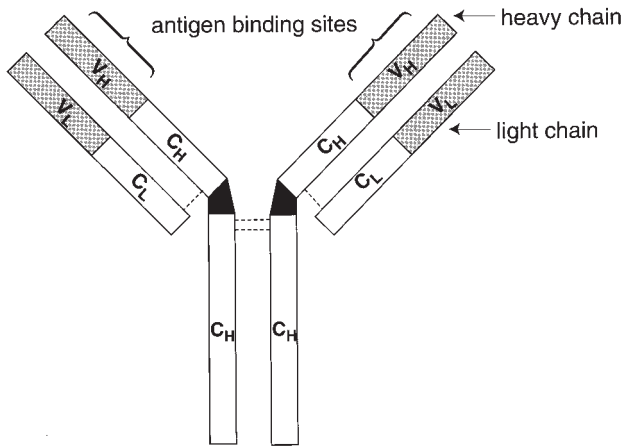


FIG. 1. Diagrammatic structure of a surface immunoglobulin (antibody) molecule. The molecule is composed of four polypeptide chains, two identical light chains, and two identical heavy chains. Each chain has a variable region ( $V_H$  and  $V_L$ ) and a constant region ( $C_H$  and  $C_L$ ). The  $V_H$  and  $V_L$  regions combine to form the two antigen binding sites on this molecule. When the molecule is on the surface of a cell, the  $C_H$  region is embedded in the cell membrane. The molecule can be enzymatically cleaved into fragments; the arms of the Y-shaped molecule, each containing one binding site, are known as Fab fragments; the tail of the Y-shaped molecule is known as the Fc fragment.

system occurs at the molecular level and is based on the complementarity in shape between the binding site of the receptor and a portion of the antigen called an *epitope* (see Fig. 2). The interaction between the recep-

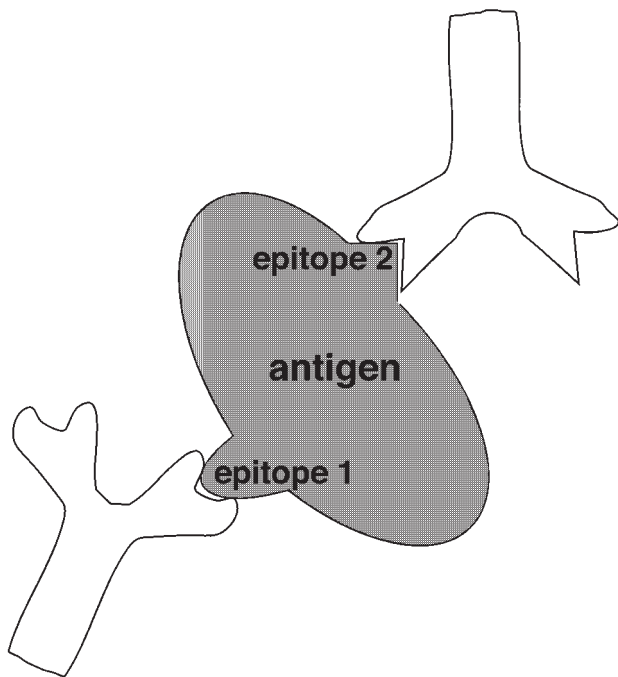


FIG. 2. The portion of an antigen that is recognized by an antibody is called an epitope. An antigen may have multiple epitopes.

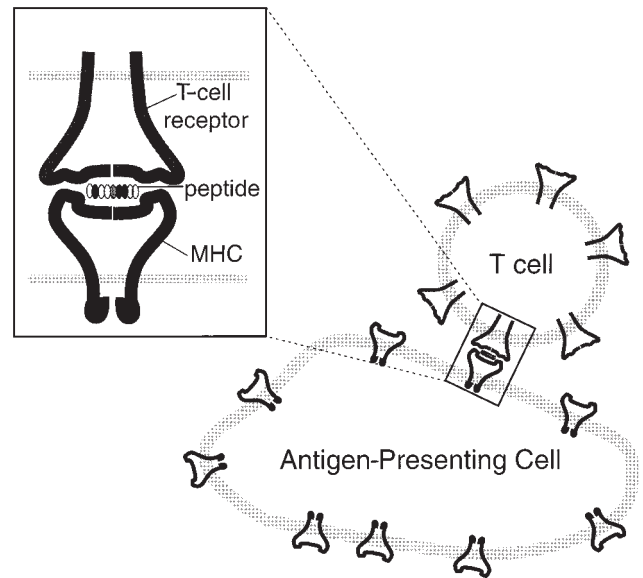


FIG. 3. T cells, via their T-cell receptor, recognize MHC-peptide complexes on the surface of antigen-presenting cells.

tor and the epitope is noncovalent and usually involves van der Waals forces, interactions among charged groups, and hydrogen bonds. These weak interactions are nevertheless strong enough to keep the macromolecules bound when the area of interaction is sufficiently large. Typical areas of interaction are  $600 \text{ \AA}^2$  (Amit *et al.*, 1986; Ajitkumar *et al.*, 1988).

B and T cell receptors see different features of an antigen. The B-cell receptor interacts with epitopes present on intact antigen molecules. Antigen molecules may be soluble or bound to a surface. The T-cell receptor interacts only with cell surface molecules. T cells secrete molecules that can kill other cells or promote their growth. Thus it is clearly important for a T cell to “know” that it is interacting with another cell rather than with a soluble molecule. One way of solving this identification process is to have the T cell recognize a cell surface molecule. Once it was thought that T cells used two receptors, one to recognize a cell surface molecule called a major histocompatibility complex (MHC) molecule and another receptor to recognize antigen. It turns out that the T-cell receptor plays the role of both of these receptors and recognizes antigen bound to an MHC molecule (Fig. 3).

There are two major classes of MHC molecules, called MHC class I and MHC class II. Class-I molecules are found on every cell, while class-II molecules are found only on a subset of cells called antigen-presenting cells.  $CD8^+$  T cells, which generally are killer cells, interact with MHC class I. Since any cell can become virally infected it makes some sense that cytotoxic T cells see antigen bound to MHC class-I molecules.  $CD4^+$  T cells, which are generally helper cells, interact with antigen bound to MHC II molecules.

The cells that express MHC class II, predominantly B cells, macrophages, and dendritic cells, are called antigen-presenting cells. Antigen-presenting cells take

up protein antigens from their environment and partially digest them, i.e., cut them into smaller parts called peptides. Some of these peptides are then bound to an MHC class-II molecule and transported to the surface of the antigen-presenting cell, where they can then interact with, or as immunologists say, be presented to the CD4<sup>+</sup> T cell. It turns out that all cells cut up a portion of the proteins that they synthesize. These self-generated peptides are in a cellular compartment in which they can interact with MHC class-I molecules. Thus both classes of MHC molecules bind peptides and “present” them to T cells. The class-I system specializes in presenting proteins synthesized within the cell, such as viral proteins made by an infected cell, while the class-II system specializes in presenting fragments of molecules picked up from the environment. Both systems present peptides from self molecules as well as from foreign molecules. T cells therefore need to discriminate between self and nonself. The self-nonself discrimination problem is discussed in Sec. I.B.3.

Each lymphocyte has on its surface  $10^4$  to  $10^5$  receptor molecules, all of the same shape, that can detect antigen. On B cells these receptors are immunoglobulin and on T cells they are simply called the T-cell receptor. A rather elaborate genetic machine underlies the construction of these receptors and to a first approximation ensures that the receptors expressed on different lymphocytes have a different randomly chosen shape. Current estimates of the *potential repertoire*, i.e., the number of possible receptors that can be constructed given the genetic mechanisms involved, are of the order of  $10^{11}$  for B cells (Berek and Milstein, 1988) and  $10^{16}$  for T cells (Davis and Bjorkman, 1988). A mouse contains of the order of  $10^8$  B lymphocytes and  $10^8$  T lymphocytes, and thus cannot contain all possible receptors. The number of different receptors that are expressed at any time, the *expressed repertoire*, is estimated to be  $10^7$ .

When B cells become stimulated they secrete a soluble form of their receptor molecule, which is called antibody. Antibodies are highly specific and can distinguish fine differences in the molecular structure of epitopes, such as the change of a single amino acid in a protein, the change of a single atom, such as a chloride, from an ortho to a para position along a substituted benzene ring, or even optical isomers such as d- and l-tartrate (Eisen, 1980).

The immune system with an expressed repertoire of  $10^7$  is capable of making of the order of  $10^7$  different antibodies at any one time. Due to their exquisite specificity the immune system uses antibodies as tags with which to label cells and molecules as foreign. Various effector mechanisms then lead to the elimination of the antigen. For example, antigen and antibody can form large complexes that are taken up and eliminated by various cells. A foreign cell with antibody attached to it is quickly eaten by large phagocytic cells such as macrophages. These phagocytic cells lack specificity and eat anything that has antibody attached. For example, they will phagocytose latex beads if they are antibody coated. Antibody bound to the surface of a cell can also initiate

a cascade of reactions among a set of high-molecular-weight serum proteins known as the complement system. This cascade of reactions causes the complement components to assemble a cylinder that penetrates the cell membrane and leads to the death of the cell by disrupting its osmotic balance. Models dealing with the complement system have been developed by Perelson and Wiegel (1979), Perelson, Goldstein, and Rocklin (1980), DeLisi and Wiegel (1983), and Dower *et al.* (1984).

## 1. Clonal selection

The most basic task of the immune system is pattern recognition. It must recognize (and then respond to) all foreign cells (e.g., viruses and bacteria) and molecules (e.g., bacterial toxins). The diversity of receptor types used by the immune system is the basis for pattern recognition. The algorithm that the immune systems uses, called *clonal selection*, was elucidated by MacFarlane Burnett (1959). Clonal selection is the idea that only those cells that recognize the antigen proliferate, thus being selected against those which do not. Clonal selection operates on both B cells and T cells. To keep matters simple, we do not distinguish between B and T cells in the discussion given below, although some of the details regarding cell stimulation do depend on the lymphocyte type.

Consider the events that follow the injection of an antigen into a mouse (Fig. 4). Given the large diversity of receptors in the expressed repertoire, whether the receptor on any particular lymphocyte detects the antigen can be viewed as a random event. The interaction of antigen with the receptors on a lymphocyte can lead to activation of the cell. Upon activation, lymphocytes proliferate and grow into a clone. A *clone* is a set of cells that are the progeny of a single cell and it might comprise anywhere from tens to thousands of cells. Cells in an activated clone respond by secreting antibody if they are B cells or by secreting growth factors if they are helper T cells. Because antigen selects which lymphocytes develop into clones, the theory is called clonal selection. The analogy with natural selection should be obvious, the fittest clones being the ones that recognize antigen best or, more precisely, the ones that are triggered best. For this algorithm to work, the receptor population or repertoire has to be diverse enough to recognize any foreign shape. The repertoire is believed to be *complete*, which means that it can recognize any shape. We shall evaluate this statement with a quantitative model in Sec. II.

## 2. Learning and memory

For protection, it is not enough only to recognize antigen. The immune system must also have sufficient resources to mount an effective response against pathogens. As in a typical predator-prey situation the size of the lymphocyte subpopulation specific for the pathogen relative to the size of the pathogen population is crucial in determining the outcome of infection. To be more

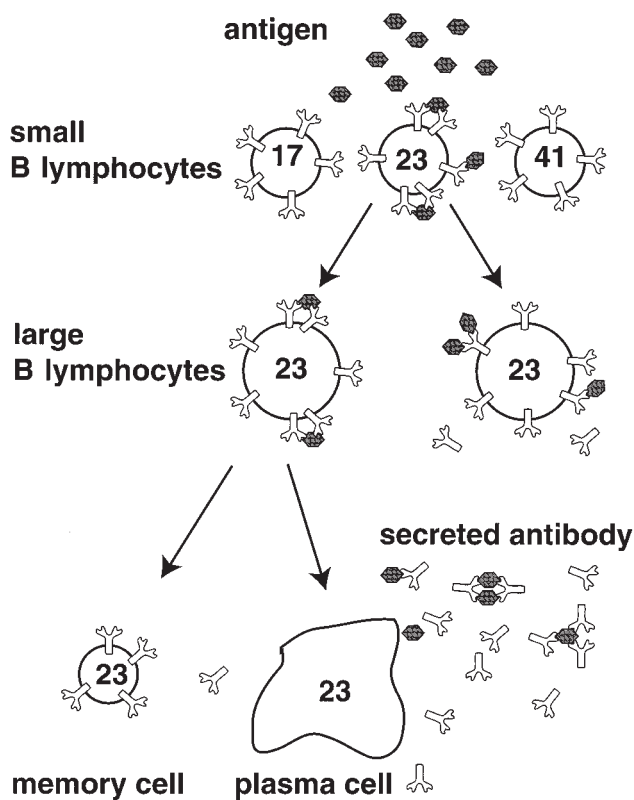


FIG. 4. Clonal selection. Small resting B cells created in the bone marrow each carry a different receptor type defined by their  $V_H$  and  $V_L$  regions (see Fig. 1). Here B cells are labeled by their receptor type. B cells of type 23 recognize the antigen and become large lymphocytes, which proliferate and differentiate into antibody-secreting cells and memory cells. The most differentiated antibody-secreting cell is a plasma cell.

precise, a mouse has approximately  $10^8$  lymphocytes. If it has a repertoire of  $10^7$ , then *on average* there are only 10 lymphocytes of any particular specificity. Learning in the immune system involves raising the population size of lymphocytes that have proven themselves to be valuable by having recognized antigen. If the immune system can learn from experience the shapes of antigenic determinants, then the immune system can maintain more lymphocytes bearing receptors of the appropriate complementary shape and be better prepared to fight an antigen if it is seen again. Thus learning in the immune system involves biasing the repertoire from random towards a repertoire that more clearly reflects the actual antigenic environment.

During the life of any individual the detailed dynamics of lymphocyte growth, differentiation, and competition between clones ultimately reflects the system's interaction with its environment. After an antigen has been seen once, the immune system responds to subsequent encounters with the same antigen with faster and larger-amplitude responses. Such responses are called *secondary* immune responses, and they can be attributed to having larger initial clone sizes. Thus, say, rather than starting the response with a clone of 10 cells, the system might start with  $10^4$  cells specific for the antigen. When

these cells secrete antibody they have a large impact. In a primary response, there is a delay due to the fact that the cell population needs to enlarge before it can secrete substantial amounts of antibody. (The more rapid and vigorous secondary response may also be due to differences between naive cells and cells that have seen antigen. For example, secondary response or memory cells may be easier to trigger than naive cells. Cells that have never been triggered are small and contain little cytoplasm. When triggered they make at least 50 new proteins. One would expect many of these molecules to remain in the cell, thus making subsequent triggering events easier and faster. Also, the affinity of antibodies for antigen may increase due to somatic mutations that occur during the growth of lymphocyte clones. This topic will be dealt with extensively in Sec. III.C.) Because the total number of lymphocytes in the immune system is regulated, increases in the sizes of some clones means other clones may have to decrease in size. The total number of lymphocytes is not kept absolutely constant. Swelling of lymph nodes, for example, allows some increase in lymphocyte populations during an immune response, but the immune system is a few percent of the total cells in the body, and that percentage cannot increase very much before affecting other bodily functions. Thus, if the immune system learns only by increasing the population sizes of specific lymphocytes, it must either forget previously learned antigens, increase in size, or constantly decrease the portion of its repertoire that is generated at random and responsible for responding to novel antigens. Because of the experimental difficulties inherent in studying individual clones *in vivo* it is not yet possible to decide to what degree each of these alternatives is followed. To gain insights into these and related questions a number of workers have developed quantitative models of cell growth and differentiation in the immune system under various scenarios of immune regulation. We discuss some of these models below.

### 3. The self-nonsel discrimination problem

The completeness of the repertoire presents a fundamental paradox for the immune system. Because all shapes can be recognized, the immune system can recognize molecules and cells of our body as well as foreign ones. For the immune system to function properly it needs to be able to distinguish between these two classes of molecules and cells, which are *a priori* indistinguishable, so as to avoid triggering an immune response against *self antigens*, i.e., the components of our body. Not responding against self antigen is a phenomenon called self-tolerance. Understanding how this is accomplished by the immune system is called the *self-nonsel discrimination problem*.

The solution to the self-nonsel discrimination problem is not yet fully at hand but an enormous amount of progress has been made in recent years. von Boehmer (1991) and others have discovered that, as T cells differentiate in the thymus, those T cells that react with self

antigens have a high probability of being eliminated. The process is, however, incomplete, and some self-reactive T cells are encountered outside the thymus. This can be understood since clonal elimination in the thymus is based on encounters between immature T cells and self antigens in the thymus, and presumably not all self antigens are present inside the thymus. As is often the case in biology, several mechanisms contribute to the same function, and self-nonself discrimination involves mechanisms other than thymic elimination. Much of the recent effort in theoretical immunology, as well as in experimental immunology, is devoted to the solution of the self-nonself discrimination problem (see Stewart and Varela, 1991; Varela and Coutinho, 1991; Neumann and Weisbuch, 1992a; De Boer and Perelson, 1993; Percus, Percus, and Perelson, 1993; Detours *et al.*, 1994; Sulzer, van Hemmen, and Behn, 1994). One approach used in this effort is the development of a theory of immune networks, to be discussed in Sec. IV.

## II. MODELING THE IMMUNE REPERTOIRE

A first example of the use of mathematics in immunology is the evaluation of the completeness of the repertoire. The arguments that we give below apply to both the B-cell and T-cell repertoires, i.e., to antibodies, to immunoglobulin receptors on the surface of B cells binding to antigens, and to the receptors on T cells binding to MHC-peptide complexes. For simplicity we state the argument in terms of receptors binding to ligands.

### A. How large does the repertoire need to be in order to be complete?

Perelson and Oster (1979) developed a simple quantitative model with which they could ask: Given a set of  $n$  distinct, randomly made receptors, what is the probability that a randomly encountered antigen is recognized by at least one of the receptors? The model is based on the notion of *shape space*. The idea is that the degree of binding between a receptor and a molecule that it binds, a ligand, generally involves short-range noncovalent interactions based on electrostatic charge, hydrogen bonding, van der Waals interactions, etc. In order for the receptor and ligand to approach each other over an appreciable portion of their surfaces, there must be extensive regions of complementarity. Oster and Perelson called the constellation of features important in determining binding among molecules the *generalized shape* of a molecule. Suppose that one can adequately describe the generalized shape of a receptor combining site by  $\eta$  parameters: the length, width, and height or the radius of curvature of any bump or groove in the combining site, its charge, etc. Then a point in an  $\eta$ -dimensional space, “shape space”  $S$ , specifies the generalized shape of a receptor binding region (Fig. 5). If an animal has a repertoire of size  $n$ , then the shape space for that animal would contain  $n$  different points. We shall assume that shape space is a bounded region of  $R^n$  with volume  $V$ , since there is only a restricted range of widths, lengths,

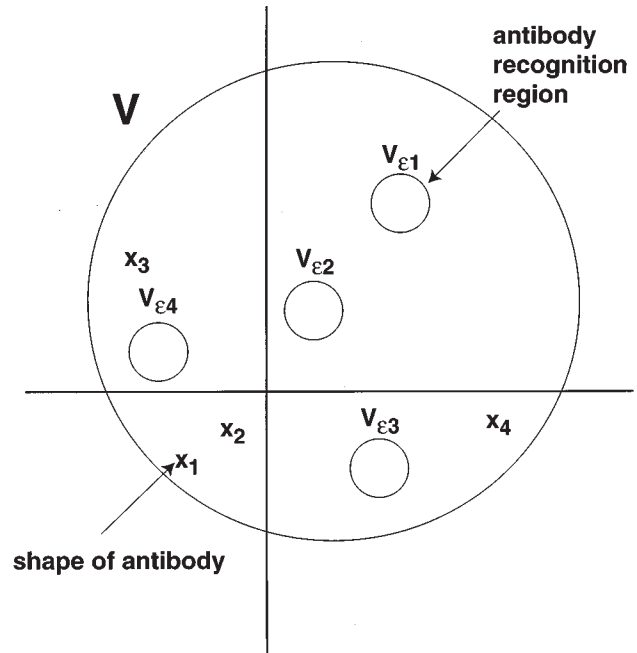


FIG. 5. Diagrammatic representation of shape space. Antibody of shape  $x_i$  recognizes those epitopes whose shapes lie within a region of shape space, of volume  $V_{\epsilon_i}$ , called a “recognition ball” or “recognition region.” The entire shape space is assumed to be a bounded region of  $R^n$  with volume  $V$ .

charges, etc. that a receptor combining site can assume. For example, one would never find a receptor with a combining site dimension of one meter.

Antigens are not recognized as whole objects but rather are parsed into small regions known as antigenic determinants or epitopes. Epitopes are also characterized by generalized shapes, which should lie within  $V$ . For example, a receptor combining site with a length of 1 nm cannot be expected to recognize an epitope 10 nm long. In order to estimate how well an animal with a receptor repertoire of size  $n$  can recognize molecular determinants, let us assume that a receptor  $i$  and antigenic determinant  $\bar{\tau}$  fit together perfectly. If the receptor and epitope shapes are not quite complementary then the two molecules may still bind but with lower equilibrium binding constant or “affinity.” At some low level of affinity, e.g.,  $10^4 M^{-1}$  ( $M \equiv$  moles/liter), immunologists say that the interaction is not specific and that the molecules are not complementary. To describe this we assume that each receptor interacts strongly enough to generate an immune response with all epitopes that are within a small region in shape space surrounding its exact complement. Although the region need not be spherical it is easiest to think of it this way and call the region a “recognition ball.” Let  $V_{\epsilon_i(K)}$  be the volume in  $S$  of the recognition ball of radius  $\epsilon_i$  for receptor  $i$ . The radius  $\epsilon_i$  is a function of the threshold affinity  $K$  for specific recognition. If the recognition region is not spherical, then  $\epsilon$  is chosen so that the recognition ball has the same volume as the nonspherical recognition region. Let  $V_{\epsilon(K)}$  be the average volume of a recognition ball in  $S$ . [If one wanted to be more precise and not use

thresholds one could assign an explicit affinity to each pair of shapes depending upon their location in shape space. This approach was taken by Segel and Perelson (1988)].

Because each receptor can recognize all antigenic determinants within a recognition ball, a finite number of antibodies can recognize an infinite number of antigens. The ability of the immune system to recognize essentially any antigen had been puzzling to immunologists who assumed each antibody was complementary to only one antigen as in the classical lock and key analogy.

To complete the model, let us assume that receptors are made with random shapes. Thus the  $n$  receptors lie scattered at random in the shape space. If each receptor has roughly the same recognition volume  $V_\epsilon$ , then the total volume covered by all of the receptors in the repertoire is  $nV_\epsilon$ . If this volume is large compared with the total volume of shape space  $V$ , then one would expect that the various antibodies would have recognition regions that overlap and completely cover shape space. In fact, each epitope would on average be recognized by  $nV_\epsilon/V$  different receptors, and the probability  $P$  that an epitope would *not* be recognized by some receptor is (Perelson and Oster, 1979)

$$P = (1 - V_\epsilon/V)^n \approx e^{-nV_\epsilon/V}. \quad (2.1a)$$

The expression on the right is the one that would result from assuming a Poisson distribution of antibodies in shape space, i.e., it is the probability of finding a point (i.e., an epitope) lying in no antibody recognition ball.

We can use Eq. (2.1a) to quantify the completeness of the repertoire. Typically, of order  $10^{-5}$  of the B cells or T cells in an animal respond to any epitope (see Klinman and Press, 1975). This value is an estimate of  $p$ , the probability that a receptor recognizes a random antigenic determinant with an affinity above the threshold value  $K$  required to stimulate a lymphocyte. To interpret  $p$  within the context of shape-space theory, notice that if one randomly places an epitope in shape space, the probability that it lands in the volume  $V_\epsilon$  surrounding any given receptor is  $V_\epsilon/V$ , the fraction of the shape-space volume covered by a single receptor. Thus, if the readout of immune recognition is lymphocyte stimulation,  $p = V_\epsilon/V \approx 10^{-5}$ , and

$$P = (1 - p)^n \approx e^{-pn}. \quad (2.1b)$$

With this rough estimate, Eq. (2.1b) predicts that animals with a repertoire of  $n = 10^5$  will have immune systems with only marginally proficient abilities to recognize foreign antigens, i.e.,  $e^{-1}$  or 37% of epitopes will escape detection. However, if  $n = 5 \times 10^5$  then  $P$  falls to  $7 \times 10^{-3}$  and less than 1% of epitopes escape detection. If  $n = 10^6$ , then  $P = 4 \times 10^{-5}$  and essentially all epitopes will be recognized. Thus a repertoire of order  $10^6$ , composed of receptors with random shapes, will be complete. This is interesting because the smallest known immune system is that of a young tadpole, which is estimated to have  $10^6$  lymphocytes and thus a repertoire of order  $10^5$  to  $10^6$  (Du Pasquier, 1973; Du Pasquier and Haimovitch, 1976). As far as we know, smaller immune

systems do not exist, and the calculation given above suggests that this is the case because such immune systems would recognize antigen so infrequently that they would provide little, if any, protective advantage.

To summarize, assuming  $p$  is of the order of  $10^{-5}$ , the receptor repertoire will be complete if three hypotheses are satisfied: (i) Each receptor can recognize a set of related epitopes, each of which differs slightly in shape. (ii) The repertoire size is of the order  $10^6$  or greater. (iii) The receptors in the repertoire have shapes that are randomly distributed throughout shape space.

Experiment has shown that hypothesis (i) is satisfied. Although binding is highly specific, antibodies can bind more than one epitope. If the epitopes have related chemical structures the antibody is called cross-reactive. If the epitopes have very different chemical structures, the antibody is called multireactive. The strength of binding may differ for different epitopes and is reflected in differences in affinity. The situation with helper T cells is similar. Helper T cells recognize peptides bound to MHC class-II molecules on the surfaces of antigen-presenting cells. By mutating the peptide, one has been able to show that a set of related peptides all bind the same T-cell receptor and are capable of leading to T-cell activation.

Although exact repertoire sizes are not known, the best current estimates for mice (the best-studied model system) place the expressed repertoire size at approximately  $10^7$  for both B cells and T cells. Thus we are reasonably confident that hypothesis (ii) is also satisfied.

Hypothesis (iii) is almost certainly not strictly satisfied. Receptors are not made by a totally random process but are constructed from genes. The genetic machinery involved in generating antibody and T-cell receptors is very diverse and error prone, so that most immunologists believe that to a good approximation shape space is covered. However, it is clear that one can breed mice to have "holes" in their repertoire. The basic genetic building blocks out of which B- and T-cell receptors are made biases the ultimate repertoire. This bias may be towards antigenic determinants that are found on common pathogens. Thus during evolutionary time the immune system may have learned that there are regions of shape space that are more important to cover than others. The repertoire may thus be biased towards this type of coverage. Work by Forrest *et al.* (1993), using simulations based on genetic algorithms, has shown how biased repertoires can develop. Also, it is now clear that elements in the repertoire that recognize self are deleted from the T-cell repertoire, further introducing holes.

A weaker form of hypothesis (iii) will suffice. Not all receptor shapes need be made at random. It will suffice if a subset of the repertoire of size  $5 \times 10^5$  to  $10^6$  is distributed randomly throughout  $V$ ; other receptors could be distributed nonrandomly and the repertoire would still be complete.

## B. Self-nonsel self discrimination and the probability of recognition

It is interesting to ask why evolution selected a value of  $p$  of order  $10^{-5}$ . If  $p = 1$ , then receptors would be

perfectly efficient and recognize everything, and a repertoire of size  $n=1$  would suffice for perfect recognition of all antigens. The answer, of course, is that the perfect antibody would stick to everything including all self molecules.<sup>1</sup> Thus, while not obvious at first, considerations of self-nonself discrimination may have played a role in selecting a reduced size for  $p$ . Percus, Percus, and Perelson (1992, 1993) have posed the problem in the following way.

Consider a repertoire of size  $n$  in an animal with  $N'$  self epitopes in an environment with  $N$  foreign epitopes. Let  $P(N, N'; n)$  be the probability that a receptor repertoire of size  $n$  has the property that all of  $N$  foreign epitopes are recognized by at least one receptor in the repertoire, but that none of  $N'$  self epitopes are recognized. Let  $p$  be the probability that a random receptor recognizes a random epitope, and the corresponding complementary probability,  $q=1-p$ . Then

$$P(N, N'; n) = (1 - q^n)^N q^{nN'}. \quad (2.2)$$

The maximum of Eq. (2.2) is achieved when

$$q = \left(1 + \frac{N}{N'}\right)^{-1/n} \sim 1 - \frac{1}{n} \ln\left(1 + \frac{N}{N'}\right). \quad (2.3)$$

If the present-day immune system has optimized  $P(N, N'; n)$ , then we would expect the probability of successfully recognizing a random epitope,  $p=1-q$ , to be computable from Eq. (2.3). Hence

$$p \sim \frac{1}{n} \ln\left(1 + \frac{N}{N'}\right). \quad (2.4)$$

Although the number of foreign and self epitopes that the immune system deals with is unknown, let us assume  $N=10^{16}$ , which is the lower limit proposed by Inman (1978). Now if the number of self epitopes  $N'=10^6$ , i.e., 10 epitopes in each of the  $10^5$  or so self proteins coded for in the human genome, then by Eq. (2.4), with  $n=10^7$ ,  $p=2 \times 10^{-6}$ . This is somewhat smaller than empirical estimates. For example, Cancro *et al.* (1978) estimate that 1.3 B cells per hundred thousand recognizes the hemagglutinin protein on influenza. Assuming that this measured frequency is an estimate of the probability that a randomly chosen B cell recognizes hemagglutinin, for this antigen  $p \approx 1.3 \times 10^{-5}$ . Since hemagglutinin is a protein found on the surface of a naturally occurring virus it is a good choice for comparison with our theory. However, as a protein it may have multiple epitopes, which may explain the fivefold higher measured frequency than our theory predicts. One might question the assumption of 10 epitopes per self protein or  $10^{16}$  foreign epitopes. However, due to the logarithmic nature of Eq. (2.4) our estimate of  $p$  is not very sensitive to changes in  $N$  and  $N'$ .

<sup>1</sup>As pointed out to us by B. Sulzer, all cells, if they used recognition as the criterion for stimulation and action, would also be called into the response. Thus graded levels of response might be difficult or impossible to obtain.

### C. Predicting the size of epitopes

So far in our consideration of receptor-ligand interactions we have not quantified the degree of match between two molecules. In this section we shall present a simple model for determining molecular complementarity and use that model to predict the optimal size of an epitope. We restrict our attention to epitopes composed of amino acids.

Farmer, Packard, and Perelson (1986) introduced the idea of using a binary string to represent the shape of a receptor. Any of a number of string-matching algorithms could then be used to determine the degree of complementarity between strings. Here we shall pursue of generalization of that idea, introduced by Percus, Percus, and Perelson (1993), in which strings chosen from an alphabet of  $m$  letters are used. The idea here is that amino acids can be classified into groups depending on their chemical properties. Thus as a simple caricature of the amino acid combining site of a receptor and the complementary epitope, we assume both are composed of  $m$  types of amino acids, with each amino acid complementary to exactly one other amino acid in the alphabet. As an example, amino acids can be classified as being hydrophobic or hydrophilic, and if they are hydrophilic as being positive or negatively charged. This leads to  $m=3$  with positive complementary to negative and hydrophobic complementary to hydrophobic. We also assume that a receptor need only be complementary to a piece of the antigen, i.e., an epitope, where an epitope is defined as a sequence of at least  $r$  letters. Let us see the consequence of this assumption on the value of the successful recognition probability  $p$ . Once we compute  $p$  as a function of  $r$ , we shall invert the function  $p(r)$  and estimate the size of an epitope,  $r$ , that is consistent with a particular value of  $p$ . Interestingly, this simple approach yields realistic estimates of epitope sizes.

Consider the simple case in which the receptor and antigen are both sequences of length  $\ell$ . Align the two sequences and denote a matching or complementary pair of letters by  $x$ , with probability  $1/m$ , and a non-matching pair by  $y$ , with probability  $(m-1)/m$ . We now compute the probability  $p$  of at least one sequence of at least  $r$   $x$ 's out of the total of  $\ell$  entries. This matching problem has a venerable history, going back at least to de Moivre (see Uspensky, 1937). We shall solve it, using generating functions, as described in Percus, Percus, and Perelson (1992). It is convenient to switch consideration to  $q=1-p$ , and hence to the probability of having no sequence of  $x$ 's longer than  $r-1$  out of a sequence of  $\ell$   $x$ 's and  $y$ 's. Let us not worry about  $\ell$  for the moment and simply construct the generating function for all sequences of  $x$ 's and  $y$ 's satisfying this condition. A typical sequence will belong to the set of  $2t+1$  groupings

$$x^{a_1} y x^{a_2} y \cdots x^{a_{t-1}} y x^{a_t} \quad (2.5)$$

where  $t \geq 1, \quad 0 \leq a_j \leq r-1.$

Summing over all  $\{a_j\}$ , we have  $(1-x^r/1-x)y\cdots y(1-x^r/1-x)$  and then over  $t$ ,  $1/[(1-x/1-x^r)-y]$ , giving us the generating function for all such sequences,

$$G(x,y) = \frac{1-x^r}{1-x-y(1-x^r)}. \quad (2.6)$$

Now we assume that  $x$  has the probability weight  $1/m$ ,  $y$  has  $(m-1)/m$ . If we give  $x$  and  $y$  a further weight  $z$ , we are then able to extract sequences of length  $\ell$  by just taking the coefficient of  $z^\ell$ . Hence, making the replacement  $x \rightarrow (1/m)z$ ,  $y \rightarrow (m-1/m)z$  in Eq. (2.6), we have

$$q = \text{coeff } z^\ell \text{ in } \frac{1-\lambda z^r}{1-z+\lambda(m-1/m)z^{r+1}} \quad (2.7)$$

where  $\lambda = m^{-r}$ . Although an exact solution can be found (Uspensky, 1937), it is not convenient for computation, especially when  $\ell \gg r$ . To proceed, we expand in  $\lambda$  as a small parameter,

$$q = \text{coeff of } z^\ell \text{ in } \frac{1}{1-z} - \lambda \left[ \frac{m-1}{m} \frac{z^{r+1}}{(1-z)^2} + \frac{z^r}{1-z} \right] + \dots, \quad (2.8)$$

which we evaluate at once as

$$q = 1 - \lambda \left[ \frac{m-1}{m} (\ell-r+1) \right] + \dots. \quad (2.9)$$

This expression can be used to compute  $r$  as function of  $p$ . Assuming  $\ell \gg r > 1$ , i.e., dropping the negligible  $[(m-1)/m]r$  and 1 in Eq. (2.9), and using the definition of  $\lambda$  we obtain

$$r = -\ln_m p + \ln_m [\ell(m-1)/m]. \quad (2.10a)$$

To obtain an estimate of  $r$  one can either use experimental estimates of  $p$  or one can substitute the optimal value of  $p$  from Eq. (2.4) and obtain

$$r = \ln_m n^\ell - \ln_m \left[ \frac{m}{m-1} \ln \left( 1 + \frac{N}{N'} \right) \right]. \quad (2.10b)$$

Thus the size of the combining site  $r$  is mainly determined by the total number of  $m$  bits in  $n$  and  $\ell$ , and, in particular, is very insensitive to the number of foreign and self epitopes,  $N$  and  $N'$ , respectively.

In the physical system, when antibody binds an antigen the binding need not involve a single uninterrupted sequence of matches. In crystal structures of antigen-antibody complexes one observes that binding can occur over an area, and several linear pieces may be involved. Thus, for successful binding, a criterion requiring, say, at least  $t$  sequences of at least  $r$  matches might make more sense. Generalizing the above to such a criterion is not difficult: we "tag" any subsequence of  $r$  or more matches by a variable  $\zeta$  in order to recognize it, thereby replacing the strict failure contribution  $(1-x^r)/(1-x)$  in Eq. (2.6) by

$$\sum_{a=0}^{r-1} x^a + \zeta \sum_{a=r}^{\infty} x^a = \frac{1-x^r}{1-x} + \frac{\zeta x^r}{1-x}. \quad (2.11)$$

When we do this, Eq. (2.6) is replaced by

$$G(x,y,\zeta) = \frac{1-x^r + \zeta x^r}{1-x-y(1-x^r + \zeta x^r)}. \quad (2.12)$$

Failing configurations are then those in which only the powers  $1, \zeta, \zeta^2, \dots, \zeta^{t-1}$  are present. Since

$$\begin{aligned} & (\text{coeff } \zeta^0 + \text{coeff } \zeta^1 + \dots + \text{coeff } \zeta^{t-1}) G(\zeta) \\ &= \text{coeff } \zeta^{t-1} [G(\zeta)/(1-\zeta)], \end{aligned} \quad (2.13)$$

we have, in the same fashion as Eq. (2.8),

$$q = \text{coeff } z^\ell \zeta^{t-1} \text{ in } \frac{1}{1-\zeta} \frac{1-\lambda(1-\zeta)z^r}{1-z+\lambda(m-1/m)(1-\zeta)z^{r+1}}, \quad (2.14)$$

from which

$$p = \lambda^t \left( \frac{m-1}{m} \right)^t \text{coeff } z^\ell \text{ in } \frac{z^{rt+t-1}/(1-z) - z^{rt+t}/m}{[1-z+\lambda(m-1/m)z^{r+1}]^t}. \quad (2.15)$$

To leading order in  $\lambda$ , Eq. (2.15) becomes

$$p \sim \lambda^t \left( \frac{m-1}{m} \right)^t \left[ \binom{\ell+1-rt}{t} - \frac{1}{m} \binom{\ell-rt}{t} \right], \quad (2.16)$$

so that, for  $\ell \gg rt$ ,

$$\ln_m p \sim -rt + t \ln_m \ell - t \ln_m \frac{m}{m-1} \dots. \quad (2.17)$$

Now, comparing with our previous estimate, Eq. (2.4), we have

$$rt = \ln_m(n^\ell) + \ln_m \{ [m/(m-1)]^t \ln(N/N') \} + \dots. \quad (2.18)$$

In other words, allowing the  $R=rt$  matching sites to be distributed in pieces indeed increases the required value of  $R$ , but not significantly until  $\ell^t$  approaches the order of  $n$ .

How reliable is the estimate given by Eq. (2.10)? A reasonable value for the size of the accessible receptor variable region is  $\ell \sim 100$  amino acids (Percus, Percus, and Perelson, 1993). Using a three-letter charge alphabet,  $m=3$ , and  $\ell=100$ ,  $n=10^7$ ,  $N \sim 10^{16}$ , and  $N' \sim 10^6$ , Eqs. (2.10a) and (2.10b) predict  $r \sim 14.3$  and 15.6, respectively. If  $\ell=70$  rather than 100, then Eq. (2.10b) predicts  $r \approx 15.3$ ; if  $N/N' = 10^9$  rather than  $10^{10}$ , and Eq. (2.10b) predicts  $r \approx 15.7$ , illustrating the insensitivity of the results to the choice of  $\ell$  and the ratio of foreign to self antigens. These predicted values are consistent with the various experimental determinations on the number of contact residues between antibody combining sites and protein antigens and the size of the region on the MHC-peptide complex that interacts with the T-cell receptor. For example, Amit *et al.* (1986) found that in an antigen (lysozyme)-antibody complex, the interface was tightly packed with 16 lysozyme and 17 antibody residues making close contact. Sheriff *et al.* (1987), looking at a second epitope on lysozyme, found that it was composed of three sequentially separated subsites containing a total of 14 residues in direct contact with the antibody. Surprisingly, Cygler *et al.* (1991) found that even

with an oligosaccharide antigen there were 15 residues in contact with the antigen. Ajitkumar *et al.* (1988) found that T cells recognized a region on peptide-MHC complexes of approximately  $600 \text{ \AA}^2$ , which is roughly the same contact area as in the antigen-antibody complexes of native proteins like lysozyme (Sheriff *et al.*, 1987) and influenza virus neuraminidase (Colman *et al.*, 1987).

Our predictions are sensitive to the alphabet size  $m$ . Thus, if  $m=4$  rather than 3, then Eqs. (2.10a) and (2.10b) give  $r \approx 11.3$  and 12.5, respectively. However, we argue in Percus, Percus, and Perelson (1993) that based on empirical data  $m=3$  appears to be a quite reasonable estimate.

Why is the result given by Eq. (2.10) interesting? First, it provides a quantitative estimate of what should be clear—that epitopes cannot be too small or too big. If epitopes were very small, say two amino acids, then the same epitope would be expected to be found on both foreign and self proteins. For example, Ohno (1991), looking at the information on the amino acids of proteins in current databases, observed that two totally unrelated proteins, on the average, shared 30 identical tripeptides, two tetrapeptides, and one pentapeptide per 500 residues. Hence receptors that recognized short patterns would be expected to bind molecules throughout the body. Thus, to be useful, receptors must recognize long strings that uniquely characterize the antigen population. Recognizing each antigen by its entire string would require a receptor for each possible antigen and would not be consistent with reasonable repertoire sizes. Thus antigens need to be recognized over regions that are long but not too long. It is interesting that this principle when made quantitative predicts epitopes sizes that are consistent with observation. Second, from a more general perspective, the calculation illustrates an important principle, namely, that the diversity seen in immune repertoires reflects not only the large number of foreign epitopes that the immune system must recognize but also, and even more importantly, the number of self epitopes that the immune system must avoid reacting with, a point further discussed in De Boer and Perelson (1993).

### III. CLONAL MODELS

A central issue in immunology is the regulation of the immune response. What determines which clones are involved, how big do the clones grow, and how is the response turned off once the antigen is eliminated?

The simplest idea, based on clonal selection, is that particular subsets of B cells (and T cells) are selected for growth and differentiation by antigen, and turn off when the antigen concentration falls below some threshold. Antibody feedback and antigen specific helper, and possibly suppressor, T cells could regulate the magnitude of the response. In this clonal selection view, antigen-specific clones respond more or less independently of one another and are primarily regulated by antigen. Furthermore, in the absence of antigen, the immune system would be predicted to be at rest.

In this section we develop models in which B cells interact with antigen and this interaction determines the kinetics of the cell's response. In Sec. IV we shall examine network models in which clones of B cells can interact with each other as well as with antigen.

#### A. Receptor cross-linking and cell activation

One of the most fundamental issues in immune system modeling is determining what the correct equations are for describing the growth of cells in the immune system. Although we should like to begin from a complete description of the properties of lymphocytes and how they vary in response to various inputs, such information is still lacking. As compared to neurobiology, where the Hodgkin-Huxley equations have provided a basis for modeling, quantitative immunology is still in its formative stages. There are no agreed upon generic equations describing the properties of single cells. Many modelers have used a “log-bell-shaped” function to describe how B cells respond as a function of antigen dose. By log-bell-shaped we mean a function that when plotted on a logarithmic scale has a shape that resembles a Gaussian. Here we give a brief description of where the log-bell-shaped function comes from and try to justify its use in this early stage of modeling in immunology.

B cells have on their surfaces between  $10^4$  and  $10^5$  immunoglobulin molecules that act as receptors for antigen. Immunoglobulin molecules are Y shaped, with the terminal portions of the arms of the Y forming the antigen binding region (Fig. 1). Because the receptors are bivalent (i.e., have two identical arms), each receptor can bind 0, 1, or 2 epitopes. Experiments have shown that monovalent antigen cannot stimulate B cells, whereas bivalent and multivalent antigen can. Frequently, anti-immunoglobulin antibodies are used as a “generic” bivalent antigen, since these molecules are capable of binding immunoglobulin receptors of all specificities. Antibody molecules can be enzymatically cleaved. A fragment, known as Fab (Fig. 1), contains one arm of the Y-shaped antibody molecule and binds monovalently. Fab fragments of anti-immunoglobulin molecules bind B cells but do not stimulate them, whereas complete bivalent anti-immunoglobulin can stimulate B cells. Experiments such as these have led to the notion that antigen binding to B cells *per se* is not the signal that triggers clonal expansion, and it has been inferred that the triggering signal involves the cross-linking or clustering of receptors on the cell surface. This has been shown to be the case in a rather direct manner on basophils, another type of white blood cell involved in allergic reactions, which respond to stimulation by releasing histamine-containing granules.

Receptor cross-linking is attained when multiple receptors bind to a single multivalent antigen. Because surface immunoglobulin molecules are bivalent, one immunoglobulin may also bind two different antigens and cause the formation of large receptor aggregates. Cross-linking brings and holds receptors close together within the cell membrane and allows subsequent intracellular

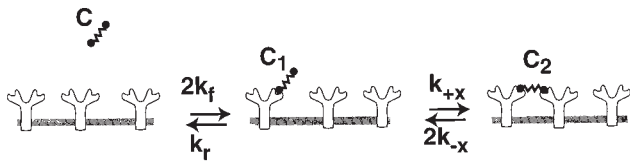
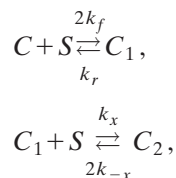


FIG. 6. Bivalent ligand in solution at concentration  $C$  reacts with bivalent surface receptors. The forward and reverse rate constants for the binding of a single site on the ligand to a single receptor site are  $k_f$  and  $k_r$ , respectively. Once the ligand is bound to the surface at one site, with concentration  $C_1$ , its second site can bind to another receptor site with forward and reverse rate constants  $k_x$  and  $k_{-x}$ , respectively, to form a doubly bound ligand  $C_2$ . Note that the second reaction, the “cross-linking step,” is a surface reaction, whereas the first reaction involves the binding from bulk solution. Thus  $k_f$  and  $k_x$  have different units and need to be distinguished.

biochemical reactions to occur that seem to be necessary for cell activation. The fraction of linked surface receptors initially increases with the free-antigen concentration. When free-antigen molecules are in excess, each receptor site tends to be bound to a different antigen molecule and few antigen molecules are simultaneously bound by several receptors. Thus we might expect the degree of receptor cross-linking first to increase with free-antigen concentration, then to reach a maximum, and then to decrease as the antigen concentration continues to rise.

Consider the following model for the cross-linking of bivalent receptors by a bivalent antigen (Fig. 6). Molecules that bind to a receptor are called ligands. We analyze a situation in which there are a fixed number of B cells, each with a constant number of bivalent receptors on its surface. Thus the total number of receptor sites in the system,  $S_0$ , is constant. Assume that the two sites on each receptor are identical and can be characterized by the same forward and reverse kinetic constants. Further assume that these binding constants are the same when the receptor is free and when it is in an aggregate. This is called the *equivalent-site hypothesis*. Let  $S(t)$  be the concentration of free sites at time  $t$ , let  $C$  be the concentration of free bivalent ligand,  $C_1$  be the concentration of ligand bound at one site, and  $C_2$  be the concentration of ligand bound at both sites. Note that  $C_2$  is the concentration of cross links. To describe the kinetics of cross-linking, let  $k_f$  and  $k_r$  be kinetic constants describing the binding and release of one site on the ligand to and from a receptor site, let  $k_x$  and  $k_{-x}$  be kinetic constants describing the binding and unbinding of the second site on a ligand already bound at one site. Also, let  $K = k_f/k_r$  and  $K_x = k_x/k_{-x}$  be the corresponding equilibrium constants. Then by the law of mass action we can write



or

$$\frac{dC_1}{dt} = 2k_fCS - k_rC_1 - k_xC_1S + 2k_{-x}C_2, \quad (3.1)$$

$$\frac{dC_2}{dt} = k_xC_1S - 2k_{-x}C_2. \quad (3.2)$$

The factors of 2 arise because either site on the ligand can bind to a receptor site, and either of the two bound sites on  $C_2$  can dissociate. By conservation of receptor sites,

$$S_0 = S(t) + C_1(t) + 2C_2(t), \quad (3.3)$$

where we have used the fact that  $C_1$  occupies one site and  $C_2$  occupies two sites. In what follows, we shall assume ligand is in excess and take  $C(t)$  to be a constant, which for simplicity we denote  $C$ .

Although approximate solutions can be found for the kinetic equations, Eqs. (3.1)–(3.3) (Perelson and DeLisi, 1980), here we shall examine only the equilibrium solution. At equilibrium,

$$C_1 = 2KCS, \quad (3.4)$$

$$C_2 = K_xC_1S/2 = KK_xCS^2. \quad (3.5)$$

Substituting into Eq. (3.3) and simplifying, one finds

$$S = S_0(1 - \beta) \left( \frac{-1 + \sqrt{1 + \delta}}{2\delta} \right), \quad (3.6)$$

where

$$\beta = \frac{2KC}{1 + 2KC} \quad \text{and} \quad \delta = \beta(1 - \beta)K_xS_0. \quad (3.7)$$

Hence the equilibrium concentration of cross links

$$C_2 = \frac{S_0}{2} \left( \frac{1 + 2\delta - \sqrt{1 + 4\delta}}{2\delta} \right). \quad (3.8)$$

Notice that  $C_2$  depends only on  $\delta$  and that  $\delta$  in turn depends on  $K_xS_0$ , a dimensionless cross-linking equilibrium constant, and on the ligand concentration  $C$ . The dependence on  $C$  is through the term  $\beta(1 - \beta)$ , which is zero when  $C = 0$ , i.e.,  $\beta = 0$ , and when  $C \rightarrow \infty$ , i.e.,  $\beta = 1$ , and which has a single maximum at  $C = 1/2K$ , i.e.,  $\beta = 1/2$ . The fraction of cross-linked receptors  $C_2$  inherits these properties and, when plotted versus  $\log 2KC$ , has a bell-shaped form with a single maximum at  $2KC = 1$ . The curve is symmetric around this maximum (see Fig. 7). The graph of  $C_2$  versus  $\log C$  has been called a cross-linking curve. Because receptors are bivalent, it is possible for a ligand to bind both arms of a single receptor. When this is taken into consideration, cross-linking curves can have two local maxima (Dembo and Goldstein, 1978).

This simple example was meant to show how a bell-shaped cross-linking function can arise. An extensive modeling effort has pursued the development of both dynamic and equilibrium models of receptor cross-linking for bivalent, trivalent, and multivalent ligands, interacting with monovalent, bivalent, and multivalent

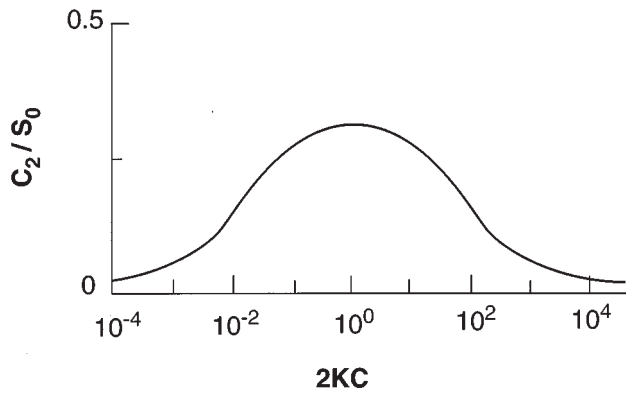


FIG. 7. A plot of the equilibrium nondimensional concentration of cross links ( $C_2/S_0$ ) vs  $\log(2KC)$ . The curve has a single peak at  $2KC=1$ , about which it is symmetric. Since the surface concentration of receptor sites is  $S_0$  and each cross link occupies two sites,  $C_2/S_0 \leq 0.5$ .

receptors. Macken and Perelson (1985a) present a general treatment using branching process methods for the analysis of multivalent ligand-multivalent receptor interactions. Macken and Perelson (1986) use renewal theory to calculate the maximum number of receptors that can be cross-linked by a randomly haptenated polymer acting as a T-independent antigen. Other references include Dembo and Goldstein (1978, 1980) DeLisi (1980, 1981), Perelson and DeLisi (1980), Perelson (1981, 1984, 1986), Wiegel and Perelson (1981), and Goldstein and Perelson (1984), Posner, Wofsy, and Goldstein (1995), Sulzer and Perelson (1996), DeBoer *et al.* (1996), and Sulzer, De Boer, and Perelson (1996). From this body of literature one learns that when ligands are not bivalent the cross-linking curve,

$$C_2 = f[\ln(C)], \quad (3.9)$$

is no longer symmetric (Perelson, 1981). Typically it has a single broad maximum over a large range of low concentrations and falls rapidly at high concentrations. However, empirical dose-response curves showing, for example, the concentration of antibody produced in mice versus the logarithm of the antigen concentration are still bell-shaped even when multivalent antigens are used (see Dintzis, Vogelstein, and Dintzis, 1982; Vogelstein, Dintzis, and Dintzis, 1982). In what follows, we shall assume that activation functions for cell proliferation and differentiation are log bell shaped and resemble the cross-linking curve derived in the example of a bivalent ligand binding to bivalent receptors without ring formation.

### B. Clonal selection models: B-cell proliferation and differentiation

Bell (1970, 1971) developed the first model of clonal selection. It was quite complete for its time, and it included the dynamics of antigen binding to B-cell receptors and the various stages of B-cell differentiation. In

the model, based on the scheme shown in Fig. 4, a set of small resting or virgin B cells are present before introduction of antigen that are capable of being stimulated into proliferation by antigen. The model assumes that in the presence of sufficient antigen the proliferating cells continue to multiply and produce antibody, which can bind to antigen and hasten its elimination. When the antigen concentration falls to a low level it is assumed that the cells stop proliferating and divide asymmetrically to become *plasma cells* and *memory cells*. Plasma cells are terminally differentiated cells that produce large amounts of antibody but that are incapable of further division (Eisen, 1980). The memory cells were assumed to be similar to virgin cells, i.e., producing no antibody and capable of being stimulated by antigen. They may be more easily triggered than virgin cells but in the model this was ignored. Interestingly, in the 25 years since the model was formulated the actual process that controls whether a proliferating cell becomes a plasma cell or a memory cell has still not been elucidated. Thus, while the assumption of half the cells' becoming memory cells and half plasma cells seems too simplistic, Bell found that the model yielded reasonable predictions.

The dynamics considered were

$$\frac{dS}{dt} = m(t) - F(R')S/T_1, \quad (3.10a)$$

$$\frac{dL}{dt} = G(R')S/T_1 + H(R')L/T_2 - L/T_2', \quad (3.10b)$$

$$\frac{dP}{dt} = \left( \frac{1 - H(R')}{2} \right) L/T_2 - P/T_3, \quad (3.10c)$$

$$\frac{dM}{dt} = \left( \frac{1 - H(R')}{2} \right) L/T_2 - M/T_4, \quad (3.10d)$$

where  $S$ ,  $L$ ,  $P$ , and  $M$  and the number per unit volume of small (virgin) lymphocytes, large (proliferating) lymphocytes, plasma cells, and memory cells, respectively. Small lymphocytes are created in the bone marrow and thus have a source,  $m(t)$ . The parameters in the model are  $T_1$ , the mean time for an optimally stimulated virgin cell to become a proliferating large lymphocyte;  $T_2$ , the mean time for a proliferating cell to divide;  $T_2'$ , the mean time for death of a proliferating cell;  $T_3$ , the mean time for death of a plasma cell; and  $T_4$ , the mean time for death of a memory cell.

The model also includes a number of functions of  $R'$ , the average number of *occupied* receptor sites per cell. Thus this model, developed before experimental information on the importance of receptor cross-linking was elucidated, assumes that cell responses are proportional to receptor occupancy. Interestingly, current models of affinity maturation by somatic mutation (Kepler and Perelson, 1993a, b), discussed in Sec. III C, also assume responses proportional to receptor occupancy. The current models are motivated by the fact that, in environments such as the spleen and lymph nodes, antigen is localized on the surface of specialized antigen-trapping

cells called follicular dendritic cells (FDC). When receptors on the B cell bind antigen on an FDC, the B-cell receptors cluster at the interface between the two cells. This bringing of the receptors close together may provide the same signals to the B cell as the cross-linking of receptors by soluble antigen.

In Eqs. (3.10a), and (3.10b),  $F$  and  $G$  are functions that control the stimulation of small lymphocytes through antigen binding to their immunoglobulin receptors. The idea is that, as receptor sites are bound, a small lymphocyte has a better chance of being activated. Thus  $F$  is chosen to be a monotonically increasing function of  $R'$ , the number of occupied receptor sites. Bell used  $F(R') = R'/(1+R')$ , but other monotonic functions should work just as well. The function  $G$  is equal to  $F$  times the fraction of virgin cells induced to proliferate rather than to die. Bell assumed that when a large fraction of the receptors on a cell were occupied the cell tended to die rather than to proliferate. This was modeled by choosing  $G(R') = (1-r')F(R')$ , where  $r'$  is the fraction of receptor sites occupied on a cell, i.e.,  $r' = R'/R_T$ , where  $R_T$  is the total number of receptor sites per cell. Note from Fig. 7 that at high antigen concentrations cross-linking decreases. Since receptor occupancy will increase monotonically with antigen concentration, Bell's function  $G$ , like the cross-linking function, decreases at high antigen. Thus Bell's model, even though it does not explicitly consider cross-linking, still incorporates the most important phenomenological feature of cross-linking, decreasing response at high antigen doses.

Lastly, Bell assumed that the fraction of large lymphocytes that still proliferate following division is  $[1 + H(R')]/2$ ; the fraction that become plasma and memory cells is thus  $[1 - H(R')]/2$ . Thus, when a proliferating cell divides, there results on average  $1 + H(R')$  proliferating cells for a net change of  $H(R')$  cells. Bell chose  $H = (R' - 1)/(R' + 1)$ , so that when many sites were occupied  $H \approx 1$  and most divisions led to proliferating cells, while when few sites were occupied,  $R' \ll 1$ ,  $H \approx -1$  and most divisions led to plasma and memory cells.

In order to compute  $R'$ , Bell also modeled the production of antibody by large lymphocytes and plasma cells and the loss of antibody by natural decay and by binding to antigen. A differential equation was also included for the total amount of antigen in the system, and chemical equilibrium equations written for the fraction of antigen bound to cells and to antibody. Thus the model comprised six differential equations and algebraic equations describing chemical equilibrium between antigen and antibody in solution and receptors on cells. The equations were solved numerically and gave rise to reasonable dynamics for an immune response.

A more elaborate version of the model was then formulated that contained a large number of different clones, each clone characterized by having a receptor with a different affinity for antigen and secreting antibody with that affinity. Equation (3.10a) was also modified by adding a term corresponding to memory cells'

being put back into the small lymphocyte pool, which could then be activated. Up to 41 different clones were followed and quantities such as the average affinity of free antibody computed. The model exhibited a phenomenon called *maturation of the immune response*, in which the average antibody affinity increased with time. This was due to the fact that cells with higher affinity would preferentially bind antigen as the antigen concentration was reduced. Thus for low affinity cells  $R'$  would be small and there would be little stimulation and little proliferation, while for high affinity cells  $R'$  would be large and proliferation would expand their numbers. Bell compared simulation results obtained with different antigen concentrations with experimental data on affinity maturation.

Perelson, Mirmirani, and Oster (1976) examined in more detail the choices a stimulated B cell has in terms of either proliferating and secreting modest amounts of antibody or giving up the ability to divide and differentiating into a short-lived plasma cell that rapidly secretes antibodies. They developed a model based on Bell's previous work that included only three populations: large lymphocytes  $L$ , plasma cells  $P$ , and antibody  $A$ . They assumed

$$\frac{dL}{dt} = pu(t)L - d[1 - u(t)]L - \mu_L L, \quad (3.11a)$$

$$\frac{dP}{dt} = d[1 - u(t)]L - \mu_P P, \quad (3.11b)$$

$$\frac{dA}{dt} = k(L + \gamma P), \quad (3.11c)$$

where  $p$  is the average proliferation rate of large lymphocytes and  $d$  is their average differentiation rate into plasma cells. It was assumed that at a given time a fraction  $u(t)$  of lymphocytes proliferated and the remaining fraction  $1 - u(t)$  were differentiating into plasma cells. Lymphocytes and plasma cells had death rates  $\mu_L$  and  $\mu_P$ , respectively, and large lymphocytes secreted antibody at rate  $k$ , whereas plasma cells secreted antibody at a rate  $\gamma \gg 1$  times larger. Using optimal control theory, Perelson, Mirmirani, and Oster (1976) asked how  $u(t)$  should be chosen in order to minimize the time needed to secrete the amount of antibody  $A^*$  required to neutralize a given dose of antigen. Thus the control problem was

$$\min \int_0^T dt, \quad (3.12a)$$

where the minimization was carried out over all functions  $u$  and where the final time  $T$  was defined by

$$A(T) = A^*. \quad (3.12b)$$

Using Pontryagin's maximum principle, they discovered that there were a number of possible strategies  $u^*(t)$  for an optimal primary response. They showed that if  $(\gamma - 1)d \leq p$ , so that plasma cells hold no advantage over large lymphocytes, then the optimal strategy is  $u^*(t) = 1$ ,  $0 \leq t \leq T$ , i.e., produce only large lymphocytes.

Parameter estimates suggest that plasma cells have a large advantage over lymphocytes and thus the immune system probably operates with  $(\gamma-1)d > p$ . In this parameter regime, the optimal strategy depends on the antigen concentration. If the antigen concentration is sufficiently low that a single generation of plasma cells could produce the target amount of antibody  $A^*$ , then the optimal control is  $u^*(t)=0$ ,  $0 \leq t \leq T$ , i.e., differentiation to plasma cells should begin immediately, with no proliferation of large lymphocytes. The more relevant case occurs when  $A^*$  is large. Plasma cells live a short time, so that immediate differentiation to plasma cells could deplete all the lymphocytes in the body that could respond to the antigen before  $A^*$  was reached. Thus with  $A^*$  large, the optimal strategy is proliferate first, i.e.,  $u^*(t)=1$ ,  $0 \leq t < t^*$ , so that a large pool of lymphocytes is created, and then switch to plasma cell differentiation,  $u^*(t)=0$ ,  $t^* \leq t \leq T$ . The switching time  $t^*$  is a function of the parameters and can be computed explicitly. The optimal solution is thus a “bang-bang” control in which  $u$  is always either 0 or 1. It is interesting that no graded response with  $u$  varying between 0 and 1 is more efficient than this extreme control with differentiation either being fully off or fully on. Using realistic parameter estimates, Perelson, Mirmirani, and Oster (1976) computed that the optimal switching time  $t^*$  should be approximately four days. This is roughly when the first plasma cells are observed experimentally.

Perelson, Mirmirani, and Oster (1978) extended their control model so that they could consider the possible consequences of repeated exposures to the same antigen. For this case they allowed the possible differentiation of a large lymphocyte into a plasma cell or a long-lived memory cell. Memory cells were assumed to be stimulated into large lymphocytes on a subsequent encounter with antigen. Thus in a second encounter with antigen, i.e., a secondary response, the initial number of large lymphocytes was the sum of the number of virgin cells stimulated plus the number of memory cells created by the end of the primary response that survived until the second encounter with antigen. In order to generate memory cells they had to modify the optimization criterion so that it included the time to complete both the primary and the secondary responses. Since memory cells did not contribute to the primary response but only to the initial conditions for the secondary response, they found, not surprisingly, that it was optimal to create memory cells only at the end of the primary response. Although Perelson, Mirmirani, and Oster (1978) found some data supporting this prediction, not all data were consistent. The major difficulty in comparing prediction to experiment was the fact that experimentalists had not fully characterized the nature of memory cells. This is still the case.

It is not clear yet whether memory in the immune system is carried by long-lived memory cells that remain at rest until a second encounter with antigen, as in the Perelson, Mirmirani, and Oster (1978) model, or if memory is a property carried by a population of proliferating cells. Models in which memory is carried dy-

namically by proliferating cell populations will be given in Sec. IV. There is also a third possibility—memory may be carried by retained antigen, with lymphocytes repeatedly encountering this retained antigen and being restimulated. Fishman and Perelson (1995) model this scenario. Data for it also exist. For example, Tew and Mandel (1979) and Tew, Phipps, and Mandel (1980) showed that protein antigens can be retained in the lymph nodes of mice for months, while more recent evidence suggests that retention may be for over a year (Tew, personal communication). Growing antigens, such as virus or bacteria, can lead to persistent low-level infections that are not cleared, and hence antigen can be present for very long periods indeed. Thus, while it was once thought that memory was due to long-lived memory cells, this view is no longer universally accepted among experimentalists (see Mackay, 1993), and other hypotheses and combinations of hypotheses about the nature of memory need to be explored.

The general problem of control of cell proliferation and differentiation in a network context has been approached by Sulzer *et al.* (1993). The nature of memory has also been examined theoretically by Behn, van Hemmen, and Sulzer (1992, 1993), and Behn *et al.* (1993). Batt and Kompala (1990) reexamined the Perelson, Mirmirani, and Oster optimization problem for a replicating antigen using a different optimization criterion. The models we have discussed have all been idealized and have not included the role of T cells in determining B-cell proliferation and differentiation. Models of immune regulation involving T-helper/T-suppressor cell circuits have been developed (see Herzenberg *et al.*, 1980; Eisenfeld and DeLisi, 1985; Kaufman, 1988; King, 1988). We shall not review these models since the very existence of T suppressor cells has been called into question. Including T cells and the cytokines that they secrete (e.g., interleukin-2) in immune system models is still an area in which much work needs to be developed. Although some recent modeling work exists (see Kevrekidis, Zecha, and Perelson, 1988; McLean and Kirkwood, 1990; Goldstein *et al.*, 1992; McLean, 1992; Michie *et al.*, 1992; Kaufman, Andris, and Leo, 1992; Kürten, 1992; Morel, Kalagnanam, and Morel, 1992; Perelson and Goldstein, 1992; Schweitzer, Swinton, and Anderson, 1992; Fishman and Perelson, 1993, 1994, 1995; Merrill, De Boer, and Perelson, 1994; De Boer and Perelson, 1994, 1995; Segel and Jäger, 1994; Morel *et al.*, 1996) we shall restrict our attention in this article to the more developed area of B-cell models.

### C. Affinity maturation

Bell's (1970) model of affinity maturation showed that as the antigen concentration decreased and became limiting higher-affinity cells would capture antigen and grow, while low-affinity cells would be unable to bind enough antigen to remain activated. Thus high-affinity cells would be preferentially selected to grow and the average affinity would increase. The model, however, assumed that cells of all possible affinities preexisted in the

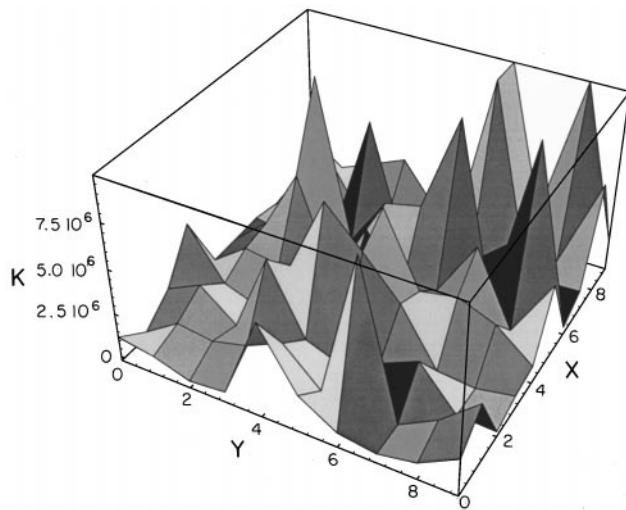


FIG. 8. A random landscape. The affinity of an antibody depends on its variable region. However, one cannot yet predict affinity from sequence. If affinities are assigned to variable-region gene sequences at random, say from a log-normal distribution, then a random landscape results. Here a two-dimensional representation of sequence space is indicated, the  $x$  and  $y$  coordinates being arbitrary indexes. Each integer value  $(x,y)$  indicates a sequence, above which a random affinity  $K(x,y)$  is plotted.

animal. Experimental measurements made in the 1980s showed that this was not the case, and that the majority of high-affinity cells were created by mutation during the course of the immune response. The process Bell modeled has been called *affinity selection* (Siskind and Benacerraf, 1969; De Boer and Perelson, 1994; Fishman and Perelson, 1995).

Recent models of affinity maturation deal with a process known as *somatic hypermutation* in which point mutations are introduced into the genes that code for the variable portion of the antibody molecule (see Fig. 1) at surprisingly high rates. Mutants with higher affinity for the immunizing antigen are selected for growth and the average affinity increases with time. Models of this process have been developed by Kauffman, Weinberger, and Perelson (1988), Macken and Perelson (1989, 1991), Macken, Hagan, and Perelson (1991), Weisbuch and Perelson (1991), Weinand (1991), Agur, Mazor, and Meilijson (1991, 1992), and most recently by Kepler and Perelson (1993a, 1993b).

The models of Kauffman, Weinberger, and Perelson (1988), Macken and Perelson (1989, 1991) and Macken, Hagan, and Perelson (1991) all deal with spin-glass-like models, in which affinity is defined as a value landscape over the space of antibody V region sequences. Affinity maturation is then modeled as a strictly uphill walk on a random landscape (Fig. 8). Because there are a large number of local optima on a random landscape, strictly uphill walks quickly get trapped at an optimum. Thus these models predict that affinity will improve for a while and then stop improving. When animals are immunized with a foreign antigen and the affinity of B cells for the immunizing antigen measured, one frequently

finds B cells that have an increased affinity for the immunizing antigen. Increases of affinity of order ten to fiftyfold are common, larger increases much rarer. After an order of magnitude or so of improvement in affinity, further point mutations tend not to lead to additional substantial improvements. Typically 8 to 10 point mutations are seen, although there is great variability from antibody to antibody; with extremes roughly between 2 and 20 mutations. This stopping of improvement in affinity is precisely what is to be expected from an uphill walk on a rugged landscape. Additionally, one can predict the probability of getting to an optimum in  $k$  steps (Macken, Hagan, and Perelson, 1991). For a random landscape the mean of this probability distribution is about 8 with a standard deviation of about 3. This is in surprisingly good agreement with immunological measurements.

Macken and Perelson (1995) have generalized their calculations of walk length to correlated landscapes which result from considering an antibody to be composed of independent parts or “blocks.” Antibody sequences and three-dimensional structures have been partitioned into framework and complementarity-determining regions (CDR). The complementarity-determining region encompasses the parts of the antibody that contact the antigen, and the framework region comprises the remainder of the molecule that provides its general structure. Assuming that the framework and complementarity-determining regions make independent contributions to the fitness of the antibody leads to a two-block model. The fitness landscape is correlated because a mutation in one block leaves the fitness contribution from the other block unchanged. Assuming that the CDR and framework blocks have evolved to different starting fitnesses allows one to fit immunological data on the number of mutations in each of these regions of the antibody molecule.

The landscape models discussed above follow the evolution of only a single antibody sequence. In an animal a large number of different B-cell clones simultaneously respond to antigen and mutate. Further, the somatic mutation process appears to be turned on and off during the course of an immune response and thus the mutation rate varies in time. Kepler and Perelson (1993a, 1993b) developed a model of B-cell growth, mutation, and competition for antigen. In their model they assumed that the rate of somatic mutation could be regulated and they sought the mutation schedule  $\mu(t)$  that maximizes, at the end of the immune response,  $\sum b_i K_i$ , where  $b_i$  is the number of B cells with affinity  $K_i$ . Since this model led to some surprising results, we summarize its main features.

B cells were assigned to discrete affinity classes. The response was assumed to be initiated by cells in single affinity class, denote by  $i=0$ , and assigned affinity  $K_0$ . Clones with  $i<0$  have decreased affinity, whereas clones with  $i>0$  have increased affinity. Mutations lead to transitions between the affinity classes, with  $m_{ij}$  defined to be the probability that a daughter of a cell in affinity class  $i$  mutated to affinity class  $j$ . These probabilities

were computed from a lower-order model but in principle could be obtained from experimental data.

The B-cell population dynamic equations used by Kepler and Perelson (1993a, 1993b) are

$$\begin{aligned}
 db_i/dt = & b_i \theta_i [-k_d(1-h_i) + k_p h_i(2m_{ii}-1)] \\
 & + 2k_p \sum_{j \neq i} m_{ji} h_j b_j \theta_j.
 \end{aligned}
 \tag{3.13}$$

Ignoring  $\theta$  for the moment, the first term on the right is the rate of death of unstimulated cells, the second term the rate of proliferation, and the third term the rate at which cells of class  $j$  have daughters that have mutated into class  $i$ . The term  $2m_{ii}-1$  represents an event in which a cell divides into two daughters of type  $i$  and the parent is lost. The factor 2 in the last term is a result of fact that either of the two daughters of a cell of type  $j$  may be of type  $i$ . The rates for proliferation and death,  $k_p$  and  $k_d$ , respectively, are multiplied by

$$h_i \equiv K_i C / (1 + K_i C),
 \tag{3.14}$$

where  $C$  is the concentration of unbound antigen. At equilibrium, the fraction of receptors on a B cell of affinity class  $i$  bound by antigen is  $h_i$ . In this model this fraction is identified with the fraction of cells  $b_i$  that are activated at antigen concentration  $C$ . Under this model, cells with higher affinity  $K_i$  grow faster and die less frequently than cells with lower affinity.

The factor  $\theta_i$ , defined to be 1 when  $b_i > 1$  and 0 otherwise, is a term included as a correction to the naive continuum description that prevents mutant populations of less than one cell per animal from growing. A more formal justification for using this correction is presented in Kepler and Perelson (1995).

Lymph nodes are designed to trap antigen, which is then retained on the surface of certain cells (follicular dendritic cells) for long periods of time. Thus, as a first approximation, Kepler and Perelson assume that antigen is conserved and obeys the equation

$$C + \sum_i \sigma b_i h_i = C_0,
 \tag{3.15}$$

where the total antigen  $C_0$  is equal to the free antigen  $C$  plus the bound antigen. The factor  $\sigma$  is a scaling constant equal to the number of antibody receptors per B cell divided by the system volume.

Using this model Kepler and Perelson (1993a, 1993b) solved the optimal control problem of choosing the mutation schedule  $\mu(t)$  that maximized  $\sum b_i(T) K_i$ , at some time  $T$  corresponding to the end of the primary immune response. The optimal solution was one in which mutation was turned on only for short periods (Fig. 9, lower panel). Thus periods of mutation-free growth were punctuated by periods in which there were bursts of high mutation rates. With this strategy, advantageous mutations are acquired sequentially rather than simultaneously (Fig. 9, upper panel). The reason that this strategy is optimal is straightforward. At high mutation rates, clones (or affinity classes) lose many daughter cells to lower affinity classes. Therefore net growth within an

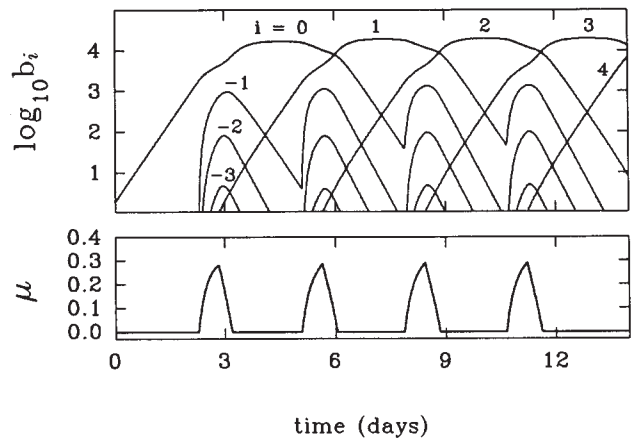


FIG. 9. The lower panel shows the optimal mutation schedule that generated the dynamics in the upper panel. There are a number of rounds of mutation, each of which produces some cells that have a one-step increase in their affinity class. After an advantageous mutant appears, mutation is turned off to maximize the growth of the mutant clone and to prevent its loss through further mutation. The upper panel shows the dynamics of the B-cell response,  $b_i$  vs  $t$ . The response begins with a single B-cell clone in affinity class  $i=0$ . Mutation, when turned on, generates cells in lower affinity classes ( $i=-1, -2, -3$ , as well as cells in higher affinity classes ( $i=1, 2, 3, 4$ ).

affinity class is greatest when  $\mu = 0$ . Because advantageous mutants are relatively rare, a large number  $N$  of mutants must be generated to assure a significant likelihood that one of them will be advantageous. For example, in Fig. 9 it was assumed that the probability of an advantageous mutation  $p_A$  is 0.01; thus  $N$  should be of the order of 100 to assure the generation of a higher-affinity mutant (in fact, it needs to be larger since in the underlying model for  $m_{ij}$  some mutations are lethal and some are silent). In the optimal solution, the population grows as quickly as possible without mutation until there are more than about  $1/p_A$  cells. Mutation is then “switched on” at a rate consistent with the rapid production of cells with a very small number of point mutations (see also Agur, Mazor, and Meilijson, 1991). After the appearance of an advantageous variant, mutation is switched off, so that the new high-affinity clone can grow as rapidly as possible and to avert the possibility that it is lost through further mutation. This cycle is then repeated until the end of the primary response.

Immunologists have discovered that somatic mutation seems to occur only in very special structures called germinal centers. It is possible that a near-optimal phasic mutation schedule arises naturally from the structure of the germinal center.

Germinal centers are found in lymphoid organs, such as spleen, lymph nodes, and tonsils, and are spatially organized into zones (Liu *et al.*, 1989). As shown in Fig. 10, cells initially enter the dark zone, where they proliferate rapidly. They then migrate to the light zone, where they stop dividing. Lymph nodes act as filters for antigen, and the cells that capture antigen, follicular den-

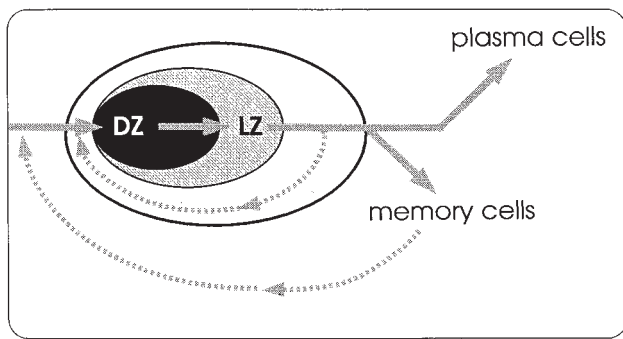


FIG. 10. Schematic illustration of a germinal center. Cells enter the dark zone DZ, a site of proliferation. They migrate to the light zone LZ, where they encounter antigen and are selected for survival based on affinity. Mutation may occur in either the dark zone or the light zone. The established pathways of cell movement are shown as solid arrows. The Kepler-Perelson model suggests that cells recycle through the germinal center using either of the pathways indicated by the broken arrows.

dritic cells, have their highest density in the light zone. Thus in the light zone, B cells can encounter antigen trapped on follicular dendritic cells and compete for binding. Cells that lose the competition die within the germinal center, whereas cells that win the competition survive. Some cells migrate out of the germinal center and differentiate into memory cells or antibody-secreting plasma cells. A phasic mutation schedule could be implemented if some cells migrated back to the dark zone and repeated the process of proliferation in the dark zone followed by antigen-driven selection in the light zone, with mutation occurring after proliferation, presumably as cells leave the dark zone or as they enter the light zone. This theory can explain the great cell-to-cell variation in the number of mutations per gene found near the end of the primary response (Berek, Berger, and Apel, 1991); some cells may have completed more cycles through the germinal center than others. Models by Oprea and Perelson (1997) and Pierre *et al.* (1997) explicitly take into account events that occur in germinal centers. Oprea and Perelson (1997) show in detail how cycling through the germinal center multiple times increases the efficiency of affinity maturation.

This consideration of the spatial structure of germinal centers points out a deficiency of essentially all existing immune system models. Current differential equation models treat the immune system as one or two (Perelson and Weisbuch, 1992a) well-stirred compartments. Models that take into consideration the spatial structure of lymphoid organs and well as the lymphocyte traffic between them still need to be developed. Cellular automata models (see Mosier and Sieburg, 1994; Seiden and Celada, 1992; Celada and Seiden, 1996), discussed in Sec. V, have included some spatial structure.

#### IV. NETWORK MODELS

Jerne (1974) hypothesized that the immune system, rather than being a set of discrete clones that respond

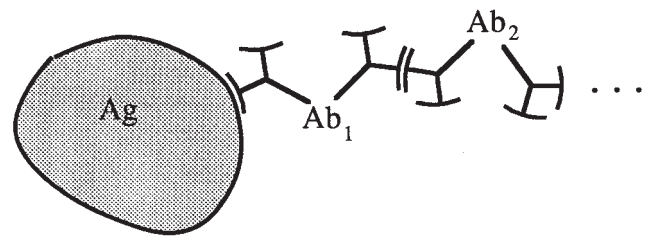


FIG. 11. Jerne idiotypic cascade. The antigen Ag is recognized by B cells, which secrete antibodies  $Ab_1$ . These antibodies are themselves recognized by “anti-idiotypic” B cells, which secrete antibodies  $Ab_2$ . Further interactions can lead to  $Ab_3$  antibodies that recognize  $Ab_2$  and so on.

only when triggered by antigen, is a regulated network of molecules and cells that recognize one another even in the absence of antigen. Because antibodies are created in part by random genetic mechanisms, they must look like novel molecules to the rest of the immune system and thus should be treated like antigens. The novel or idiosyncratic parts of an antibody are called *idiotopes*. The set of idiotopes that characterizes an antibody is called its *idiotype*. Due to the completeness of the repertoire, the immune system should recognize the idiotopes on its own antibodies and make antibodies against them. Jerne suggested that during an immune response antigen would directly elicit the production of a first set of antibodies  $Ab_1$ . These antibodies would then act as antigens and elicit the production of a second set of “anti-idiotypic” (anti-id) antibodies  $Ab_2$ , which recognize idiotopes on  $Ab_1$  antibodies (see Fig. 11). Similarly, a third set of antibodies  $Ab_3$  could be elicited that recognized  $Ab_2$  antibodies, and so forth. Anti-id antibodies have been found to occur naturally (Binion and Rodkey, 1982) and when injected into animals profoundly alter the animal’s antibody repertoire in later life (Eichmann, 1978; Takemori and Rajewsky, 1984; Vakil *et al.*, 1986; Freitas *et al.*, 1988). Furthermore, by idiotypic interactions one clone or an antibody carrying its idiotope should be able to stimulate its anti-idiotypic partner. Such stimulatory idiotypic interactions have been described (Eichmann and Rajewsky, 1975; Cosenza, 1976). Suppressive idiotypic interactions have also been found (Hardt *et al.*, 1972; Vakil *et al.*, 1986). Whether idiotypic interactions regulate or play a part in regulating the immune system, especially given other levels of control (e.g., antigen processing, interleukins, helper and suppressor T-cell circuits, etc.), is still unresolved. One of the major thrusts of theory in immunology has been to evaluate the network hypothesis and illustrate the types of phenomena that can result from network interactions. Unfortunately, theory has lagged behind experiment, and in the 1990s experimental immunologists have largely abandoned working on the network hypothesis. There are probably many reasons for this but a major factor is that the experiments that can easily be done have been done, and new experiments are no longer producing exciting and novel results or generating new ideas. Whether theory can lead the way

to the design of experiments that can give insights into the complex interactions that underlie network behavior remains to be seen.

**A. The B model**

De Boer (1988), De Boer and Hogeweg (1989b), Weisbuch, De Boer, and Perelson (1990), De Boer and Perelson (1991), Perelson and Weisbuch (1992b), and Stadler, Schuster, and Perelson (1994), all considered variations of the following model for B-cell clonal dynamics. It is one of the simplest models that can be conceived, yet it still exhibits interesting properties. We call it the B model since it deals only with B cells. In Sec. E we shall generalize the model so that it includes both B cells and antibodies.

The time evolution of the population  $x_i$  of clone  $i$  is described by the following differential equation:

$$\frac{dx_i}{dt} = m + x_i[pf(h_i) - d], \tag{4.1}$$

where  $m$  is a source term corresponding to newly generated cells coming into the system from the bone marrow,  $p$  is the rate of cell proliferation, the function  $f(h_i)$  defines the fraction of cells proliferating as a function of the “field”  $h_i$ , and  $d$  specifies the per capita rate of cell death. Because cells only proliferate when they are activated,  $f(h_i)$  is called an activation function or sometimes a proliferation function.

For each clone  $i$ , the total amount of stimulation is considered to be a linear combination of the populations of other interacting clones  $j$ . This linear combination is called the field  $h_i$  acting on clone  $x_i$ , i.e.,

$$h_i = \sum_j J_{ij}x_j, \tag{4.2}$$

where  $J_{ij}$  specifies the interaction strength (or affinity) between clones  $x_i$  and  $x_j$ . The choice of a  $J$  matrix defines the topology of the network. For simplicity,  $J_{ij}$  values are typically chosen as 0 and 1, although some authors (e.g., De Boer and Perelson, 1991; Detours, Sulzer, and Perelson, 1996) also use intermediate values to model circumstances in which one wants to be truer to the biology in which interactions need not be all-or-none.

The most crucial feature of this model is the shape of the activation function  $f(h_i)$ , which is taken to be a log-bell-shaped dose-response function

$$f(h_i) = \frac{h_i}{\theta_1 + h_i} \left( 1 - \frac{h_i}{\theta_2 + h_i} \right) = \frac{h_i}{\theta_1 + h_i} \frac{\theta_2}{\theta_2 + h_i}, \tag{4.3}$$

with parameters  $\theta_1$  and  $\theta_2$  chosen such that  $\theta_2 \gg \theta_1$  (see Fig. 12).

The function  $f(h_i)$  is composed of two factors. The first factor increases from 0 to 1, reaching its half-maximal value at  $\theta_1$ , the second factor decreases from 1 to 0, reaching its half-maximal value at  $\theta_2$ . For  $\theta_2 \gg \theta_1$ , the maximum,  $\theta_2 / (\sqrt{\theta_1} + \sqrt{\theta_2})^2$ , is approximately one. This maximum is attained at  $h = \sqrt{\theta_1 \theta_2}$ . Because

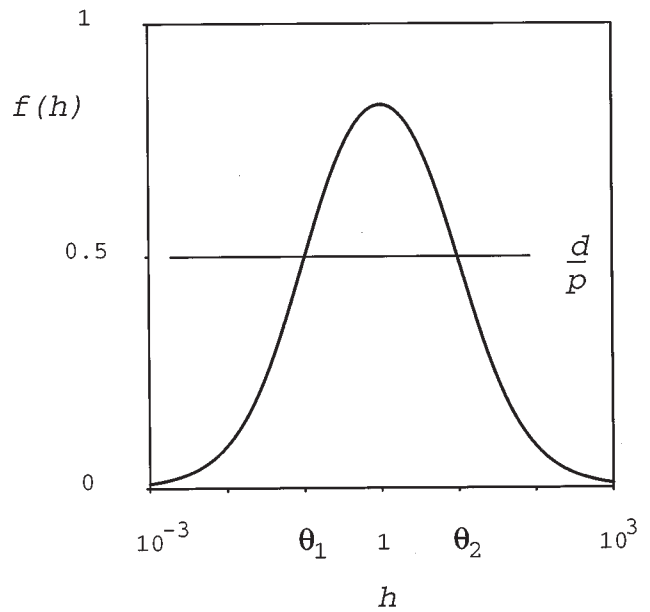


FIG. 12. The log-bell-shaped activation function  $f(h)$  defined by Eq. (4.3). As discussed in the text, when  $m$  is small, intersections of the line  $y = d/p$  with the bell-shaped curve define the activating and suppressive field values,  $L$  and  $H$ , respectively. For the parameters used here,  $p = 1$  and  $d = 0.5$ , these intersections occur near the field values  $\theta_1$  and  $\theta_2$ .

$0 \leq f(h) < 1$ , we derive from Eq. (4.1) that the B cells can maximally grow at a rate  $p - d$ . Thus in order to allow for net clonal expansion  $p$  must be greater than  $d$ . Maximally stimulated cells divide about once every 16 h, so  $p = 1 \text{ day}^{-1}$  is a typical rate of proliferation. Cells live a few days, so that  $d = 0.5 \text{ day}^{-1}$  is a typical death rate. Although different experiments may lead to slightly different estimates of  $p$  and  $d$ , we shall assume throughout that  $p > d$ , so that net clonal expansion can occur when cells are activated.

Below the maximum of  $f(h_i)$ , increasing  $h_i$  increases  $f(h_i)$ ; we call this the *stimulatory regime*. Above the maximum, increasing  $h_i$  decreases  $f(h_i)$ ; we call this the *suppressive regime*. Plotted as a function of  $\log h_i$ , the graph of  $f(h_i)$  is a bell-shaped curve. As discussed in Sec. III.A, an important argument for the use of a log-bell-shaped function is that receptor cross-linking (Fig. 6) is involved in B-cell activation. The log-bell-shaped function is also observed experimentally in the response of the immune system as a function of the dose of antigen (Celada, 1971, 1992; Dintzis, Vogelstein, and Dintzis, 1982; Vogelstein, Dintzis, and Dintzis, 1982). The function  $f(h)$ , given by Eq. (4.3), should be considered as a phenomenological description of B-cell activation, motivated by the chemistry of cross-linking and experimental observations. The exact functional form that is being used was chosen for its algebraic simplicity and other similarly shaped functions could also be used (cf. De Boer *et al.*, 1996).

**B. The two-clone problem**

Before analyzing large networks, we discuss the simple case of two interacting populations. One popula-

tion,  $x_1$ , reacts with the antigen, while the other population,  $x_2$ , reacts with  $x_1$ . In idiotypic network theory, the population  $x_1$  is called the idio type and  $x_2$  the anti-idio type. The interaction constants are  $J_{12}=J_{21}=1$  and  $J_{11}=J_{22}=0$ . Thus the fields are  $h_1=x_2$  and  $h_2=x_1$ . The system of equations (4.1) now becomes

$$\frac{dx_1}{dt} = m + x_1[pf(x_2) - d], \quad (4.4a)$$

$$\frac{dx_2}{dt} = m + x_2[pf(x_1) - d]. \quad (4.4b)$$

In the presence of antigen at concentration  $A$ , the field  $h_1$  experienced by  $x_1$  is given by  $h_1=x_2+J_{1,A}A$ . Antigen is eliminated by reacting with antibody and hence as a simple model one might assume

$$\frac{dA}{dt} = -kAx_1,$$

where  $k$  is a rate constant. Here we are interested in the long-time behavior of the system after antigen presumably has been eliminated. After an introduction of antigen, first  $x_1$  and then  $x_2$  increase, and by the time the antigen is eliminated they reach some value that we take as the initial conditions for the solution of system (4.4).

We are interested in the attractors of system (4.4). For most parameter values of immunological interest, the two isoclines,  $\dot{x}_1=0$  and  $\dot{x}_2=0$ , intersect in five points, of which only three are stable. We call these stable configurations virgin, immune, and tolerant.

The *virgin* configuration is obtained when the activation function is very small, i.e.,  $pf(h) \ll 1$ . It has coordinates

$$x_1=x_2 \approx m/d \equiv V. \quad (4.5)$$

In the limit of small  $m$ , the other possible steady solutions correspond to intersections of the activation function with the decay term (see Fig. 12). In this limit, steady-state solutions occur when  $f(h_i)=d/p$ . Since  $p > d$ , there are two intersections of the line  $y=d/p$  with the curve  $y=f(h)$ , one on each side of the maximum of the bell-shaped curve. (If the source  $m$  is small but non-zero, then the steady states will be somewhat below the two intersection points.) We call the field values at the intersection points  $L$  and  $H$ . In Fig. 12 because of our choice  $d/p=0.5$  these intersection points occur at approximately  $\theta_1$  and  $\theta_2$ . The steady-state field  $L$ , which is below the maximum of the log-bell-shaped activation curve, is called *stimulatory* since increasing the field above  $L$  increases the proliferation rate. The field  $H$ , which is above the maximum, is called *suppressive*, since increasing the field above  $H$  reduces proliferation.

One stable steady state, *the immune state*, occurs when  $x_1$  experiences the low stimulatory field  $L$ , and  $x_2$  the high suppressive field  $H$  (Weisbuch, De Boer, and Perelson, 1990). In this state the idiotypic B cells  $x_1$  have a large population and generate a large, and hence suppressive, field on the anti-idiotypic  $x_2$ . The anti-idiotypic B cells thus have a small population and generate a small, and hence excitatory, field on the idio type.

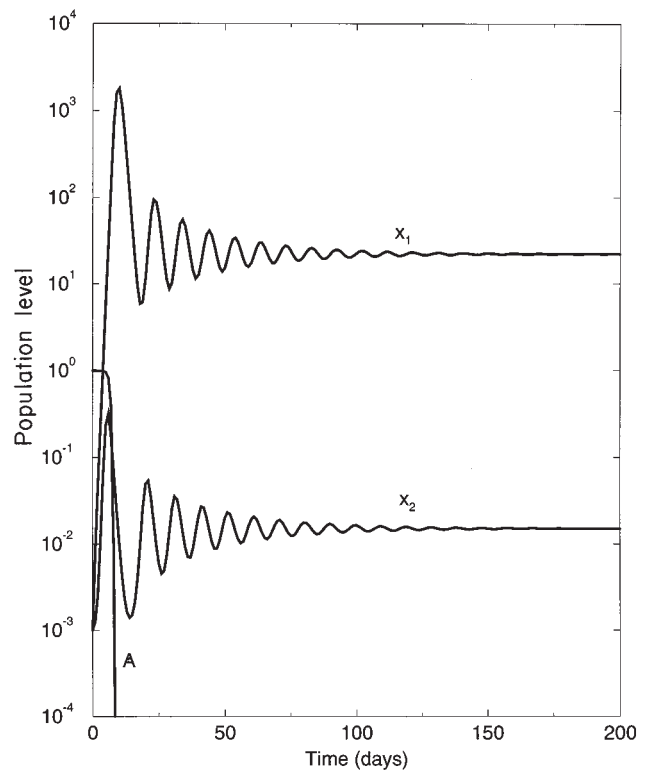


FIG. 13. Dynamics of a response induced by injecting antigen  $A$  that results in the system's approaching the immune attractor. The clone population sizes are plotted vs time in days. In the immune configuration the largest population is localized at the first level.  $x_1$  is high ( $H$ ) and is sustained by interacting with  $x_2$ , which is at a lower level ( $L$ ).

We can compute, via a simple approximation, the population sizes  $x_1$  and  $x_2$  in the immune state. For small and large fields  $f(h)$  can be approximated by  $h/\theta_1+h$  and  $\theta_2/\theta_2+h$ , respectively. By assuming  $m/d$  is small when compared with  $\theta_1$ , one obtains for the immune steady state

$$x_1 = H = \frac{(p-d)\theta_2}{d}, \quad x_2 = L = \frac{d\theta_1}{p-d}. \quad (4.6)$$

Since  $(p-d)/d$  is of order 1, for  $\theta_2 \gg \theta_1$ ,  $x_1 \gg x_2$ .

This attractor is called immune because if antigen  $A$  is injected into the system its elimination is much faster than when the system is in the virgin state. This is due to the fact that the clone that recognizes antigen,  $x_1$ , is present at a much higher population than when the system is in the virgin state. An interesting feature is that the  $x_1$  population remains large even in the absence of the antigen. Thus, if this steady state was obtained by perturbation of the virgin state by antigen, as shown in Fig. 13, a memory of the original response is kept by the  $x_1$ - $x_2$  couple, which sustain each other. Linear-stability analysis shows that the immune state is stable, but because the eigenvalues have an imaginary part, attenuated oscillations towards the attractor are expected and indeed observed in numerical solutions to Eqs. (4.4) (Fig. 13).

The *tolerant* attractor is obtained by exchanging  $x_1$

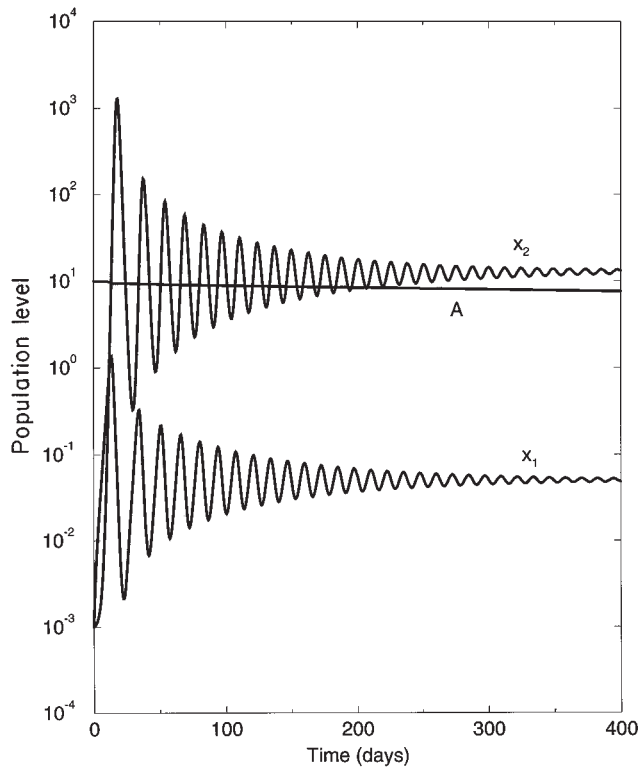


FIG. 14. Dynamics of a response induced by antigen  $A$  that results in the system's approaching the tolerant attractor. At the attractor,  $x_2$  is high ( $H$ ) and is sustained by  $x_1$ , which is at  $L$ .

and  $x_2$ . Thus in this configuration  $x_1$  has a low population  $L$  and  $x_2$  has a high population  $H$ . The attainment of the tolerance attractor is shown in Fig. 14. This configuration is interpreted as tolerance because, if antigen is presented, clone  $x_1$  is not able to react with a strong intensity, since it is experiencing a high (suppressive) field due to clone  $x_2$ , and antigen will increase its field and make it even more suppressive.

There are also two symmetric steady state solutions with both  $x_1$  and  $x_2$  having suppressive (high) or stimulatory (low) fields. Both of these symmetric states are unstable (Fig. 15).

### C. Network topology

In the previous section we examined interactions between two B-cell clones. In models with more than two clones one needs to specify the interconnections between the clones, i.e., the topology of the network that is formed and the strengths of the connections.

Due to the great diversity of the immune system and the fact that on average only one cell in  $10^5$  responds to a particular epitope, it has been extremely difficult to examine experimentally interactions between particular clones, as would be required to gain a detailed understanding of idiotypic networks. Clones in immune networks can communicate with each other over long distances by broadcasting signals in the form of anti-idiotypic antibodies. These antibodies can react with

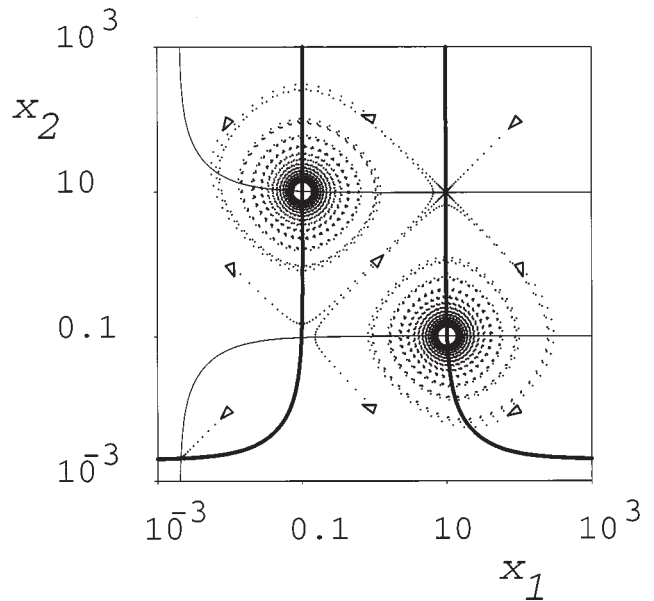


FIG. 15. Phase portrait of the dynamics of two interacting clones. Of the five singular points in the plane, only the virgin state  $(x_1, x_2) = (L, L)$ , the tolerant state  $(x_1, x_2) = (H, L)$ , and the immune state  $(x_1, x_2) = (L, H)$  are attractors. The two symmetric states  $(L, L)$  and  $(H, H)$  are unstable.

complementary receptors on the surface of B cells and T cells throughout the body. In neural networks, one can trace *in vivo* the connections between neurons, for example by using horseradish peroxidase staining, and thus learn the topology of a network. In the immune system there is no equivalent technique available, and thus one is forced to rely on models to gain even a rudimentary understanding of the degree of interaction among cells.

One of the major stumbling blocks in formulating a faithful mathematical model of an idiotypic network is determining a realistic topology for the network. In a system with a repertoire of, say,  $10^7$  elements how can one ever determine all of the possible interactions? A number of different theoretical approaches have been taken. In the first, one simply assumes that the topology and connection strengths are given. By studying a number of different cases one then hopes to gain an understanding of how the network behavior depends on the connections. Some examples of this approach are Hoffmann's plus-minus network theory (Hoffmann, 1975, 1979, 1980; Gunther and Hoffmann, 1982), which dealt with only two specificities, an antigen-specific population and its anti-idiotypic partner. Richter (1975, 1978) dealt with a linear network, which is a linear sequence of clones and their anticlones  $(Ab_1, Ab_2, \dots, Ab_\ell)$ , in which antibodies and/or lymphocytes (a distinction between the two was not made) at idiotypic level  $i$  interact with populations at levels  $i-1$  and  $i+1$ , and antigen is defined to be level 0:

$$\text{Antigen} \rightarrow Ab_1 \rightarrow Ab_2 \rightarrow \dots \rightarrow Ab_\ell.$$

Although  $\ell$ , the number of levels in the network,

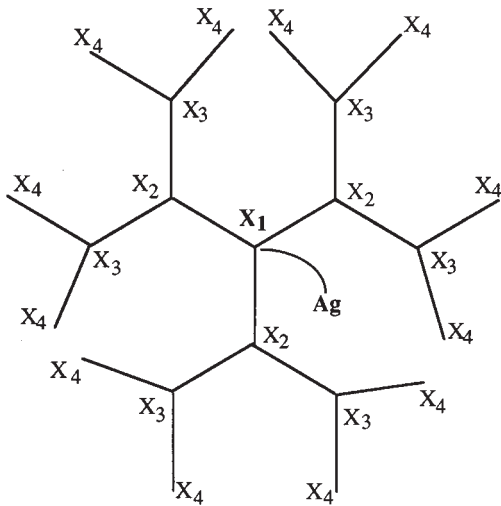


FIG. 16. A Cayley tree. This is a network without loops, in which each clone interacts with a fixed number  $z$  of other clones. A Cayley tree with  $z = 3$  is illustrated. Here only clone  $x_1$  reacts with the antigen Ag.

could be very high, in early simulation studies  $\ell$  was generally taken to be rather small, i.e.,  $\ell < 10$ . Hiernaux (1977) noticed that the dynamical behavior of Richter's model depended upon whether the network had an even or odd number of levels. Thus even in the case of a linear network, topology was important. To avoid the artificial choice of even or odd networks, Hiernaux (1977) analyzed a model in which the linear chain was converted into a simple cyclic network by identifying  $Ab_1$  with  $Ab_\ell$ .

More recent models have analyzed much larger networks and have considered more complex and possibly more realistic topologies. Weisbuch, De Boer, and Perelson (1990), Weisbuch (1990a), Neumann and Weisbuch (1992a), and Anderson, Neumann, and Perelson (1993) have all considered models with a Cayley tree topology (Fig. 16), work that is reviewed in detail in Sec. IV.D. Neumann and Weisbuch (1992b) examined other discrete topologies that arise by adding connections to the Cayley tree, which form even or odd loops (see Sec. IV.D.4).

Another approach to specifying the interactions between clones is to set up an "affinity" or  $J_{ij}$  matrix (De Boer, 1988). The nonzero elements in the matrix represent interactions and the magnitude of the elements represents the strength of the interaction. The affinity matrix is the equivalent to a matrix of synaptic weights in

neural network models. If one takes the point of view that the network is so large and complex that it is impossible to determine the relationships between the elements, then one can assign the elements at random with a specified fraction of nonzero elements (see De Boer, 1988; Hoffmann *et al.*, 1988; Parisi, 1990). Alternatively, specific terms can be placed in the matrix to represent networks of a given topology (Stewart and Varela, 1989). Some data are available from experiments by Zöller and Achnich (1991), Kearney, Vakil, and Nicholson (1987), and Holmberg *et al.* (1984) on the structure of networks in neonatal mice, which can guide the construction of realistic forms for the affinity matrix.

A different approach, pioneered by Perelson, assumes that the interactions in a network are determined by the specific chemical interactions between the various cells and molecules in the immune system. The basis of these interactions is what we previously called generalized shape (see Sec. II). Thus if one knew the shape of each molecule one could predict which molecules would react and the affinity of their interaction. Even though we do not know the actual shapes of molecules we can develop simple mathematical representations of antibodies that allow us to compute the degree of complementarity between molecules and even assign an affinity to their interactions. In one approach, first introduced by Farmer, Packard, and Perelson (1986), one represents the antibody binding site by a binary string of length  $n$ . An antigen containing a single epitope is represented by a single binary string, whereas antigens with multiple epitopes are represented by multiple strings (Seiden and Celada, 1992). With this representation shape space is a hypercube of dimension  $n$ . If one chooses  $n=32$ , then one can represent  $2^{32} \approx 4 \times 10^9$  different epitopes in this shape space. This is a diversity comparable to that expressed in the mammalian immune system.

Complementarity between molecules represented as strings can be defined by any of a number of rules, and the degree of complementarity can be quantified and used as a measure of the affinity of the antigen-antibody interaction. For example, two  $n$ -bit strings are complementary if at least some critical number of their bits are complementary; the number of complementary bits exceeding the threshold can be taken proportional to the affinity of the interaction (Fig. 17). Other rules can also be used for determining complementarity. For example, since the strings represent molecules they need not be aligned when they interact. Thus one can also use a matching rule in which the sequences are shifted and then checked for complementarity. Furthermore, molecules generally do not interact over their entire length,

```

Antigen: 1100100101101001101010000100001111010011001010101001010100110101
Antibody: 001101010100101001011100010101110101101110001100110010010010111
XOR:      11111 1 111111 1 1 1 1 1 1 1 11 1 111 1 1

```

FIG. 17. Generalized shapes of molecules, represented by strings. The degree of complementarity between two binary strings can be computed using the exclusive or (XOR) function. The number of positions at which a 0 matches a 1 can be used as a measure of the interaction strength between the molecules.

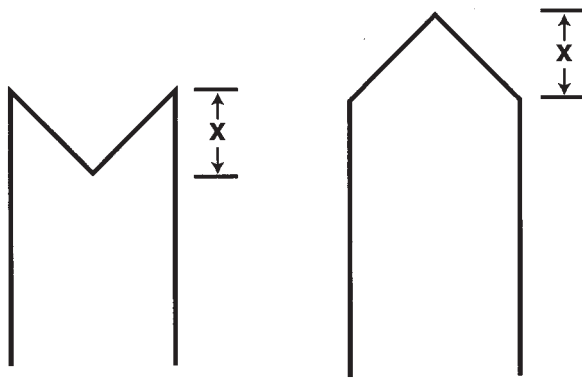


FIG. 18. Antibody shapes described by a real number, for example, the height ( $+x$ ) or depth of the antibody binding site ( $-x$ ), in continuous shape space.

but rather in localized areas. To model this one can use a complementarity rule in which the number of adjacent complementary bits is important. This type of approach was used in Sec. II.C to predict the size of epitopes and will be used again in Sec. IV.G in an idiotypic network model. Papers that use bit-string models include those of Farmer, Packard, and Perelson (1986), Perelson (1989a), De Boer and Perelson (1991), Celada and Seiden (1992, 1996), Percus, Percus, and Perelson (1992, 1993), Seiden and Celada (1992), Forrest *et al.* (1993), Rose and Perelson (1994), Detours, Sulzer, and Perelson (1996), and Perelson, Hightower, and Forrest (1996).

Another approach, which emphasizes the effects of cross-reactivity among clones, uses the continuous shape space of Segel and Perelson (1988). In this approach, which we discuss in detail in Sec. IV.F, one describes the shape of a molecule by one or more continuous “shape” variables and constructs a system of partial differential equations for the dynamics. For example, in Segel and Perelson (1988) it was assumed that a single (positive or negative) number  $x$  characterizes the generalized shape of antibody (or antigen). This variable  $x$  could be viewed as the height or depth of the antibody combining site (Fig. 18). Thus an antibody with  $x = -2$  has a binding site that is deeper than an antibody with  $x = -1$  and can better bind an antigen with a bump of height  $x = +2$ . Recent structural determinations of idiotype–anti-idiotype complexes indicate that a bump on one antibody fits into a groove of the other as envisioned in this simple model. A potential difficulty of a one-dimensional shape space is that an antibody has only one natural complement and the complement of the complement is the original antibody. To generate richer idiotypic structures requires higher-dimensional models and more complex matching rules. Recent work by Stewart and Varela (1991), De Boer, Hogeweg, and Perelson (1992), and De Boer, Segel, and Perelson (1992) considers two-dimensional shape spaces. Weinand (1991) considers a three-dimensional shape space. Weisbuch and Oprea (1994) and Detours, Sulzer, and Perelson (1996) consider high-dimensional “digit-string” spaces.

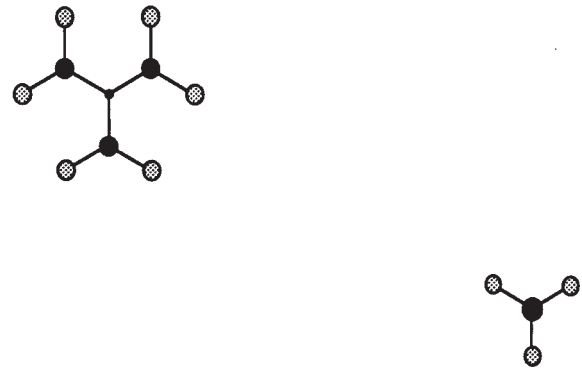


FIG. 19. Localized patches of clones perturbed by different antigenic presentations. Two immune and one tolerant attractor are represented. The immune attractor patches involve one idiotypic clone (dark dot) and three anti-idiotypic clones, while the tolerance attractor patch involves one more level.

We consider some explicit examples of these various approaches in the sections that follow.

#### D. Localized attractors

As a memory device, the immune system needs to obey certain constraints: it should be sensitive enough to change attractor under the influence of antigen. It should not be too sensitive and overreact when antigen is present in very low doses. The immune system should also discriminate between self antigens and foreign antigens. Finally, it should be robust—memories of previously presented antigens should not be lost when a new antigen is presented. Thus, in some sense, the system should be able to generate independent responses to many different antigens. This independence property is achieved when attractors are localized, i.e., when the perturbation induced by an encounter with antigen remains localized among the clones that are close to those that actually recognize the antigen (see Fig. 19). Below, we systematically search for localized attractors.

##### 1. Cayley tree

The topology of the immune network is defined by the  $J_{ij}$ 's of Eq. (4.2). Unfortunately our knowledge of the actual  $J_{ij}$ 's is very restricted. Some educated guesses can be made about the structure of the network from experiments or simplified considerations about the basis of immune recognition. One might also be tempted to use a well-defined network structure: a regular lattice, a complete graph with random connection strengths, a Cayley tree, etc. The Cayley tree is in fact an intermediate ap-

proximation between the two-clone model and more realistic networks. Its relevance comes from one of its features, localized attractors, which as we show below can be interpreted in terms of phenomena seen in experimental immunology. We discuss Cayley tree networks in this section, and later discuss changes in dynamic behavior that might be expected when more “realistic” architectures are used.

Let us consider a Cayley tree architecture (Weisbuch, De Boer, and Perelson 1990) with  $z$  connections per site (see Fig. 16), and  $J_{ij}$ 's which can only be 0 (no interaction) or 1 (maximum interaction). The root of the tree is selected by the presented antigen. For simplicity, it is assumed that a single antigen is presented to the system and only one clone, the root, reacts with that antigen. According to their distance to the root, the clones are numbered 1 (and called  $Ab_1$  for the antigen specific clones), 2 (for the  $Ab_2$  anti-idiotypic clones, specific for some  $Ab_1$ ), 3, ...,  $i$ . The different fields for clones 1, 2, 3, ...,  $i$  in the absence of antigen are given by

$$\begin{aligned} h_1 &= zx_2 \\ h_2 &= x_1 + (z-1)x_3, \\ h_3 &= x_2 + (z-1)x_4, \\ &\dots\dots\dots \\ h_i &= x_{i-1} + (z-1)x_{i+1}. \end{aligned} \quad (4.7)$$

Our problem is to classify the different attractors of the network and to interpret the transitions from one attractor to another under the influence of antigen perturbation. Let us start with the simplest virgin configuration, corresponding to the hypothetical case in which no antigen has yet been encountered and all populations are at level  $m/d$ , i.e., all proliferation functions are close to 0. After presentation of the first antigen, memorization is obtained if some populations of the network reach stable populations different from  $m/d$ . In the case of a localized response, there will be a patch close to the antigen-specific clone in which cells are excited out of the virgin state. Each antigen presented to the network will result in a patch of clones that are modified by the presentation. As long as the patches corresponding to different clones do not overlap, the various antigens presented to the network can all be remembered. Once the idea of localized noninteracting attractors is accepted, everything is simplified: instead of solving  $10^8$  equations, we have only to solve a small set of equations for those neighboring clones with large populations, supposing that clones that do not belong to the set with large populations are nearly virgin, i.e., have populations of order  $m/d$ . A practical approach to studying localized attractors is to combine computer simulations and analytic checks of the attractors by solving the field equations (see below).

#### a. Immunity

Let us examine the case of antigen presented to clone  $Ab_1$ , which results in excitation of clones  $Ab_2$ , with

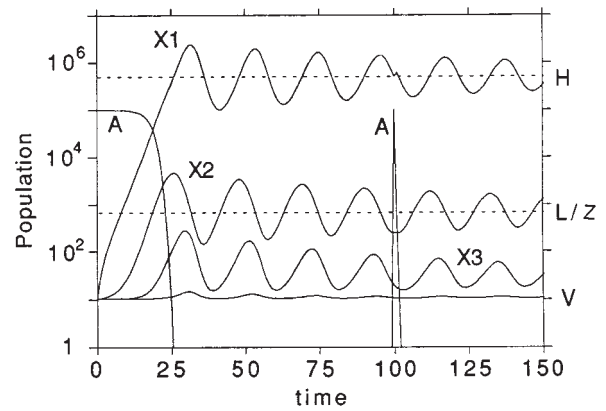


FIG. 20. Dynamics of an immune response generated by a network with a Cayley tree topology when antigen  $A$ , recognized by a clone at level 1,  $x_1$ , is injected into a system in the virgin state. The response causes the system to approach the immune attractor. In the immune configuration the largest population is localized at the first level.  $x_1$  is high ( $H$ ) and is sustained by interacting with  $x_2$ , which is at an intermediate population level ( $L/z$ ). In a network with a Cayley tree topology, where  $z$  is the number of clones connected to any clone, one sees that clones  $x_3$  as well as the rest of the clones in the network are virgin ( $V$ ) (or almost virgin) after the system settles into this attractor. When antigen is presented again, it is eliminated faster than the first time. Simulation parameters were as follows:  $k=10^{-6}$ ,  $A_0=5000$ ,  $d=0.5$ ,  $p=1$ ,  $z=3$ ,  $m=10^{-3}$ ,  $\theta_1=2000$ , and  $\theta_2=10^5$ . From Neumann and Weisbuch, 1992a, reproduced with permission.

clones  $Ab_3$  remaining close to their virgin level (see Fig. 20). In analogy with the two-clone problem, we expect that  $Ab_1$  will experience a low field,  $L$ , while  $Ab_2$  will experience a large suppressive field,  $H$ . From the field equations we can compute the populations  $x_i$ . Recall, from Eqs. (4.7) and (4.6),

$$h_1 = zx_2 = L = \frac{d\theta_1}{p'}, \quad (4.8)$$

$$h_2 = x_1 + (z-1)\frac{m}{d} = H = \frac{p'\theta_2}{d}, \quad (4.9)$$

where  $p' = p - d$ . Of course, the solution remains localized only if the field  $h_3$  on  $x_3$  is nonexcitatory, i.e., is much less than  $L$ , otherwise  $x_3$  would also proliferate. Thus we require

$$h_3 = \frac{L}{z} + \frac{(z-1)m}{d} < L. \quad (4.10)$$

This is possible only if  $z$  is larger than 1 (multiple connectivity is essential to localization) and if the following inequality, derived by using the value of  $L$  in Eq. (4.8), is fulfilled:

$$\frac{p'zm}{d^2} < \theta_1. \quad (4.11)$$

This is equivalent to the statement that the field due to  $z$  virgin clones,  $zm/d$ , should be small compared to the proliferation threshold  $\theta_1$ , since  $p'/d$  is approximately one.

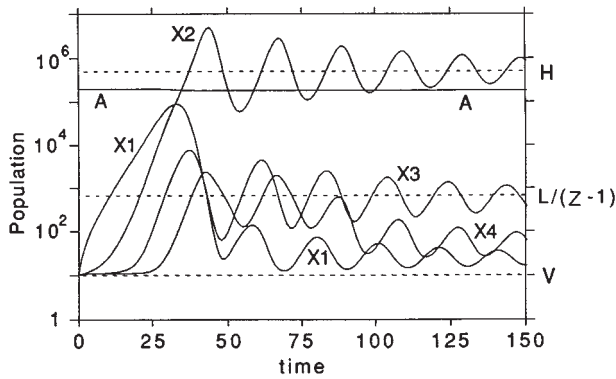


FIG. 21. Dynamics of a response generated by a network with a Cayley tree topology that results in the system's approaching the tolerant attractor. Antigen  $A$  at a high concentration is injected into a system in the virgin state. At the attractor,  $x_2$  is high ( $H$ ) and is sustained by  $x_1$ , which is an intermediate population  $[L/(z-1)]$  of  $x_3$ . Here  $x_1$  is oversuppressed by the  $x_2$  and is not able to remove the antigen. Simulation parameters were the same as for Fig. 20, in which the immune attractor is attained except that the rate of antigen elimination is tenfold lower,  $k=10^{-7}$ , and the initial antigen concentration is tenfold higher,  $A_0=5\times 10^4$ . From Neumann and Weisbuch, 1992a, reproduced with permission.

To decide which attractor is reached when antigen is presented, one needs to solve Eqs. (4.1), to which a supplementary equation describing the dynamics of antigen  $A$  is added,

$$\frac{dA}{dt} = -kAx_1. \tag{4.12}$$

In the presence of antigen, the field acting on  $Ab_1$  due to the antigen is added to the field due to  $Ab_2$ . Thus

$$h_1 = zx_2 + J_A A, \tag{4.13}$$

where  $J_A$  is the antigen interaction constant. An immune attractor is usually reached for an intermediate initial antigen concentration  $A_0$  and intermediate decay constants  $k$  (for further details see Sec. IV.D.3 on the window automaton). If the initial antigen concentration is too low or if the antigen decays too fast (large  $k$ ), the immune attractor is not attained and the system returns to the virgin configuration, i.e.,  $Ab_1$  and  $Ab_2$  populations increase only transiently and ultimately return to the virgin  $m/d$  level. Thus no memory of an antigen encounter is retained.

*b. Tolerance*

Another localized attractor corresponds to tolerance, a condition in which further response to the antigen is prevented (see Fig. 21). A strong suppressive field acts on  $Ab_1$  due to  $Ab_2$ 's, the  $Ab_2$ 's proliferate due to a low field provided by  $Ab_3$ 's, but  $Ab_4$ 's remain nearly virgin. The field equations once more allow one to compute the populations:

$$h_2 = x_1 + (z-1)x_3 = L = \frac{d\theta_1}{p'}, \tag{4.14}$$

which can be solved for  $x_3$ , if one neglects  $x_1$  which is small. Further,

$$h_3 = x_2 + \frac{(z-1)m}{d} = H = \frac{p'\theta_2}{d}. \tag{4.15}$$

Thus for small  $m/d$

$$h_1 = zx_2 \approx zH. \tag{4.16}$$

Substituting  $h_1$  in Eq. (4.1) gives a very small value for  $f(h_1)$ , which shows that  $x_1$  is of the order of  $m/d$ . The  $Ab_1$  population, experiencing a field several times higher than  $H$ , is said to be *oversuppressed*. One can also show that  $h_4$  is small, i.e.,  $h_4 \approx L/(z-1)$ , and that  $x_4$  is nearly virgin.

As in the case of the immune attractor, one can study the conditions under which the tolerance attractor is reached when antigen is presented. One finds that tolerance is obtained for large initial antigen concentrations, slow antigen decay rates (small  $k$ ), and large connectivity  $z$  (see Sec. IV.D.3 and Neumann and Weisbuch, 1992a).

*c. Extended localization*

In another type of steady-state configuration, which we call *extended localization*, the pair of neighboring  $H$  and  $L$  fields propagate further than levels 2 and 3. Equations similar to (4.14)–(4.16) for higher levels can then be used to find the corresponding populations. Extended localization is usually obtained in a number of narrow-parameter regimes that are in the vicinity of boundaries between other dynamic behaviors. See the phase-transition diagram in Fig. 22. Consider the case of a response localized at levels 3 and 4. Clone  $x_1$  is at the virgin level, clones  $x_2$  are oversuppressed, clones  $x_3$  are excited to a high population sustained by clones  $x_4$ . Clone  $x_1$  is then able to proliferate and it gives a transient response if the antigen is again presented. But this response cannot be transmitted to any neighboring clone since clones  $x_2$  are oversuppressed. After antigen elimination, clone  $x_1$  returns to the nearly virgin level it started from. The transient response resembles a primary response, since the  $x_1$  population starts from a virgin level—as opposed to a secondary response, which is obtained when the  $x_1$  population starts from a higher level.

*d. Percolation*

Some parameter values, such as a low excitation threshold  $\theta_1$ , allow an excitation to propagate from the initial node across all of the tree. In such a case percolation is observed, which corresponds to a nonlocalized dynamic response (Fig. 23). This may not be a healthy condition, and in some autoimmune diseases, such as systemic lupus erythematosus, a large number of different autoantibodies are detected as if there were perco-

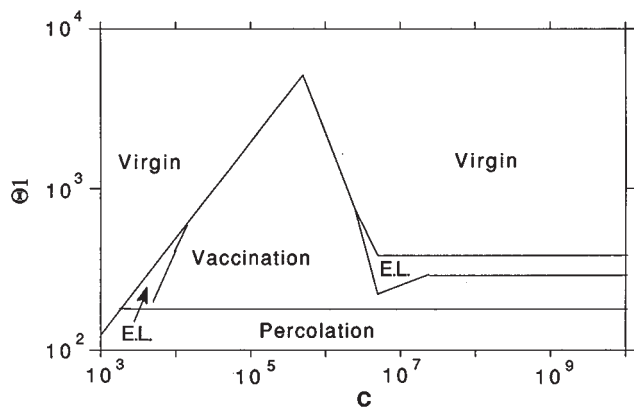


FIG. 22. Phase diagram derived from the window-automaton model [defined by Eq. (4.17)].  $\theta_1$  is the excitation threshold and  $C$  is related to the antigen elimination time [see Eq. (4.22)]. The transition from virginity to excitation is different for the three regimes of  $C$ . The transition from percolation to vaccination is independent of  $C$ . Two extended-localization regimes, denoted E.L., are observed. This diagram corresponds to a relatively low initial antigen concentration,  $A_0 = \sqrt{\theta_1 \theta_2}$ . (A large initial antigen concentration, which can result in tolerance, would further complicate this phase diagram.) From Neumann and Weisbuch, 1992a, reproduced with permission.

lation of an immune response within an idiotypic network (Shoenfeld and Moses, 1990).

2. Number of attractors

The Cayley tree model predicts localized attractors that can be interpreted in terms of immunity or tolerance. Because these attractors are localized they are somehow independent: starting from a fully virgin configuration, one can imagine successive antigen encounters that leave footprints on the network by creating

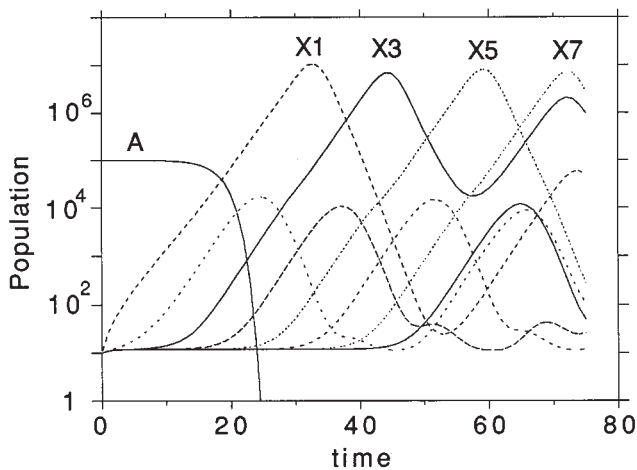


FIG. 23. Dynamics of a network undergoing percolation. The parameters are  $k=10^{-5}$ ,  $A_0=10^5$ ,  $d=1.0$ ,  $p=1.5$ ,  $z=3$ ,  $m=10$ ,  $\theta_1=300$ , and  $\theta_2=10^6$ . From Neumann and Weisbuch, 1992a, reproduced with permission.

nonvirgin patches, each of these involving a set of  $p$  perturbed neighboring clones. An immune patch contains  $1+z$  clones, a tolerant patch  $1+z^2$  (see Fig. 19). Independence of localized attractors implies a maximum number of attractor configurations that scales exponentially with  $N$ , the total number of clones. The following simplified argument gives a lower bound. Divide the network into  $N/(1+z^2)$  patches. Each patch can be in three possible configurations: virgin, immune, or tolerant. This gives a number of attractors that scales as  $3N/(1+z^2)$ . Few of these attractors are of interest. The relevant question is the following: A living system must face frequent encounters with antigen during its life. Self antigen should elicit a tolerant response, whereas dangerous external antigens should elicit immune responses and subsequent immunity. The nature of the localized response on each individual site of the network is then determined by the fact that the presented antigen should be tolerated or fought against. In this context, we can ask, "How many different antigens can be presented so that no overlap among different patches occurs?"

In the case of random antigen presentation, simple reasoning (Weisbuch, 1990b; Weisbuch and Oprea, 1994) is sufficient to derive the scaling law relating  $m$ , the memory capacity (i.e., the maximum number of remembered antigens), to  $N$ , the total number of clones. Let  $n_s$  be the number of suppressed clones involved in a patch.

We first compute the probability  $\pi_i$  that a clone is able to proliferate on encounter with antigen given that  $i-1$  different antigens have already been presented and resulted in the creation of  $i-1$  non-overlapping patches of  $n_s$  clones each:

$$\pi_i = 1 - \left( \frac{(i-1)n_s}{N} \right),$$

where the term in parentheses corresponds to the probability that the clone relevant for the  $i$ th antigen is not able to proliferate because it is involved in another attractor and already suppressed. The probability  $P_m$  that  $m$  successive antigens are recognized by nonsuppressed clones, and generate responses is then the product of the  $\pi_i$  probabilities for  $i$  running from 1 to  $m$ , which can be expressed as

$$P_m = \prod_{i=1}^{m-1} \left[ 1 - \left( \frac{in_s}{N} \right) \right].$$

Hence

$$\begin{aligned} \log P_m &= \sum_{i=1}^{m-1} \log \left[ 1 - \left( \frac{in_s}{N} \right) \right] \approx \sum_{i=1}^{m-1} \left[ - \left( \frac{in_s}{N} \right) \right] \\ &= - \frac{n_s m(m-1)}{2N}. \end{aligned}$$

For  $m \gg 1$ ,

$$P_m \approx \exp \left[ - \frac{m^2}{2} \left( \frac{n_s}{N} \right) \right].$$

$P_m$  is close to 1 for small  $m$  and decreases exponentially to 0 when  $m$  is larger than a transition value corresponding to the argument of the exponential being 1. The transition for  $m$  is given by

$$m \approx \sqrt{\frac{2N}{n_s}},$$

and this provides an estimate for the mean memory capacity of the network. Since  $P_m$  is Gaussian, the transition width is also  $\sqrt{2N/n_s}$ , which implies a rather extended probability distribution.

The above scaling law applies to any network topology that accommodates local attractors. The only assumption is the random character of the network with respect to antigens, i.e., the network is not organized to respond to the set of presented antigens. On the other hand, it can be argued that the clones expressed by mammals have been selected by evolution according to the environment of the immune system, e.g., to be tolerant to self molecules and responsive to frequently encountered parasites and pathogens. If the system were optimized to the antigens in its environment, the network could be filled compactly with nonoverlapping patches. The number of antigens (patches) would then scale linearly, i.e.,

$$m \propto \frac{N}{n_s}.$$

A rough estimate of the number of different pathogens encountered in a lifetime is of the order of  $10^3$ . The same figure also holds for the number of self peptides that need to be tolerated after clonal deletion has occurred in the thymus (von Boehmer, 1991). If we take  $N$ , the number of clones in the network, to be of order  $10^7$ , and  $n_s$ , the number of suppressed clones per patch, of order 10, then the square root scaling law predicts a memory capacity of  $10^3$ , while the maximum capacity is of order  $10^6$ . Since one might expect the network to be partially random and partially optimized, its most likely capacity is enough to handle the expected number of self and foreign antigens. A comparison of the results of Weisbuch and Oprea (1994) with the scaling laws obtained for Hopfield's version of neural networks (Hertz, Krogh, and Palmer, 1991) is of interest. In both cases, exponential scaling laws are obtained for the total number of attractors, while "useful" attractors scale as power laws in  $N$ .

Weisbuch and Oprea (1994) discuss more thoroughly the capacity limits of model immune networks with localized responses. They verify by numerical simulations the square-root scaling law for the memory capacity. They also examine a number of other features of the network. They show that when the number of presented antigens increases, failures to remove the antigen occur, since the relevant clone has been suppressed by a previous antigen presentation. They also show that previous immune or tolerant attractors are rather robust in the sense that destruction of these local attractors by new encounters with antigen is rare, and that the complete reshuffling of the attractors, as in Hopfield nets (Hertz, Krogh, and Palmer, 1991), is never observed.

The questions that we addressed in this section have some relation to those discussed in Secs. II.A and II.B. However, the results cannot be directly mapped on one

another for the following reasons: In Sec. II, we derived the size of the repertoire needed to respond to *any* antigen that could be presented to the immune system. Here we discussed the capacity of the network in terms of a set of  $m$  successive antigens presented to the network. Further, the computations in Sec. II were made for a clonal model in which only clones responding to the antigen (idiotypic clones) were considered. Overlap of patches in shape-space models corresponds to cross-reactivity, i.e., the phenomenon of the same clone's recognizing several different antigens, and rather than being a problem it is a desirable feature, since it allows a large number of clones to respond to any antigen. On the other hand, in a network model, overlaps of patches are to be avoided since they set the limit of the memory capacity.

### 3. Basins of attraction and the window-automaton approximation

The above analysis describes the attractors of the dynamics, but does not predict which attractor is reached according to the conditions of antigenic stimulation. Determining which attractor is attained under a prescribed set of conditions is precisely the question immunologists want to answer. Numerical simulations allow such predictions, but techniques are not available to allow us to make this prediction analytically for the nonlinear model given by Eq. (4.1). However, replacing the nonlinear proliferation function  $f(h)$  by a piecewise linear function, a window automaton, allows analytical treatment and prediction of which attractor is reached under any given antigenic stimulation protocol (Neumann and Weisbuch, 1992a). A *window automaton* (Weisbuch, 1990a) is a function whose value is a nonzero constant when its input is between a low and a high threshold; otherwise its value is zero. We have chosen as threshold  $L$  and  $H$ , those values of the field where the function  $f(h)$  intersects the horizontal line  $y = d/p$ . Thus

$$L \approx \frac{d}{p-d} \theta_1, \quad H \approx \frac{p-d}{d} \theta_2.$$

The window-automaton proliferation function (see Fig. 24) is then defined by

$$\begin{aligned} h < L: & \quad f(h) = 0, \\ L < h < H: & \quad f(h) = 1, \\ H < h: & \quad f(h) = 0. \end{aligned} \tag{4.17}$$

Using the window automaton instead of the continuous proliferation function, we find that the differential equations (4.1) become piecewise linear, and hence the time variation of all clone populations can be described by simple exponential functions, except in the vicinity of the virgin population ( $V$ ), where the source term cannot be neglected and constant terms enter the solution. Indeed, on a time diagram of the numerical simulations, one observes piecewise linear evolution when plotting the logarithm of the populations [e.g., compare the time plots obtained with the continuous function  $f(h)$  in Fig.

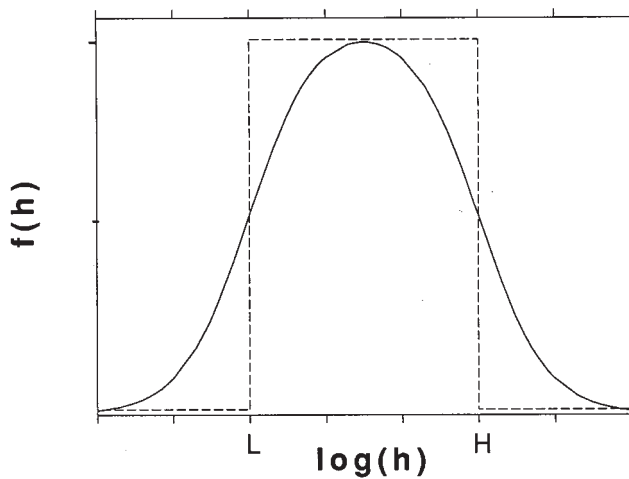


FIG. 24. The activation function  $f(h)$  and its approximation by a window automaton. From Neumann and Weisbuch, 1992a, reproduced with permission.

23 with those obtained with the window automaton in Fig. 25]. If the source can be neglected, then according to the field  $h_i$ ,  $x_i(t)$  varies as

$$\begin{aligned} h_i < L: \quad x_i(t) &= x_i(\tau) e^{-d(t-\tau)}, \\ L < h_i < H: \quad x_i(t) &= x_i(\tau) e^{(p-d)(t-\tau)}, \\ H < h_i: \quad x_i(t) &= x_i(\tau) e^{-d(t-\tau)}, \end{aligned} \quad (4.18)$$

where  $\tau$  is the last time a threshold was crossed. This approximation enables us to divide the dynamics into short time stretches, where the dynamics of each clone is an exponential growth or decay.

Another favorable feature of the window-automaton approach is that the antigen dynamics is also simple.

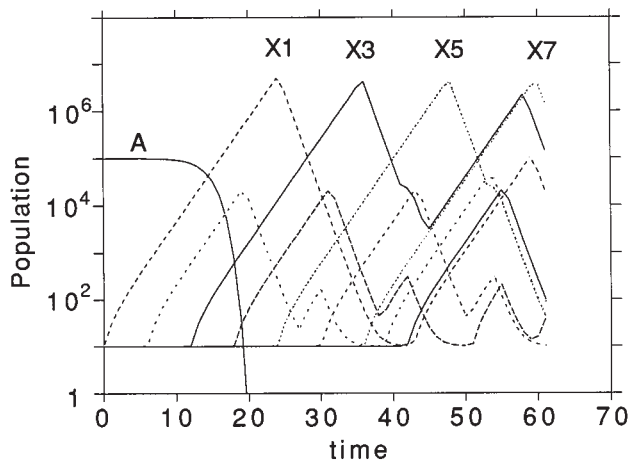


FIG. 25. Dynamics of a network undergoing percolation predicted with the window-automaton model. The dynamics are very similar to those illustrated in Fig. 23 for the log-bell-shaped proliferation function, apart from a slight difference in time scales. The same parameters were used in both simulations:  $k=10^{-5}$ ,  $A_0=10^5$ ,  $d=1.0$ ,  $p=1.5$ ,  $z=3$ ,  $m=10$ ,  $\theta_1=300$ , and  $\theta_2=10^6$ . From Neumann and Weisbuch, 1992a, reproduced with permission.

Starting from an excitatory concentration of antigen,  $L < A_0 < H$ , the antigen concentration first decays very slowly until the idiotypic clone population is large enough to decrease it substantially. Since the clone population increases exponentially, further antigen reduction is then very fast (see Fig. 25). Once the antigen concentration reaches 1, it is close to being eliminated (Fig. 25). We thus approximate the dynamics of antigen concentration by a step function, constant up to time  $t_A$  defined by  $A(t_A)=1$ , and then vanishingly small,

$$\begin{aligned} t < t_A: \quad A(t) &= A_0, \\ t > t_A: \quad A(t) &= 0. \end{aligned} \quad (4.19)$$

The time  $t_A$  can be computed by using Eqs. (4.12) and (4.18),

$$\frac{dA}{dt} \frac{1}{A(t)} = -kx_1(0)e^{(p-d)t}. \quad (4.20)$$

Integrating until  $t_A$ , with the initial condition  $x_1(0) = m/d$ , gives

$$t_A \approx \frac{1}{p-d} \ln \left[ \frac{(p-d)}{k} \frac{d}{m} \ln A_0 \right]. \quad (4.21)$$

Thus the antigen elimination time is almost independent of the initial antigen population  $A_0$ . It can be seen that  $t_A$  is approximately the time that  $x_1$  takes to proliferate from  $m/d$  to  $C$  cells, where

$$C = k^{-1}(p-d) \ln A_0. \quad (4.22)$$

In most cases  $C$  is the single parameter that suffices to characterize antigenic stimulation.

The following sections describe the application of the window-automaton technique to the computation of two transition lines.

#### a. From virginity to excitation

As seen in Fig. 26, to escape the virgin state, excitation of  $x_1$  above  $L$  needs to be maintained by  $x_2$  after antigen elimination.

For a Cayley tree with a coordination number  $z$ , let  $t_{Lz}$  be the time for  $x_2$  to reach  $L/z$ , the level needed to sustain  $x_1$  at a field  $L$ . In order to escape the virgin attractor by antigen perturbation,  $t_{Lz}$  should be small and  $t_{1d}$ , the time for  $x_1$  to decay back to  $L$ , thus preventing  $x_2$  from further proliferation, should be large. The condition for escape from virginity is therefore written as (see Fig. 26)

$$t_L + t_{Lz} < t_A + t_{1d}. \quad (4.23)$$

On the left-hand side,  $t_L$  is the time for  $x_1$  to grow from  $V$  to  $L$  so as to excite  $x_2$ . The quantity  $t_L + t_{Lz}$  is further called the two-level time delay because it involves the time necessary to excite two levels (here levels 1 and 2) to a population sufficient to generate an excitatory field. It also plays an important role in other transitions that will be discussed later. On the right-hand side of Eq. (4.23),  $t_A$  is the antigen elimination time [Eq. (4.21)]. Expression (4.23) is exact and valid under any antigenic stimulation, but the evaluation of  $t_{Lz}$  and  $t_{1d}$  from the

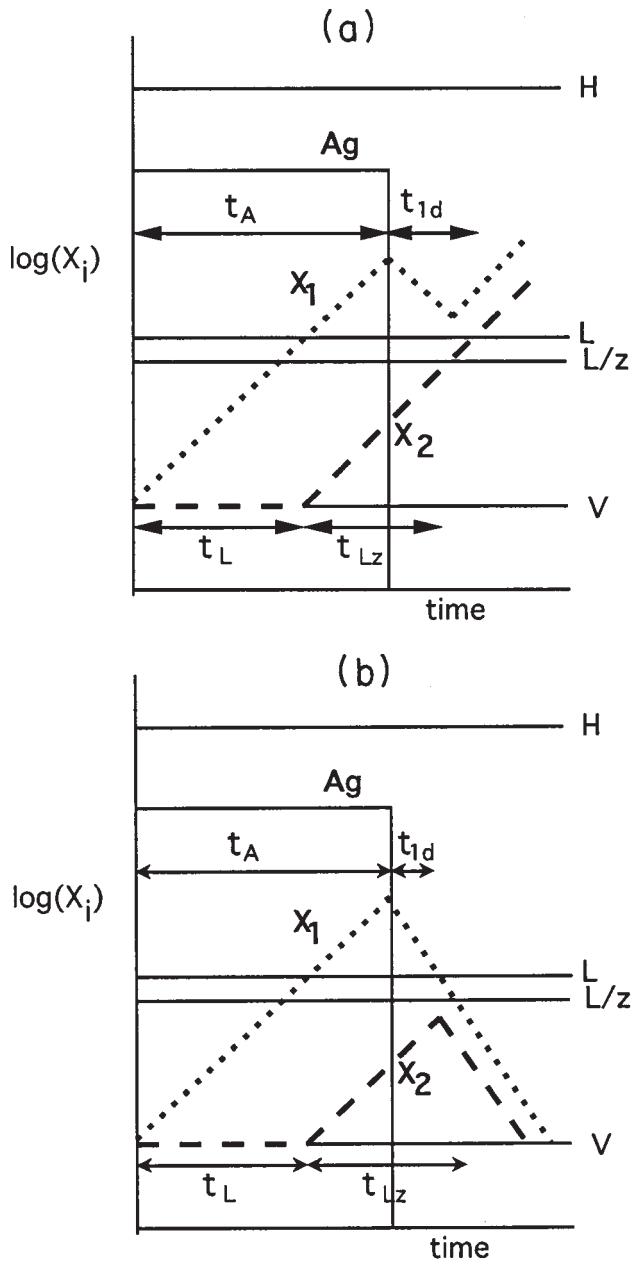


FIG. 26. Dynamics predicted with the window-automaton model at the transition from virginity to excitation.  $x_2$  starts to proliferate when  $x_1$  passes  $L$ .  $x_1$  starts to decay when antigen is eliminated. (a) Escape from virginity: excitation of  $x_2$  to  $L/z$  (the dashed line:  $t_L + t_{Lm}$ ) is faster than the decay of  $x_1$  back to  $L$  (the dotted line:  $t_A + t_{1d}$ ). (b) Failure of vaccination:  $x_2$  excitation is too slow and it cannot sustain  $x_1$ . From Neumann and Weisbuch, 1992a, reproduced with permission.

parameters  $\theta_1$ ,  $\theta_2$ ,  $A_0$ , etc. depends upon the conditions of antigenic stimulation.

In the simpler case when  $C$  [defined by Eq. (4.22)] is smaller than  $H$ , the growth of  $x_2$  up to  $L/z$  is monotonic. The following expressions for the time intervals are obtained:

$$t_L = \frac{1}{p-d} \ln \left[ \frac{L}{V} \right] \quad (4.24)$$

and

$$t_{Lz} = \frac{1}{p-d} \ln \left[ \frac{L}{zV} \right]. \quad (4.25)$$

Proliferation and decay times ( $t_p$  and  $t_d$ , respectively) between the same two concentrations are related by

$$(p-d)t_p = dt_d \quad (4.26)$$

and  $t_{1d}$  is then computed from the time it takes for  $x_1$  to proliferate from  $L$  to its maximum concentration, reached when antigen is eliminated,

$$t_{1d} = \frac{p-d}{d} t_A - \frac{1}{d} \ln \left( \frac{L}{V} \right). \quad (4.27)$$

When one replaces the times in inequality (4.23) by their expressions given by Eqs. (4.24)–(4.27) and then replaces the variables  $A_0$ ,  $V$ , and  $L$  by their corresponding expressions in terms of the parameters  $\theta_1$ ,  $z$ ,  $m$ ,  $d$ , and  $p$ , the condition for escape from the virgin attractor appears as the following scaling law:

$$\theta_1 < \theta_1^V \equiv \frac{p-d}{d} \left( \frac{m}{d} \right)^\alpha \theta_2^\beta (z-1)^\gamma \left[ \frac{(p-d) \ln A_0}{k} \right]^\delta, \quad (4.28)$$

$$\alpha = \gamma = \frac{d}{p+d}, \quad \beta = 0, \quad \delta = \frac{p}{p+d}.$$

If the threshold  $\theta_1$  is too high, the idiotypic clone  $x_1$ , even if excited, does not remain above  $L$  long enough to allow the relay of the antigenic stimulus by anti-idiotypic stimulation, and the network falls back to the virgin state.

### b. Tolerance vs vaccination

When excitation remains localized to the first levels, there are special cases in which tolerance (see Fig. 21) is observed instead of vaccination (see Fig. 20). The window-automaton approximation can be further refined to take into account the fact that, under strong antigenic stimulation,  $A_0 > \sqrt{\theta_1 \theta_2}$ , the field experienced by  $x_1$  is sufficiently large that the proliferation rate of  $x_1$ , as computed from  $pf(h_1)$ , is significantly smaller than  $p$  but not zero. Thus, for fields that are outside the window because of high antigen, we use  $p' - d$  as the growth rate of  $x_1$ , i.e.,

$$L < h_1 < H: \quad x_1(t) = x_1(\tau) e^{(p'-d)(t-\tau)} \quad (4.29)$$

where  $p'$  is the proliferation rate due to the initial antigen population,

$$p' \approx pf(h_1 = A_0), \quad d < p' \leq p. \quad (4.30)$$

A large initial antigen concentration slows down the rate of proliferation of clone  $x_1$  to  $p'$  and favors tolerance. In fact,  $x_1$  and  $x_2$  “race for suppression” (Fig. 27).

Assuming that  $C > H$ , so the proliferation rate of  $x_1$  is constantly  $p'$ , and neglecting the role of  $x_3$  in the field  $h_2$ , we derive the scaling law for the transition from vaccination to tolerance,

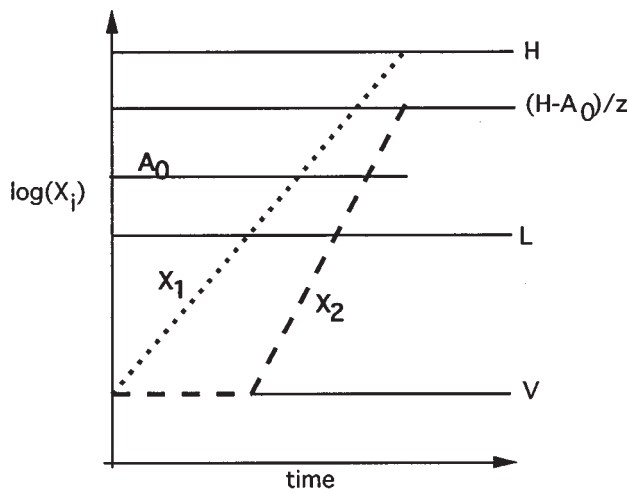


FIG. 27. Time diagram at the transition from tolerance to vaccination. In order for tolerance to occur,  $x_2$  has to be excited by  $x_1$ , reach  $(H-A_0)/z$ , and suppress  $x_1$  (the dashed line) before  $x_1$  reaches  $H$  and suppresses  $x_2$  (the dotted line). This is made possible by a large initial antigen concentration (which implies a smaller proliferation rate for  $x_1$ ) and by large  $z$ . From Neumann and Weisbuch, 1992a, reproduced with permission.

$$\theta_1 < \theta_1^T \equiv \left(\frac{p-d}{d}\right)^{2-\beta} \left(\frac{m}{d}\right)^\alpha \theta_2 (\theta_2 - A_0)^{-\beta} z^\gamma \quad (4.31)$$

where

$$\alpha = \beta = \gamma = \frac{p' - d}{p - d}.$$

In conclusion, the window-automaton analysis allows the determination of the basins of attraction of this dynamical immune system model. Note that attractor selection is rather unusual; the attractor is selected as a result of a competition between the growth of clones toward an excitation or a suppression threshold.

The steps taken in this method are the following:

- (1) Dividing the whole dynamics, using the window-automaton approximation, into shorter time intervals in which the time variations are simpler.
- (2) Expressing the conditions for the different dynamic regimes as inequalities among these time sequences.
- (3) Transposing the inequalities in terms of populations (e.g.,  $V, L, H, C$ ) and then in terms of the parameters (e.g.,  $\theta_1, \theta_2, p, d$ , etc.).

These steps allow the derivation of the scaling laws for transitions from one attractor to another and can be applied in a similar manner to determine transitions to other dynamic regimes such as percolation and extended localization. The eight transition lines of Fig. 22 were drawn according to the algorithm described above. The method also gives us more insight into the relevant quantities that determine the dynamics, the antigen elimination time, and the population of the idiotypic

clone at this time,  $C$ , and the two-level time delay  $t_L + t_{Lz}$ , which determines the possibility of excitation and of triggering.

#### 4. More realistic topologies

The Cayley tree topology with equal connection strengths is a strong idealization. In general, one would expect networks to contain loops and to have unequal interaction strengths  $J_{ij}$ .

##### a. Loops

The standard interpretation of recognition based on complementary shapes implies a network with loops.

Even loops are a likely feature of any model of recognition based on bit strings or shape space. We expect that if the idiotype ( $Ab_1$ ) recognizes by complementarity two similar anti-idiotypes ( $Ab_2$  and  $Ab'_2$ ), any third antibody  $Ab_3$  complementary to one of the anti-idiotypes has a good chance of recognizing the other anti-idiotype as well, giving rise to a four-membered loop. Even loops give only quantitative changes to the phase diagram, as discussed by Neumann and Weisbuch (1992b), and they do not change our basic conclusions about the dynamics of Cayley tree networks.

Odd loops are far less likely to occur within a model based on rigid structures. Antibodies with shapes that are self-complementary can stimulate themselves and give rise to loops of length 1. In a bit-string model with a matching rule that allows the strings to match when they are in any alignment, self-complementarities and odd loops arise. Rather nonspecific rules for recognition can also account for odd loops. On the other hand, odd loops are more probable if recognition involves soft molecular structures that can bend and have deformations to adhere to each other. In fact odd loops are present in experimental connection structures obtained by cross-reactivity tests on panels of antibodies from newborn mice (Kearney and Vakil, 1986; Holmberg *et al.*, 1986). Multispecific clones, which give rise to large connectivities and odd loops, are frequent in newborn animals and seem to disappear or become infrequent in adults (Holmberg *et al.*, 1986).

There are several situations in which odd loops result in tolerant attractors. We then obtain a very consistent view of some possible mechanisms for the establishment of localized tolerance attractors at prenatal and neonatal stages when multispecific clones and odd loops are present. These attractors once established remain stable, even when the multispecific clones disappear. On the other hand, those clones that remained virgin during early development are able to react and memorize antigen presentation by reaching vaccination attractor configurations.

##### b. Distribution of $J_{ij}$ values

We have no *a priori* reason to suppose that all connection strengths are equivalent. But when one uses different connection strengths, the weaker connections seem to have more influence on the population levels

than the stronger connections. Let us first consider the case of a single idotype  $Ab_1$  related with different connection strengths to two anti-idiotypes,  $Ab_2$  with intensity  $J$ , and  $Ab'_2$  with intensity  $J_w < J$ . After antigenic stimulation,  $Ab_2$  gets excited when its field,  $h = Jx_1$ , reaches  $L$ . This occurs as soon as  $Ab_1$  reaches  $L/J$ . By a similar argument,  $Ab'_2$  only gets excited when  $Ab_1$  reaches  $L/J_w$ , the corresponding excitation threshold for  $Ab'_2$ , provided that the suppression threshold for  $Ab_2$  is high enough,

$$J_w \frac{H}{J} > L \quad (4.32)$$

(otherwise  $Ab'_2$  remains nearly virgin).  $Ab'_2$  proliferates, and so does  $Ab_1$  until their populations become stabilized at a level such that  $Ab_1$  suppresses  $Ab'_2$  and  $Ab'_2$  stimulates  $Ab_1$ , i.e.,

$$x_1 = \frac{H}{J_w}, \quad x'_2 = \frac{L}{J_w}. \quad (4.33)$$

Both populations increase when  $J_w$  decreases. Furthermore,  $Ab_2$  experiences a very strong field  $J(H/J_w)$  and is oversuppressed: its level is of order  $m/d$  rather than  $L$ . Paradoxically, it plays no role in fixing the level of  $Ab_1$ .

Since the population of  $Ab'_2$  can be large, it now may become higher than the excitation threshold of a clone at level 3 with which it is connected. If we assume the connection strength  $J_{2'3}$  is stronger than  $J_w$ , then the condition for the excitation of  $Ab_3$ ,

$$J_{2'3} \frac{L}{J_w} > L, \quad (4.34)$$

is satisfied. Excitation is no longer localized at levels 1 and 2 as is usual in the case of a vaccination. The equivalent process can be described from level 3 to level 5: a weak connection between levels 3 and 4 gives rise to higher populations at these levels and  $Ab_4$  is high enough to excite  $Ab_5$ . An avalanche progresses along weak/strong connections and localization of the response is then lost. Neumann and Weisbuch (1992b) discuss the range of parameters for which this type of percolation can occur. They argue that any continuous distribution of  $J_{ij}$  results in percolation. Under these conditions localized attractors can no longer exist, and hence it would be difficult to have memory storage in a network.

Boutet de Monvel and Martin (1995) have derived an upper bound on the number of fixed points (which are not necessarily attractors) corresponding to memory or immune steady states against presented antigens, for a random network with a continuous distribution of  $J_{ij}$ . They show that the maximum number of such fixed points scales as  $\log N$  where  $N$  is the total number of clones. They thus conclude that a system with random connectivities and a continuous distribution of affinities will have a memory capacity that is "essentially nil." This conclusion, which is rather pessimistic, may be very sensitive to the choice of a bell-shaped activation func-

tion  $f(h)$  used in the network model. Recently, De Boer *et al.* (1996) introduced a new bell-shaped activation function derived from a physical chemical model of receptor cross-linking that greatly reduces the possibility of percolation in networks with a distribution of  $J_{ij}$ . How the number of fixed points and attractors scale in systems using this new activation function remains to be determined.

A number of authors, e.g., Varela *et al.* (1988), accept the idea of an immune network working in the chaotic regime that results from avalanches. But in our view, their predictions concerning the functional role of the network are unsatisfactory. For instance, they have to postulate the existence of two kinds of clones, those that are functionally connected to the net and those that are not, to account for both tolerance and clonal expansion.

If we want to maintain the existence of localized attractors in a network with many different connection strengths, we have to consider improvements to the original model. The most convincing improvement takes into account the role of T cells (cf. Carneiro *et al.*, 1996; Carneiro, Coutinho, and Stewart, 1966). Recent work of Neumann and Perelson (unpublished results) show that the control of B-cell proliferation by T cells can prevent percolation from occurring.

## 5. Biological interpretations of the localized attractor model

The simple B-cell model allows one to understand how the same network can support different independent attractors that can be interpreted as virgin, immune, and tolerant states. Which attractor is reached depends on the local topology of the network and the conditions of antigen presentation. With the additional assumption that the parameters of the model change between early life and adulthood one can understand how self-nonself discrimination is accomplished by the immune system. Assume that a self antigen is seen only by clone  $Ab_1$ . Recall that tolerance can be achieved by the suppression of the idiotypic clone  $Ab_1$  by the anti-idiotypic clone  $Ab_2$ . Once the tolerance attractor is achieved, secondary presentation of the antigen does not give rise to any immune response, because the antigen only increases the suppression on clone  $Ab_1$ . Thus the tolerance attractor, once reached, is robust against secondary presentation of the antigen. If we now assume that the anatomical and physiological situation during prenatal and neonatal life gives rise to parameters such that self antigen presentation results in tolerance, then no response to self antigen will be observed after the tolerance attractor is attained. During childhood, system parameters may change so responses to newly encountered and presumably foreign antigens will predominantly give rise to immune responses and attainment of the immune attractor rather than the tolerance attractor. Thus vaccination against new (foreign) antigens will occur, except for those with very large concentrations that generate suppressive fields. Even though system parameters change, the (self) antigens presented in the first stage will continue to be tolerated; the tolerance attrac-

tor is not removed by the change of parameters, but it can no longer be reached from the virgin state.

“Abnormal” presentation of self antigen during early life can, according to this model, result in autoimmune diseases. The dynamic approach may shed some light on the specific role of certain MHC molecules in autoimmunity. Since self peptides need to be presented by MHC molecules, the local parameters (connectivity and  $J_{ij}$ 's) that describe network topology and antigen presentation are under the influence of the MHC. The same logic may explain the existence of only a limited set of autoimmune diseases: although we have discussed mainly a homogeneous network, it is clear the immune system is inhomogeneous. Around each node in the network, connectivity and  $J_{ij}$ 's may vary and we might expect that some tolerant attractors are more fragile than others.

The view that autoimmune disease can result from dynamic effects is not shared by most experimentalists whose attention is focused on immunogenetics (Coutinho and Kazatchkine, 1994).

### E. Antibody/B-cell network models

The network models that we have discussed so far have dealt solely with B cells. A more realistic set of models have been developed that include both B cells and the antibody that they secrete. When the lifetimes of B cells and antibody differ significantly, new phenomena arise in these network models. In this section we describe the class of AB (antibody/B-cell) models and their properties.

#### 1. The AB model

Let  $b_i$  be the density of B cells of type  $i$  and  $a_i$  the concentration of antibody of type  $i$ . Then a generalization of the model given by Eq. (4.1) is

$$\frac{db_i}{dt} = m + b_i[\rho f(h_i) - d_B], \quad (4.35a)$$

$$\frac{da_i}{dt} = s b_i f(h_i) - d_C h_i a_i - d_A a_i, \quad (4.35b)$$

where the field

$$h_i = \sum_j J_{ij} a_j, \quad (4.36)$$

is determined by the concentration of antibodies capable of reacting with a B cell. If antigen is present, its concentration is added to the field with an appropriate weighting coefficient. As in the B model,  $p$  is the rate of proliferation of B cells and  $f(h)$  is taken to be the log-bell-shaped function given by Eq. (4.3). Here  $m$  is the rate of generation of cells from the bone marrow, and  $d_B$  is the rate of B-cell death. We assume that when B cells become activated they secrete  $Ab$  at rate  $s$ . Antibody has a natural rate of decay  $d_A$ . Antibody can also be eliminated by binding to anti-idiotypic antibody to form a complex, which is then assumed to be eliminated

(by macrophages and other phagocytic cells) at rate  $d_C$ . Formation and clearance of antibody-antibody complexes has been measured in man (Davies *et al.*, 1990). Because complex formation is a chemical process that should occur on a time scale of seconds to minutes, we have assumed that the concentration of complex is that at chemical equilibrium. Thus we assume that the concentration of complexes containing antibody  $a_i$  is proportional to  $C_i = \sum_j J_{ij} a_j a_i = h_i a_i$ . Since the “affinities”  $J_{ij}$  are scaled to be between 0 and 1, the actual concentration of complexes is obtained by multiplying  $C_i$  by a typical affinity  $K$  for idio-anti-idiotypic interactions, e.g.,  $10^6 \text{ M}^{-1}$ . This affinity constant is then subsumed within the parameter  $d_C$ .

In this model we have assumed that activated cells proliferate and secrete antibodies, and that the signals for doing so can be summarized by the field through the single function  $f(h)$ . Other models (e.g., those of Varela *et al.*, 1988; Sulzer *et al.*, 1993) assume that different functions of the field govern proliferation and differentiation into an antibody-secreting state.

To reduce the number of parameters in this model we nondimensionalize the equations, choosing the B-cell lifetime as a time scale. Equations (4.35) and (4.36) become

$$\frac{dB_i}{dT} = \sigma + B_i[\rho f(h_i) - 1], \quad (4.37a)$$

$$\frac{dA_i}{dT} = \delta[B_i f(h_i) - A_i] - \mu A_i h_i, \quad (4.37b)$$

where  $T = t d_B$ ,  $B_i = b_i s / (\alpha d_A)$ ,  $A_i = a_i / \alpha$ ,  $\alpha$  is a typical antibody concentration,  $\delta = d_A / d_B$ ,  $\sigma = m s \alpha / (d_A d_B)$ ,  $\mu = d_C / d_B$ , and  $\rho = p / d_B$ . Further, since the activation function  $f(h)$  is symmetric around its maximum when plotted on a logarithmic scale, we can choose  $\alpha$  such that  $h = 1$  corresponds to the maximum level of activation and replace  $\theta_1$  and  $\theta_2$  by a single parameter  $\theta$  with

$$f(h) = \frac{h \theta}{(\theta^{-1} + h)(h + \theta)}. \quad (4.38)$$

A discussion of this nondimensionalization is given by De Boer, Perelson, and Kevrekidis (1993a).

#### 2. The two-clone case

De Boer, Perelson, and Kevrekidis (1993a) study the case of two clones with no self interaction,  $J_{11} = J_{22} = 0$ , and a symmetric connection matrix,  $J_{12} = J_{21} = 1$ . The steady states of this model can be analyzed completely. At steady state, Eqs. (4.37) become

$$0 = \sigma + B_1[\rho f(A_2) - 1], \quad (4.39a)$$

$$0 = \sigma + B_2[\rho f(A_1) - 1], \quad (4.39b)$$

$$0 = \delta[B_1 f(A_2) - A_1] - \mu A_1 A_2, \quad (4.40a)$$

$$0 = \delta[B_2 f(A_1) - A_2] - \mu A_1 A_2. \quad (4.40b)$$

Hence, from Eq. (4.39) with  $\sigma \neq 0$ ,

$$B_1 = \frac{\sigma}{1 - \rho f(A_2)}, \quad (4.41a)$$

$$B_2 = \frac{\sigma}{1 - \rho f(A_1)}. \quad (4.41b)$$

Equations (4.40) give, for  $\delta \neq 0$ ,

$$B_1 = \frac{A_1(\mu A_2 + \delta)}{\delta f(A_2)}, \quad (4.42a)$$

$$B_2 = \frac{A_2(\mu A_1 + \delta)}{\delta f(A_1)}. \quad (4.42b)$$

Equating the right-hand sides of Eqs. (4.41a) and (4.42a) and the right-hand sides of Eqs. (4.41b) and (4.42b), one obtains

$$\sigma \delta f(A_2) = A_1 [1 - \rho f(A_2)] (\mu A_2 + \delta), \quad (4.43a)$$

$$\sigma \delta f(A_1) = A_2 [1 - \rho f(A_1)] (\mu A_2 + \delta), \quad (4.43b)$$

equations whose solution give the steady-state values of  $A_1$  and  $A_2$ .

One class of solutions are the symmetric solutions with  $A_1 = A_2 = A$ . From Eq. (4.43a), with  $A_1 = A_2 = A$  and the substitution of Eq. (4.38) for  $f(A)$ , one obtains

$$A \{ \mu \theta A^3 + [\mu + \delta \theta - \mu \theta^2 (\rho - 1)] A^2 + [\mu \theta + \delta - \delta \theta^2 (\rho - 1)] A + \delta \theta (1 - \sigma \theta) \} = 0. \quad (4.44)$$

One solution is  $A = 0$ . In this state both antibody populations are zero. De Boer, Perelson, and Kevrekidis (1993a) call this state ZZ (for zero-zero). The B-cell populations, from Eq. (4.5), are  $B_1 = B_2 = \sigma$ . Hence the ZZ state is a virgin state in which no antibody is present. The AB model also has another type of virgin state, akin to the one in the B model, in which antibody is present but its concentration is so low that the field it generates is insufficient to activate either B cell. This type of virgin state, which is denoted by VV, can be found by further analyzing Eq. (4.44) as discussed below.

The other symmetric solutions are the real positive roots of the cubic given in brackets. If  $\sigma \theta < 1$ , then the cubic will have two or no real positive roots. For what we consider to be typical parameter values,  $\rho = 2$ ,  $\theta = 10$ ,  $\delta = 0.1$ ,  $\mu = 20$ , and  $\sigma = 1.48 \times 10^{-3}$ , there are two positive roots. These roots correspond to the two symmetric states of the B model, in which either both clones have high fields or both clones have low fields. The VV state is negative (see Fig. 28) and hence not physically realizable. When  $\sigma \theta > 1$ , the cubic has one or three real solutions. The case of one solution occurs when  $\sigma$  is large. Then there are always many B cells present and the system can only produce large amounts of antibody and hence high fields. The one steady state is then the HH, or high-high, state. The case of three real solutions corresponds to the VV, LL, and HH states that also occur in the B model (see Sec. IV.A and Fig. 15).

Once the symmetric states are found, Eqs. (4.43a) and (4.43b) can be analyzed for their asymmetric steady-state solutions. Combining these equations, one obtains a high degree polynomial that can be factored, with one

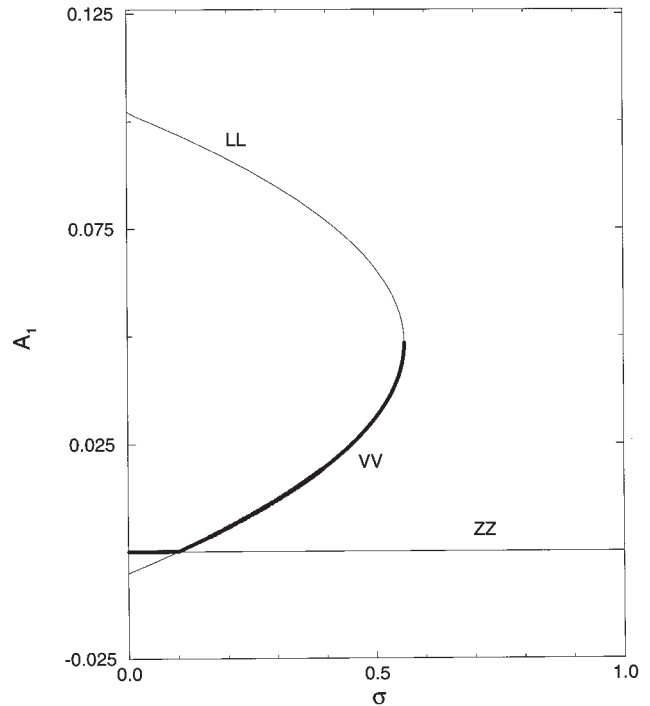


FIG. 28. Bifurcation diagram of AB model. Here the nondimensional source  $\sigma$  is varied and the equilibrium concentration of antibody  $A_1$  plotted. For low values of  $\sigma$  the virgin state with low amounts of antibody present, the VV state, is negative, and only the ZZ virgin state with no antibody present is a physically realizable solution to the AB model equations. The dark line indicates a stable steady state. For  $\sigma > 0.1$ , the ZZ state is unstable and the VV state is the virgin state for this system. For values of  $\sigma > 0.56$  this system has no virgin state.

factor being Eq. (4.44). The remaining factor is a sixth degree polynomial, which has not been analyzed algebraically. The asymmetric steady states are those in which one field is high and one low. In the B model, we distinguished between the two possible asymmetric states and called one immune and the other tolerant. Here we shall not introduce antigen and there is no reason to distinguish these states; in fact, their stability properties are identical.

Numerical studies (De Boer, Kevrekidis, and Perelson, 1990) indicated that the AB model could show oscillatory and chaotic behavior when antibody lifetimes were greater than B-cell lifetimes, i.e., when  $\delta = d_A / d_B < 1$ . More precise analysis was carried out by De Boer, Perelson, Kevrekidis (1993a) using numerical continuation methods. This work showed that when  $\mu = 0$ , so that there was no antibody-antibody complex formation, continuation of either of the asymmetric (or immune) steady states with  $\delta$  as a bifurcation parameter led to a supercritical Hopf bifurcation at  $\delta = 0.98$ . Continuation of the Hopf bifurcation as a function of the two antibody lifetime parameters  $\delta$  and  $\mu$  allowed De Boer, Perelson, and Kevrekidis (1993a) to map the parameter region where the immune states are stable—and where the principal behavior of the model is stationary—as well as the region where the immune states are unstable—and where the principal behavior

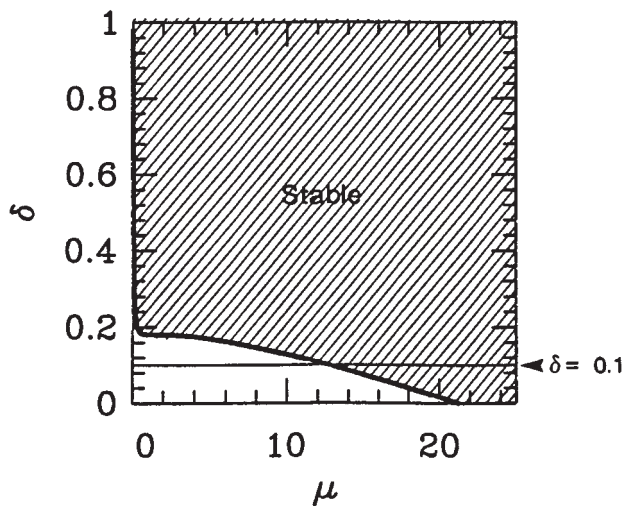


FIG. 29. Stability of the immune state in the AB model as a function of the parameters  $\mu$  and  $\delta$ .

turns out to be oscillations and/or chaos. The immune states are stable in the shaded area in Fig. 29.

Using  $\delta=0.1$  as a realistic estimate of the ratio of B-cell and antibody lifetimes, this analysis suggests that the immune states would be stable whenever  $\mu$  was sufficiently large, i.e.,  $\mu > 12.6$ . Using biological data, De Boer, Perelson, and Kevrekidis (1993a) estimated that  $\mu \approx 200$  and hence predicted that immune states should be stable.

An overview of the dynamic behavior of the AB model can be gleaned from Fig. 30, where the complex formation parameter  $0 \leq \mu \leq 15$  is varied (for  $\delta=0.1$ ). For these parameters the immune states are unstable

when  $\mu < 12.6$ . At  $\mu \approx 12.6$  the immune states undergo a subcritical Hopf bifurcation (see Fig. 29). The dots in Fig. 30 are values of  $\ln(B_1/B_2)$  attained at a Poincaré section defined by  $\ln A_1 - \ln A_2 = 0$ . This Poincaré section is a plane of symmetry.

Figure 30 exhibits three distinct regions of behavior. For  $0 \leq \mu < 3.7$ , there is an apparently chaotic attractor that seems to be born via a period-doubling cascade. For  $3.7 \leq \mu < 14$ , there is an apparently chaotic attractor (and complicated limit cycles in its periodic windows). The texture of this region is much lighter (and is even white for  $3.75 < \mu < 6$  because the zero-order continuation has difficulties following the attractor). Lastly, for  $\mu > 14$ , the apparently chaotic attractor has disappeared, and there appear to be no further orbits intersecting the Poincaré plane.

### 3. Chaos

One of the interesting dynamical features of the AB model is the existence of apparent chaotic dynamics. Further details about the oscillatory and chaotic behaviors observed in AB models can be found in De Boer, Kevrekidis, and Perelson (1990), Stewart and Varela (1990), Perelson and Weisbuch (1992a), Anderson, Neumann, and Perelson (1993), De Boer, Perelson, and Kevrekidis (1993a, 1993b), Bersini and Calenbuhr (1995), and Calenbuhr *et al.* (1995).

Are such behaviors characteristic of the immune system or are they simply behaviors of a complex nonlinear dynamic model operating in a possibly nonphysical parameter regime? At the moment we do not know. There have been three experimental reports (Rodkey and Adler, 1983; Lundkvist *et al.*, 1989; Varela *et al.*, 1991)

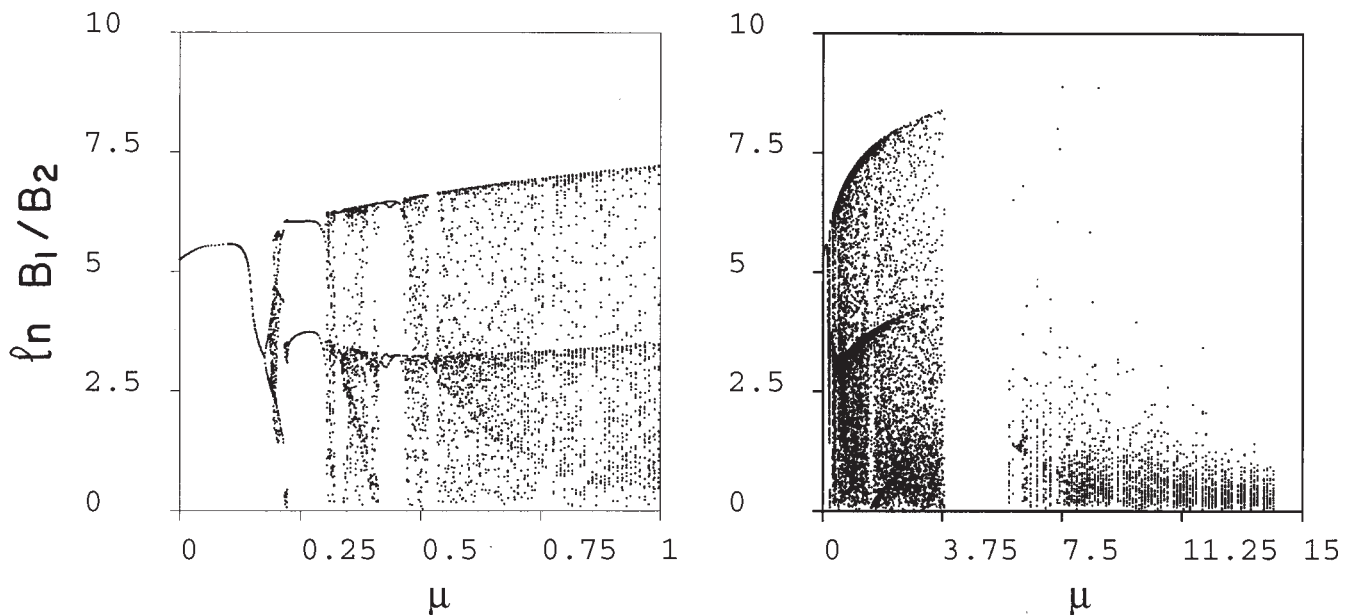


FIG. 30. Dynamics of the AB model as seen by trajectories going through the Poincaré section defined by  $A_1 - A_2 = 0$ . The behavior of the model is either stationary, periodic, or apparently chaotic, depending upon the value of  $\mu$ .

suggesting that concentrations of particular idiotype/anti-idiotype pairs fluctuate in an irregular and possibly chaotic manner. However, because the data reported in these papers contained very short time series, with of the order of ten points, it is not possible to reach any conclusions about the possible existence of chaos in the immune system.

When high-dimensional AB models operate in the chaotic regime, perturbations tend to percolate throughout the network (De Boer and Perelson, 1991; Anderson, Neumann, and Perelson, 1993). Thus, in contradistinction to the localized attractor models where clones can maintain either a high (immune) or low (suppressed) level for long periods, in AB models when clones are in the chaotic region their levels tend to fluctuate between high and low, although in restricted parameter domains fluctuations around only the immune or suppressed state have been observed (Anderson, Neumann, and Perelson, 1993). In the presence of percolation and large-scale fluctuations it is difficult to envision how immune memory might be maintained by a network. Thus one can conclude that either responses are localized or that memory is maintained by non-network mechanisms, e.g. memory cells or retained antigen (see Fishman and Perelson, 1995).

### F. The continuous-shape-space approach

Another approach to the study of immune networks suggested by Segel and Perelson (1988, 1989a, 1989b, 1989c, 1990) involves using partial differential equations rather than systems of ordinary differential equations. Here the shape of a receptor that characterizes a B-cell clone is described by a continuous variable  $x$ . For concreteness one can think of  $x$  as the height of a wedge-shaped region on the receptor, with positive  $x$  corresponding to a protuberance and negative  $x$  to an indentation (see Fig. 18). Perfect complementarity, and hence maximum binding affinity, occurs when the protuberance on one molecule and the indentation on another molecule are of the same length. For definiteness, the falling off of binding affinity for less complementary shapes is described by a Gaussian function of the distance between a given shape and its complement. These considerations lead to the following model (De Boer, Segel, and Perelson, 1992):

$$\partial b / \partial t = m + b[pf(h) - d], \quad (4.45)$$

where  $b(x, t)$  is written as  $b$ , and  $f(h)$  is again given by the log-bell-shaped activation function,  $f(h) = h\theta_2 / [( \theta_1 + h)(\theta_2 + h)]$ .

The field  $h(x; b)$  felt by B cells of shape  $x$  is

$$h(x; b) = \int_{-L}^L g(x, \hat{x}) b(\hat{x}, t) d\hat{x}, \quad (4.46)$$

where  $[-L, L]$  is taken to be the extent of shape space and

$$g(x, \hat{x}) = G(2\pi\sigma^2)^{-1/2} \exp[-(x + \hat{x})^2 / 2\sigma^2]. \quad (4.47)$$

TABLE I. Stability properties of the uniform steady states.

State	Stability to perturbation uniform	sinusoidal	Most dangerous perturbation
Virgin	stable	stable	-
Immune	unstable	unstable	$\cos kx$
Suppressed	stable	unstable	$\sin kx$

In Eq. (4.47)  $G$  and  $\sigma$  are constants determining the amplitude and width of the Gaussian, respectively. If each shape is complementary to only a small fraction of all possible shapes,  $\sigma \ll L$ . Because we can scale  $\theta_1$  and  $\theta_2$ , we can set  $G = 1$  without loss of generality (De Boer and Perelson, 1991). This has the advantage that for  $L \gg \sigma$

$$\int_{-L}^L g(x, \hat{x}) d\hat{x} \approx 1. \quad (4.48)$$

For a multidimensional shape space, we replace Eq. (4.47) with

$$g(\mathbf{x}, \hat{\mathbf{x}}) = G(2\pi\sigma^2)^{-l/2} \exp[-(\mathbf{x} + \hat{\mathbf{x}})^2 / 2\sigma^2],$$

where  $l$  is the dimension of the shape space and  $\mathbf{x}$  and  $\hat{\mathbf{x}}$  are  $l$ -dimensional vectors. The use of different variances in different shape-space directions is also possible in this multidimensional model. Sometimes periodic boundary conditions are used to avoid end effects. To study the effects of finite shape-space size, other boundary conditions are employed wherein clone sizes whose shapes lie outside a certain interval are fixed at zero magnitude.

As might be deduced from our considerations of discrete networks (Secs. IV.B and IV.D), whenever  $m \ll \theta_1 \ll \theta_2$ , Eq. (4.45) formulated on the infinite domain or using periodic boundary conditions has three spatially uniform equilibria  $b(x, t) = \bar{b}$ , the *virgin*, the *immune*, and the *suppressed* or *tolerant* states, respectively. By Eqs. (4.46) and (4.47) the fields of the uniform states satisfy  $h(x; \bar{b}) = \bar{b} = \text{const}$ , for all  $x$ . Each of the three states has its own typical range of values of the field. As in the case of the discrete network one can greatly simplify the analysis by approximating  $f(h)$  differently in each of the three states, and easily obtain analytic expressions for the B-cell population levels in the three uniform states. In the virgin state,  $\bar{b} \approx m/d$ , in the immune state,  $\bar{b} \approx \theta_1 / [p/d - 1]$ , and in the suppressed state,  $\bar{b} \approx (p/d - 1)\theta_2$ . The stability of the uniform states can be analyzed by rather standard analytical methods (De Boer, Segel, and Perelson, 1992). The stability of the uniform states is described in Table I.

Many nonuniform steady states also exists, which can be found by numerical methods (see Fig. 31). Analysis of the nonuniform solution is a type of pattern formation problem, in which the patterns form in shape space. Learning and memory in this system correspond to obtaining patterns in which clonal populations that are complementary to encountered antigens are high and remain high after subsequent antigen challenges. Patterns also form in the absence of antigen, which reflect

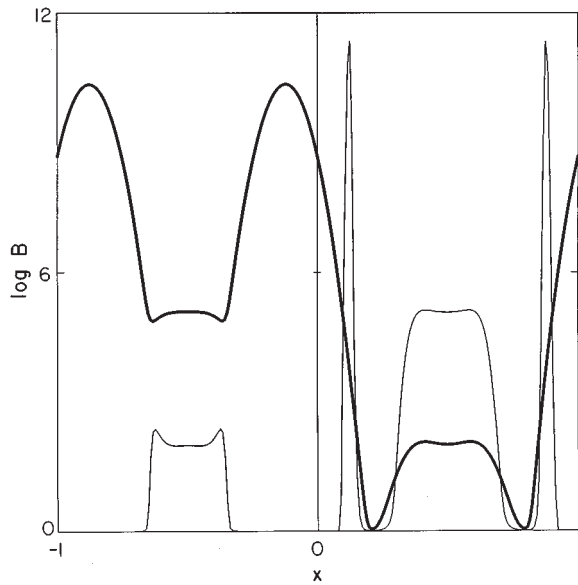


FIG. 31. Pattern formed in a continuous one-dimensional shape space by an AB model. Here  $x$ , the shape variable, is the horizontal axis. We show the distribution of the B-cell population (light lines) and of the field (heavy lines) attained long after a destabilizing perturbation of the suppressed state. The B-cell population, which is plotted on a logarithmic scale ranging to  $10^{12}$ , exhibits two unrealistically large peaks, which are sustained by self-stimulation. In addition one sees a region for  $0.2 < x < 0.6$  where the population is in the immune state, and a complementary region in the negative part of shape space in which the population is suppressed.

the intrinsic activity of the network.

Numerical solutions of a discrete representation of Eqs. (4.45)–(4.48) showed that networks do not always reach an equilibrium; clones can continue to grow due to self-stimulation. Antibodies that are self-binding have been discovered and are called *autobodies* (Kang and Köhler, 1986a, 1986b). To see how antibodies arise, consider the effect of a single clone at  $x = x_1$ , where  $x_1 > 0$ . Let

$$b(x) = b_1 \delta(x - x_1),$$

where  $\delta$  denotes the delta function. Then, by Eq. (4.46),

$$h(y) = \int g(x+y)b(x)dx = b_1 g(x_1+y).$$

The field is maximal at  $y = -x_1$  and falls towards zero as  $y$  approaches  $x_1$ . If, at some value  $\hat{y}$ ,  $h(\hat{y}) \approx \sqrt{\theta_1 \theta_2}$  then a clone at  $\hat{y}$  will be maximally stimulated. If this maximal stimulation occurs at  $\hat{y} = x_1$ , then the clone at  $x_1$  will stimulate itself maximally. This will occur if  $b_1 g(2x_1) \approx \sqrt{\theta_1 \theta_2}$  or  $x_1 = \sigma \sqrt{2 \log \eta / 2}$ , where  $\eta = b_1 / \sqrt{2 \pi \sigma^2 \theta_1 \theta_2}$ . Thus  $x_1$  is of order  $\sigma$ , i.e., near the origin. Notice that the larger  $b_1$ , the further from the origin is the clone that maximally stimulates itself. Thus we expect the peak near the origin to move gradually to the right as it grows, which in fact is observed in the simulations.

Self-stimulation of clones near the origin makes sense because shapes near zero are supposed to match them-

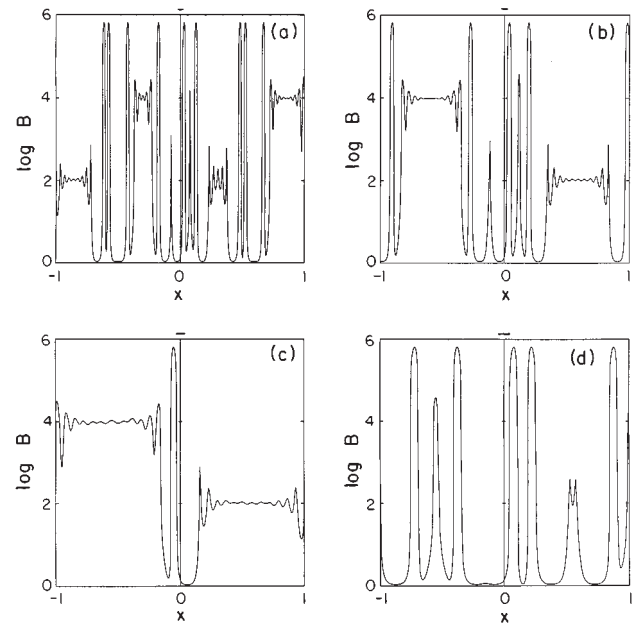


FIG. 32. The equilibrium distributions of B-cell populations as a function of the range of interaction in shape space. The interaction range is indicated by the heavy horizontal line at the top of each panel. See De Boer, Segel, and Perelson (1992) for details.

selves closely. B-cell clones that produce antibodies have been discovered in mice. These clones can become large and dominate immune responses. Similarly, in this model a low-affinity antibody can grow large enough to sustain its own proliferation, and—as a side effect—dominate a large proportion of the shape space.

A simple solution to the problem of unrealistically large population sizes formed by antibodies is to incorporate a self-limiting term in the growth equation for each population. Thus one can multiply the maximum proliferation rate  $p$  by the density-dependent function  $r(b)$ , so that Eq. (4.45) is replaced by

$$\partial b / \partial t = m + b[pf(h)r(b) - d], \quad (4.49)$$

where  $r(b)$  is

$$r(b) = \frac{\theta_3}{\theta_3 + b}.$$

Instead of  $\theta_3 / (\theta_3 + b)$  a variety of other functions could be used. For example, Segel and Perelson (1988) suggested  $e^{-\lambda b}$ . The logistic-type term  $(1 - b/b_{\max})$  could also be used.

With the inclusion of the self-limitation term  $r(b)$ , networks now reach an equilibrium. In equilibrium some populations are close to the maximum  $\theta_3$ , while other populations attain values around the immune and suppressed states. As was to be expected, the antibody close to the origin  $x = 0$  grows to the maximum level.

In Fig. 32 we show a number of equilibrium patterns as a function of the standard deviation  $\sigma$  used in the Gaussian. This parameter controls the range of interaction among clones. The main result is that the smaller

$\sigma$  the more peaks there are in the equilibrium distribution. However, analysis of the patterns that formed reveal another interesting feature. Recall that the uniform states of the system corresponded to clones' being in one of three states: virgin, immune, or suppressed. Similarly, in two-clone networks these three types of states also appeared with the added complication that the only stable states were with both clones virgin or with one clone at a high level (immune) and the other at a low-to-intermediate level (suppressed). In the nonlinear patterns that develop in continuous shape space, clones spontaneously organize into clusters of immune clones, and in regions of shape space that are complementary, clusters of suppressed clones are found (Fig. 32). It is not surprising to see immune and suppressed clones in complementary parts of shape space since the bell-shaped activation function requires an immune clone to see a low field as generated by a suppressed clone, and a suppressed clone to see a high field of the type generated by an immune clone. What is surprising is that we find localized regions of shape space, of width much larger than the field sensed by any single clone, in which all clones are activated. Furthermore, this region is complementary in shape to a region of roughly equal size in which all clones are suppressed. These higher-order localized structures are emergent properties of our model. The structures are not only present at equilibrium as shown in Fig. 32, but appear while the network is attaining equilibrium. During the oscillatory approach to equilibrium all of the clones in a cluster have related behavior, and idiotypic and anti-idiotypic clusters oscillate as if they were two interacting antibody species (not shown). An interesting implication is that one should be able to formulate a model in terms of interactions between clusters of clones. To our knowledge this has not yet been done.

Another open problem is to demonstrate learning and memory. Patterns that form once a system is challenged with antigen tend not to be preserved if the system is challenged with a second antigen. In a sense, responses percolate through the system preventing memory from being retained. It would be interesting to see if some basic modifications to the fundamental equations could be made that would allow memory retention. The localized responses seen in fixed-topology models (Sec. IV.D) do allow preservation of memory. Here localized responses can only be obtained if  $\sigma$  is taken sufficiently small that clones act independently, and hence if the network is destroyed. Immunologists, such as Coutinho (1989), have suggested that networks may not be involved in generating immune responses (see also Rose and Perelson, 1994). If this is in fact the case, then not being able to retain memory of previous antigen encounters may not be a failing of the model but rather a reflection of the properties of an immune network.

The model presented above was one dimensional. The general analysis of pattern formation in multidimensional shape spaces is a challenging task and remains to be resolved. Some approaches that are currently being explored involve using window-automaton models (Sec.

IV.D.3) in which the log-bell-shaped activation function  $f(h)$  is replaced by a piecewise linear function that is 1 when  $h$  is between  $\theta_1$  and  $\theta_2$ , and 0 elsewhere (De Boer, Hogeweg, and Perelson, 1992; Stauffer and Weisbuch, 1992; De Boer, van der Laan, and Hogeweg, 1993; Stauffer and Sahimi, 1994; see also Stewart and Varela, 1990) and (Sec. V.D). While such approaches are interesting mathematically and give some impression of patterns, it is not clear whether they will provide additional immunological insights beyond those that can be obtained with the bit-string models discussed below.

## G. Bit-string models of the network

The main advantage of the previously discussed B and AB models is that their simplicity allows for mathematical analysis. Thus in the continuous shape space model one can easily analyze the stability of the three homogeneous steady states of the model to uniform and sinusoidal perturbations (De Boer, Segel, and Perelson, 1992). In the discrete network model we were able to find conditions for the existence of localized attractors. However, a major disadvantage is that these models ignore the turnover of clones in the network and have rather simple, idealized topologies.

In the immune system the bone marrow produces novel clones with new receptors at a rate that is sufficient to replace all clones in the network in a few days. Thus it seems that in the network the addition and deletion of clones takes place on a time scale that is similar to the growth and decay rates of B cells. The addition and deletion of clones was first considered in the simulation model of Farmer, Packard, and Perelson (1986). Farmer *et al.* (1987), as well as Varela *et al.* (1988), have used the term "metadynamics" to denote the change in dynamics of the system owing to the replacement of clones. By adding a form of metadynamics to a class of network models, De Boer and Perelson (1991) have attempted to account for the effects of clonal insertion and deletion processes in the network. Because the immune network seems to be significant during early life (Coutinho, 1989; Holmberg *et al.*, 1989), the model was used to study the development of the immune network. They were particularly interested in two emergent properties—the size and the connectivity of the network.

### 1. Model equations

The model is composed of a varying number of B-cell clones of different specificities that form a network. Each clone is characterized by its specific antibody receptor, which is specified in the model by a bit string that reflects the "shape" of the antibody (see Farmer, Packard, and Perelson, 1986). A source, intended to model the bone marrow, supplies novel B-cell clones that can be incorporated into the network. Two clones can interact via soluble antibodies whenever their receptor shapes (i.e., bit strings) are complementary. Cells that become activated proliferate and differentiate into antibody-secreting cells. This maturation process takes a

few days. Free antibodies may also react with complementary antibodies to form *complexes*. These complexes, which are analogous to antigen-antibody complexes, are removed from the system.

The field of a clone is defined as in Eq. (4.36). The activation function  $f(h_i)$  is the log-bell-shaped function, Eq. (4.3).

To model the dynamics of the various B-cell clones they assumed that cells proliferate at rate  $p$  upon idiotypic stimulation and decay at rate  $d_B$ . Thus

$$\frac{dB_i}{dt} = B_i[pf(h_i) - d_B]. \quad (4.50)$$

This differential equation differs from that in the B and AB models, Eqs. (4.1) and (4.35), respectively, in that it has no source  $m$ . To model the time-dependent aspects of antibody production De Boer and Perelson (1991) used a “gearing up” function  $G(t)$  that accounted for the time lag associated with the differentiation of stimulated B cells. This approach was first introduced by Segel and Perelson (1989b). In this model, a separate gearing up function was used for each clone so that  $G_i(t)$  could be interpreted as the proportion of fully differentiated B cells of type  $i$ .  $G_i(t)$  was given by

$$\frac{dG_i}{dt} = k[f(h_i) - G_i], \quad (4.51)$$

where  $k$  is a constant that determines the characteristic time for gearing up. At  $t=0$ ,  $G_i(0)=0$  so that there is no initial secretion. After antibodies are secreted they are free in solution. Free antibodies  $A$  decay at rate  $d_A$  and form complexes with complementary antibodies, which are eliminated at rate  $d_C$ . Thus

$$\frac{dA_i}{dt} = sB_iG_i - d_C A_i h_i - d_A A_i, \quad (4.52)$$

where  $s$  is the rate at which a fully mature B cell produces antibody. Note that this equation differs from Eq. (4.35b) in the basic AB model by using  $G_i$  rather than  $f(h_i)$  as the modifier of  $s$ .

To summarize, the model consists of  $3n$  differential equations, where  $n$  is the number of clones in the system. The size of the network  $n$  is determined by the metadynamics.

## 2. Metadynamics

As in Farmer, Packard, and Perelson (1986) and Perelson (1988), the shape of each antibody molecule is represented as a bit string of length  $L$ . Antibody molecules are assumed to recognize each other whenever their bit strings can be matched complementarily. The specific rule that we used was to align the bit strings and require a complementary match over a stretch of at least  $r$  adjacent positions. If the strings match over exactly  $r$  adjacent positions, we assigned a low affinity,  $J_{ij}=0.1$ . If the strings match over more than  $r$  adjacent positions, we assigned a high affinity,  $J_{ij}=1$ . We set  $L=32$  and varied  $r$  in order to vary the *a priori* matching probability  $P(\text{match})$  of receptors. For the matching rule de-

scribed above,  $P(\text{match})$  is the probability of finding a “success run” of at least length  $r$  in a sequence of  $L$  Bernoulli trials (e.g.,  $r$  “heads” in a row in a sequence of  $L$  coin tosses). For a binary string generated with equal probabilities of 0 or 1 at each position, Feller (1968) shows that  $P(\text{match})$  can be approximated by the following formula, which becomes reasonably accurate for  $L \geq 2$ :

$$P(\text{match}) \approx 1 - r \frac{2-x}{(r+1-rx)x^{L+1}},$$

where  $x$  is the smallest root in absolute value of

$$1 - x + \left(\frac{x}{2}\right)^{r+1} = 0.$$

[One can also approximate  $P(\text{match})$  by the methods used by Percus, Percus, and Perelson (1993) and discussed in Sec. II.C.] Using Feller’s result, we find for  $L=32$  and  $r=6, 7, 8, 9, 10$ , and  $11$ ,  $P(\text{match}) \approx 0.205, 0.103, 0.05, 0.024, 0.012$ , and  $0.005$ , respectively. Experimental data suggest that during early life clones are connected to 20–25% of all the clones in the network (Holmberg *et al.*, 1984; Kearney, Vakil, and Nicholson, 1987). For  $L=32$  such a connectivity, i.e.,  $P(\text{match}) \approx 0.2$ , is expected around  $r=6$ .

In the simulation of De Boer and Perelson (1991),  $M$  novel clones were produced each day, with each clone containing about 10 cells. Using the string-matching algorithm, each newly generated clone was compared with the clones already in the network. A new clone was incorporated in the network only if it recognized at least one other clone and if these interactions were sufficiently stimulatory so that  $dB_i/dt > 0$ . At time intervals of one day, clones were removed if  $B_i < 1$  and  $A_i < \theta_1/10$ , i.e., if the clone consisted of fewer than one cell or if its antibody population was too small to have any effect. As an initial condition the simulation was started with a few randomly generated antibodies, assumed to represent maternal antibodies.

## 3. Simulation results

Figure 33 shows how some global characteristics of the network change in time for several values of the clonal production rate (i.e.,  $M=10, 20, 40$ ; lines increase in thickness with  $M$ ). The number of clones  $n$  in the network [Fig. 33(a)] has a large peak during the first month, whose height increases with  $M$ . This early peak sharply declines by the third month, and the network attains an equilibrium size around which it fluctuates. The total amount of antibody produced by the network is shown in Fig. 33(b). After a slow decline of the maternal antibodies, the total antibody concentration increases until a steady-state level of about  $3 \times 10^6$  units is attained, where a unit is the amount of antibody secreted by a single activated B cell during one day. This level corresponds to roughly 1 mg/ml, the physiologically observed serum level of IgM. The daily average number of connections per clone, i.e., the connectivity of the network, is shown in Fig. 33(c). As in Fig. 33(a), Fig.

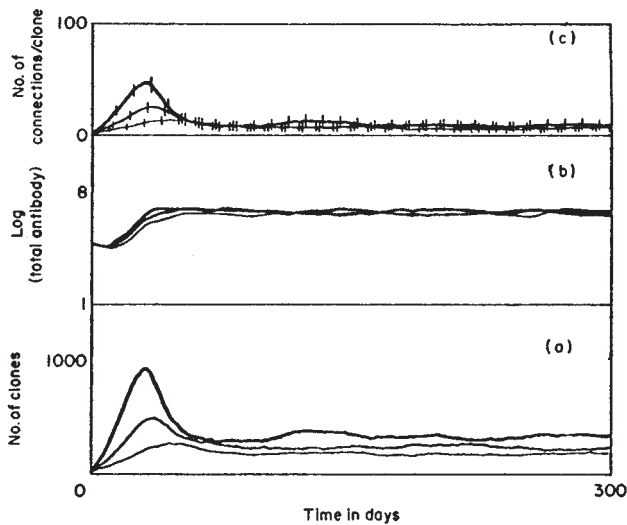


FIG. 33. Time-dependent characteristics of a sample network. Parameters  $p=1$ ,  $d_B=0.5$ ,  $d_A=0.05$ ,  $m=1$ ,  $d_C=10^{-3}$ ,  $\theta_1=10^2$ ,  $\theta_2=10^4$ ,  $k=0.2$ ,  $T=8$ ,  $P(\text{match})=0.05$ . We show three values of bone marrow production:  $M=10$ ,  $M=20$ , and  $M=40$ . Lines increase in thickness with  $M$ . (a) The number of clones in the network; (b) the total antibody concentration on a logarithmic scale (base ten); (c) the average connectivity. (The bars indicate one standard deviation.)

33(c) shows an early peak and attains an equilibrium around day 100. This equilibrium is about 6–9 connections per clone.

The fact that equilibrium levels are attained in Fig. 33 shows that the idiotypic network has certain self-structuring properties. Interactions within the network determine the network's size and connectivity and determine the total serum antibody level. The existence of stable “emergent” properties is one of the most interesting features of this network model. As we all know, one of the characteristics of living systems is their ability to maintain themselves in the face of constant turnover of their components. Thus, while as a whole the immune system behaves as a coherent system, we know that the cells and molecules that make up the system constantly change. The De Boer-Perelson network model has precisely this property. Stable properties characteristic of the immune system arise even though individual components may have only short lifetimes within the system and may even oscillate in concentration while they are present. For example, the serum concentration of one particular idio type may oscillate, consistent with the measurements of Lundkvist *et al.* (1989) and Varela *et al.* (1991), whereas the total serum antibody concentration remains quite constant. This is significant because there is no explanation of what physiological processes maintain the constant serum immunoglobulin concentrations. The De Boer-Perelson model is thus the first quantitative model to address this question.

The emergent properties of the network were further investigated by analyzing a series of networks in which both  $P(\text{match})$  and  $M$  were varied (Fig. 34). The equilibrium size of the network strongly depended on

$P(\text{match})$  [Fig. 34(a)]. Networks comprised of sticky receptors [e.g.,  $P(\text{match}) > 0.1$ ] remained small and contained fewer than 200 clones. Conversely, whenever receptors were specific [e.g.,  $P(\text{match}) < 0.01$ ], the networks became larger and could contain thousands of clones. From the shape of the observed curves one can conclude that the number of clones was inversely related to  $P(\text{match})$ . Thus systems with highly specific receptors generated very large networks.

The light lines in Fig. 34(c) depict the dynamic connectivity of the network, i.e., the average number of connections per clone realized during the simulation. For low values of  $P(\text{match})$  the dynamical connectivity increased with  $P(\text{match})$  until it saturated at about 10 connections per clone. This saturation was surprising because it meant that the connectivity no longer depended on the matching probability. It also showed that one cannot always deduce  $P(\text{match})$  from connectivity data. The experimental estimate of a connectivity of 20–25 % is only a transient in this model, which is attained during the early peak shown in Fig. 34. This is consistent with experiments by Holmberg *et al.* (1984) and Kearney, Vakil, and Nicholson (1987) in which connectivities of around 20% were observed in newborn mice and then decreased by at least 10-to-100-fold in adult mice (Holmberg *et al.*, 1986, 1989; Zöller and Achtnich, 1991).

The “expected connectivity” of a network, i.e., the  $P(\text{match})$  multiplied by  $n$ , the number of clones in the network [as provided in Fig. 34(a)], is shown by the heavy lines in Fig. 34(c). Because the connectivity was always smaller than the expected connectivity, one can conclude that networks in equilibrium select for growth and survival, within the network, of clones with low connectivity. Within this framework, low connectivity is not an intrinsic property of any particular antibody but rather is determined by the random structure of a clone's receptor and the shapes of the receptors on the other clones present in the system. A clone that is low connectivity in one simulation may be a high-connectivity clone in another simulation—the collection of clones within the system at any given time determines whether a clone will have high or low connectivity. This is a prediction of the model that may be able to be tested in experimental animals.

The fact that the observed equilibrium size of the networks is inversely related to  $P(\text{match})$  accounts for a “self-regulatory completeness” of the repertoire: the higher the specificity of the receptors the larger the number of clones becomes in the immune network. Thus over a large range of specificities the size of the system changes so that the repertoire remains complete. This completeness also provides an explanation for the fact that the networks attain an equilibrium size. The networks grow until every bit string is expected to be connected to a sufficient number of other clones to remain stimulated. De Boer and Perelson (1991) explain this in more detail.

The incorporation of metadynamics in this model was an attempt to account for the rapid turnover of clones in

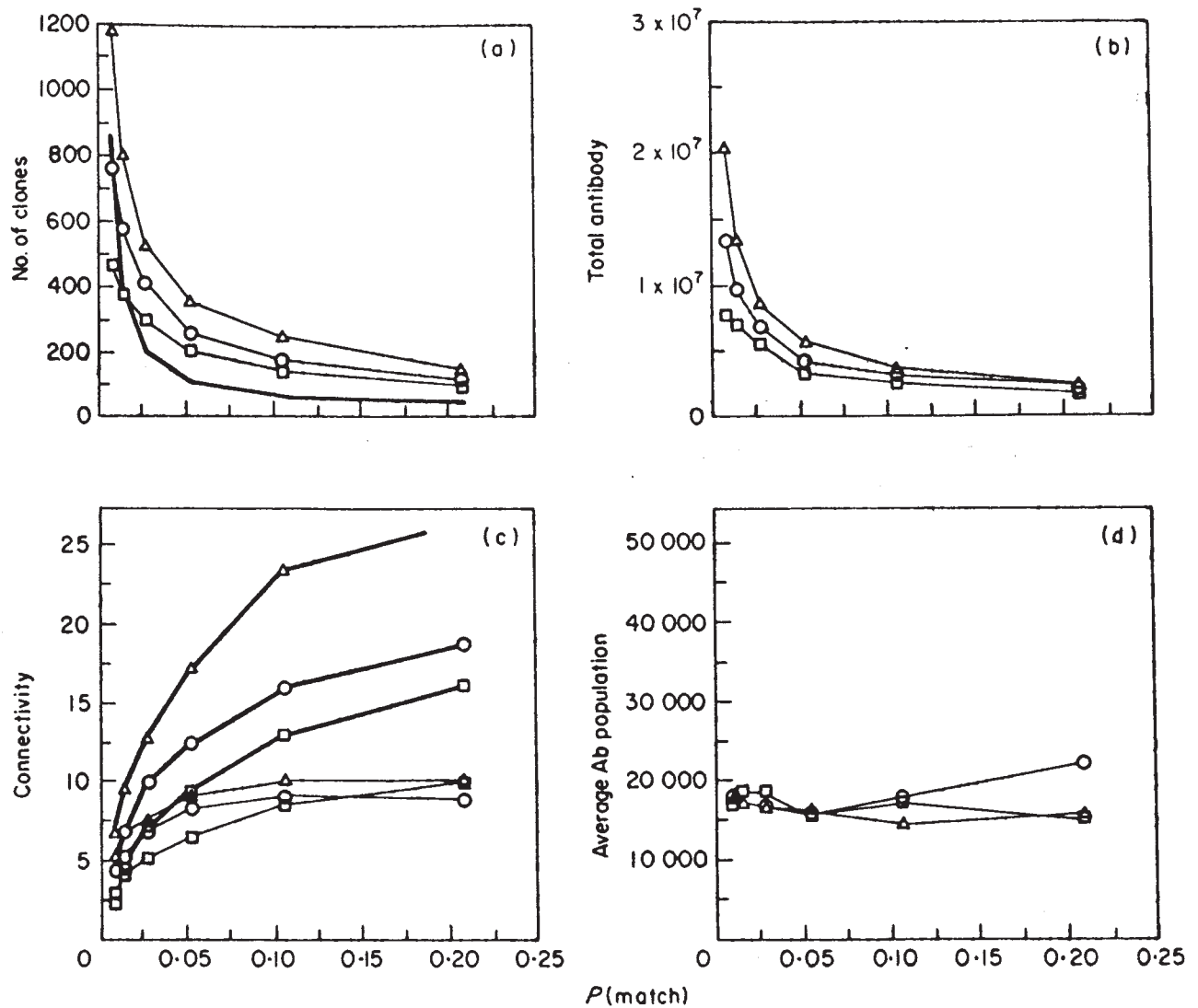


FIG. 34. Equilibrium characteristics of a series of networks varying  $P(\text{match})$ . Parameters as in Fig. 33. The equilibrium values were determined by averaging over the last 100 days of a simulation. We show three values of  $M$ :  $\square$ ,  $M=10$ ;  $\circ$ ,  $M=20$ ;  $\triangle$ ,  $M=40$ . (a) The total number of clones (light lines). (b) Total antibody. (c) The network connectivity (light lines) and the expected network connectivity (heavy lines), defined by  $P(\text{match})$  multiplied by the number of clones, as given in (a). (d) Average antibody per clone.

the network. Unfortunately, due to current computational limitations, it is impossible to perform the simulations for realistic values of  $M$ . In the immune system the bone marrow produces of the order of  $M=10^5$  to  $M=10^6$  novel clones per day. Thus systems with of order of a million differential equations might need to be solved. We have simulated up to  $M=500$  (De Boer and Perelson, 1991). In an attempt to model systems with larger values of  $M$ , De Boer, Hogeweg, and Perelson (1992) approximated  $f(h)$  by a window automaton (Sec. IV.D.3; Neumann and Weisbuch 1992a) and implemented this AB model with gearing up in a two-dimensional shape space as a cellular automaton. They found that all of the conclusions presented above remained true as  $M$  reached realistic values (see also De Boer, van der Laan, and Hogeweg, 1993). Further discussion of automaton models is given below.

## V. AUTOMATON APPROACHES

Networks of automata are dynamical systems that are the discrete equivalent of differential systems. Recently they have been widely used, for instance in neural nets and cellular automata, to model complex systems such as the brain or complex fluids. The theory of these networks has been actively developed during the last ten years. We shall not try to redefine this formalism here. The interested reader might refer to Meżard *et al.* (1988), Hertz *et al.* (1990) or Weisbuch (1990a), for simple introductions. One of the main advantages of these networks for a biologist involved in modeling is that the construction of a model requires a minimal knowledge about the numerical values of the parameters that define a system. The differential equation systems described in the previous sections required biological

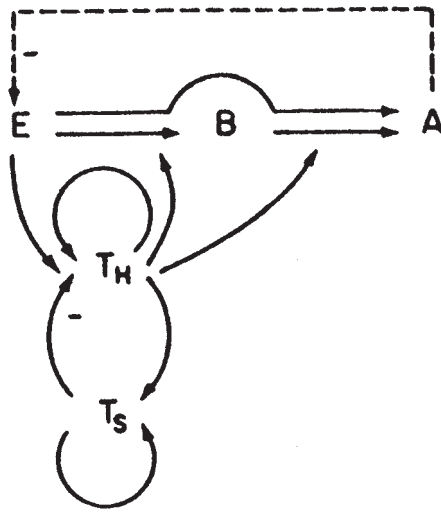


FIG. 35. Boolean model of B-T cell interactions was based upon the interaction scheme shown above in which  $E$  stands for epitope (the antigen),  $B$  for B cells,  $A$  for antibody,  $T_H$  and  $T_S$  for helper and suppressor T cells. From Kaufman, Urbain, and Thomas (1985), reproduced with permission.

data on cell lifetimes, cell supply from the bone marrow, thresholds for activation, affinity constants, etc. Most automata models do not require these data. The basic assumption is that cell populations need only be described by a set of discrete values, often 0 and 1, where 0 means that a population is absent, while 1 means that it is present at a high level. Interactions among populations are represented by logical functions, i.e., Boolean functions, which most often are equivalent to threshold automata (i.e., for physicists, spin variables at zero temperature). Since the  $J_{ij}$  are unknown they are usually taken equal to 1, or set at random as in spin-glass models.

We describe some examples, usually in their simplest version. Since these models often try to follow some of the intricacies of the immune system in terms of the cellular specificities, a faithful description would take us too far into cellular immunology and into the idiosyncrasies of each model (at least in the two first cases).

#### A. Modeling B-T interactions

A discrete model for B-cell/T-cell interactions was proposed by Kaufman, Urbain, and Thomas (1985). These authors were interested in the simplest way to describe the logic of the interactions among a number of different cell types and their results in terms of the immune response. Figure 35 shows the simplest version of their network. The binary variables are  $B$ , the B-cell population,  $A$ , the secreted antibody concentration, and  $H$  and  $S$ , helper and suppressor T-cell populations, respectively. Antigen is assumed to be either present or absent and hence is represented by  $e$ , a binary parameter. Thus in this model suppression is taken into account by an explicit cell population, suppressor T cells, rather than by a suppressive region in the proliferative

response function of B cells. The network is represented by the following set of logical expressions:

$$B = e \cdot h,$$

$$H = e \cdot \bar{s} + h,$$

$$S = h + s$$

$$A = e \cdot b \cdot h.$$

The bar over  $s$  ( $\bar{s}$ ) is to be read as a NOT logical function, multiplicative sign ( $\cdot$ ) is to be read as an AND logical function, and the  $+$  sign as an OR. The model uses a specific kind of sequential updating so that one has to make a distinction between states represented by lower-case letters and updating functions represented by upper-case letters. In the absence of antigen, the attractors of the dynamics are  $bhsa = 0000, 0110, 0010$ , which can be interpreted as virgin, memory (in which there are neither antibody nor B cells, but there are helper and suppressor cells), and a nonresponsive or suppressed state (the leftmost bits represent variable  $b$ , the second  $h$ , the third  $s$ , and the last  $a$ ). This analysis is extended to more complicated networks taking into account different stages of development of B cells, and to systems of differential equations by Kaufman and Thomas (1987) and Kaufman (1988).

#### B. A model of autoimmune diseases

Immunologists interested in autoimmune diseases often work on animal models instead of humans. Experimental autoimmune encephalomyelitis (EAE) is a disease that can be induced in mice and Lewis rats and which serves as a model of multiple sclerosis (MS) in humans. Adjuvant arthritis is an animal model of rheumatoid arthritis. Experiments on animals allow cellular immunologists to isolate and culture those cells, T cells in the above-mentioned models, involved in the development or the suppression of the disease (Cohen, 1986). The knowledge available to the theorist about an autoimmune disease is then which cell types have large populations, what kind of interaction—help or suppression—might exist among the different cell types, and, at some “macroscopic level,” the result of immunizations or cell transfers on the course of the disease. This knowledge can then be incorporated into one or several models, whose dynamical behavior can be compared with experimental results. Although one can use a differential equation model (cf. Segel and Jäger, 1994), here we focus on automaton models. Figure 36 represents an early and very simple attempt to model by a network of threshold automata the local network involved in the response to the self antigen myelin basic protein, as might occur in the diseases EAE or MS (Weisbuch and Atlan, 1988a).

A five-cell-type network is shown in Fig. 36. Automaton #1 represents killer cells in a resting state, #2 killers activated by the presence of the antigen, #3 and #5 suppressor cells, and #4 helper cells. The arrows represent “synaptic connections” of either sign. The strengths of

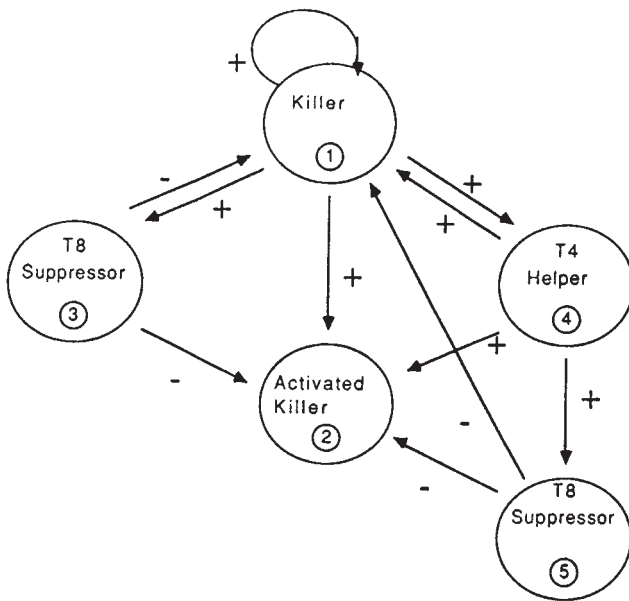


FIG. 36. Boolean net analyzed by Weisbuch and Atlan (1988a), reproduced with permission.

all synaptic connections are taken equal to 1. The thresholds are positive and less than 1. The iteration process involves parallel updating of the automata. Such a net can be in any of the 32 configurations corresponding to different populations of the five cell types. The dynamics of this network has two attractors, one with all automata in state 0, which can be interpreted as a virgin state corresponding to the absence of any cell type specific for the antigen. The other attractor has binary representation 10111, which indicates a small concentration of activated killers and a large concentration of all other cell types. It corresponds to a healthy carrier state, with killer cells only in a resting state, thus unable to harm the organism by developing an active autoimmune reaction. The basin of attractors of these two attractors are obtained by the iteration of all the 32 possible configurations. Attractor 10111 is preceded for instance by configuration 10111, with active killer cells. If one survives this critical period one reaches attractor 10111, the vaccinated carrier state.

More elaborate versions of this approach were developed by Atlan and Cohen (1992). Chowdhury and Stauffer discussed extensions of the small-network approach to AIDS and cancer (see their review paper published in 1992). Cellular-automaton models have also been formulated for the interactions between helper T-cell subsets (Brass, Grecis, and Else, 1994), for HIV infection of T cells and macrophages (Pandey and Stauffer, 1990; Pandey, 1991; Mosier and Sieburg, 1994), and for more general immune system models (Celada and Seiden, 1992, 1996; Seiden and Celada, 1992).

The Seiden and Celada (1992) approach is particularly noteworthy since an attempt is being made to build a general immune system simulator. Their model begins with a bit-string description of receptors on B cells and T cells, as well as major histocompatibility complex

(MHC) molecules on antigen-presenting cells. Antigen, 8 bits long, interacts with an 8-bit MHC molecule and under the correct matching conditions a complex is formed which has 4 antigen bits and 4 MHC bits “exposed.” This complex is now capable of interacting with an 8-bit T-cell receptor. The full 8-bit antigen can also interact with 8-bit antibodies secreted by B cells that were stimulated by interacting with the antigen and appropriate T helper cells. The number of cells and molecules are discrete variables, and events such as cell division or antigen-antibody binding occur probabilistically, with probabilities chosen so that the relative rates of different processes can be modeled. The simulation is done on a two-dimensional grid, and cells and molecules migrate over the grid; interactions occur only among cells and molecules in the same automaton cell. The model incorporates a lot of immunological details, and parameters have been tuned to give realistic-looking immune responses. Questions related to the optimal number of MHC molecules and the process of affinity maturation have been addressed with the model.

### C. Spin-glass models

Spin glasses and neural nets have also inspired some models in theoretical immunology that are direct implementations of these formalisms. Parisi (1988), for instance, used a spin-glass formalism with symmetrical random connections to show that even in the case of large connectivity resulting in many clones  $Ab1$  that recognize the antigen, the anti-idiotypic clones  $Ab2$ , unlike the internal image of the antigen-specific clone, have little chance to be excited since the field they experience is the result of random contributions. Only the clone corresponding to the internal image has some chance to be excited since its field results from a coherent contribution from the first-level clones. Lefèvre and Parisi (1993) have examined learning and memory in spin-glasslike immune networks.

Weisbuch and Atlan (1988b) used a dilute neural net formalism as a generalization of the simple neural network model discussed in Sec. V.B. With this formalism they studied the transition between organized behavior (localized attractors and cyclic attractors with short periods) and chaos (nonlocalization and aperiodic dynamics). In the dilute random-neural-nets formalism, localized behavior is observed only when a sufficiently large threshold  $\theta$  is applied to the automata. The condition found by Weisbuch and Atlan was

$$\theta > \sqrt{z \log(z)},$$

where  $z$  is the connectivity of the network.

### D. Automata on a 2-dimensional shape space with metadynamics

Stewart and Varela (1991), De Boer, Hogeweg, and Perelson (1992), De Boer, Segel, and Perelson (1992),

and De Boer, van der Laan, and Hogeweg (1993) have proposed and analyzed automaton models in a two-dimensional (2-d) shape space. We first describe the Stewart and Varela model. As in the De Boer and Perelson (1991) bit-string model described in Sec. IV.G, Stewart and Varela were interested in a metadynamics in which new clones are constantly generated from the bone marrow. Their basic algorithm consists in the generation of new clones at each time step. A new clone is randomly assigned a position on the 2-d space, with population 1. Fields on each clone are computed by adding contributions from neighboring clones. Individual contributions to the field are weighted by a Gaussian distribution according to the distance between clones as in the Segel and Perelson (1988) continuous-shape-space model (Sec. IV.F), but instead of using a single shape plane with maximum complementarity at opposite sites in the plane, Stewart and Varela use a representation with two sheets of complementary clones, white and black, and maximum complementarity occurs for clones of different colors at the same place. With our notation, the field  $h_i$  acting on clone  $i$ , is given by

$$h_i = \sum_j e^{-d_{ij}/c^2}, \quad (5.1)$$

for all  $j$  clones of opposite color, where  $d_{ij}$  is the distance between clone  $i$  and  $j$ , and  $c$  is a scaling constant. All clones, old and new, are set to zero population except if they experience an intermediate field,  $L < h < H$ , in which case their population is set to 1. This dynamics results in the appearance of black and white stripes in the shape space (see Fig. 37). Black stripes apply large suppressive fields which exclude white clones. The parallel stripes of white clones create intermediate fields sufficient to sustain the black clones. These regions are stabilized by the presence of self antigens. The large fields created by these self antigens is sufficient to suppress complementary clones of opposite color in their immediate neighborhood, but excite them at a distance (see Fig. 37). A generalization of this black-white model to a system using differential equations to model the relevant dynamics is given by Detours *et al.* (1994).

A related model is that of De Boer, Segel, and Perelson (1992). Their model is formally a coupled map lattice model rather than an automaton model. Using a 2-d shape space, they let  $B = \ln b$ , where  $b$  is the B cell concentration at position  $(x, y)$  in shape space. With  $m = 0$ , Eq. (4.45) then becomes

$$\partial B / \partial t = pf(h) - 1, \quad (5.2)$$

where the B-cell death rate was set to 1 by an appropriate choice of the time scale, and  $p \approx 2$  in these units. Because  $0 \leq f(h) \leq 1$ ,  $-1 \leq \partial B / \partial t \leq p - 1 \approx 1$ . Thus the derivative is bounded, and using an Euler integration method with step size one gives

$$B(x, y, t + 1) = B(x, y, t) + pf(h) - 1. \quad (5.3)$$

Since  $B = 0$  corresponds to  $b = 1$ , i.e., one B cell, it seems reasonable to require that  $B(x, y)$  never become smaller than zero. Thus De Boer, Segel, and Perelson (1992) assume

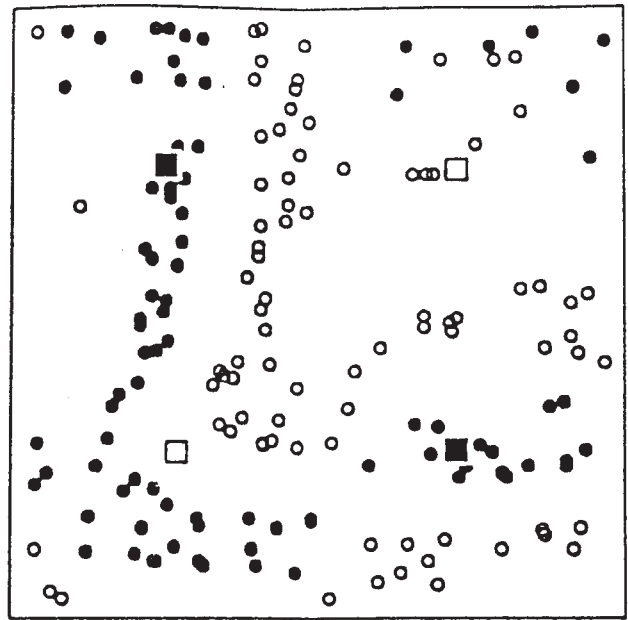


FIG. 37. Simulation of a two-dimensional shape space with window automata. Black and white clones recognize each other with strength decaying according to a Gaussian function of the distance. Homogeneous stripes are organized around self-antigens, represented by squares. From Stewart and Varela, 1991, reproduced with permission.

$$B(x, y, t + 1) = \max[0, B(x, y, t) + pf(h) - 1]. \quad (5.4)$$

Computing  $h(x, y)$  by a discrete representation of (4.46), i.e., similar to Eq. (5.1), converts this model into a 2-d lattice map. Figure 38 shows the distribution of clones and field values that result from a typical simulation of this type. At each location  $(x, y)$  the gray scale indicates the size of clone  $B(x, y)$  [Fig. 38(a)] and the size of the field  $h(x, y)$  [Fig. 38(b)]. The patterns seen in the figure are roughly circular due to the use of a truncated Gaussian function for  $f(h)$ . Were we to use a square local neighborhood rather than the circular Gaussian neighborhood used here, the patterns would be more rectangular. The distribution of clone sizes and fields form a landscape of hills and valleys that resemble the distribution seen in the one-dimensional shape space illustrated in Figs. 31 and 32.

Restricting  $B$  to a small set of integer values and choosing  $f(h)$  as a window automaton converts the model into a cellular automaton. Dasgupta (1992) studies this model with  $B$  restricted to values 0, 1, and 2 and with a stochastic updating rule. Stauffer and Weisbuch (1992) and De Boer, van der Laan, and Hogeweg (1993) use only two values, 0 and 1. These models are computationally efficient and have been used to study pattern formation in shape space and the effects of high rates of cell recruitment into the network (De Boer, Hogeweg, and Perelson, 1992; De Boer, van der Laan, and Hogeweg, 1993).

In these models the patterns that appear represent the immune activity in the animal. Memory to an antigen or

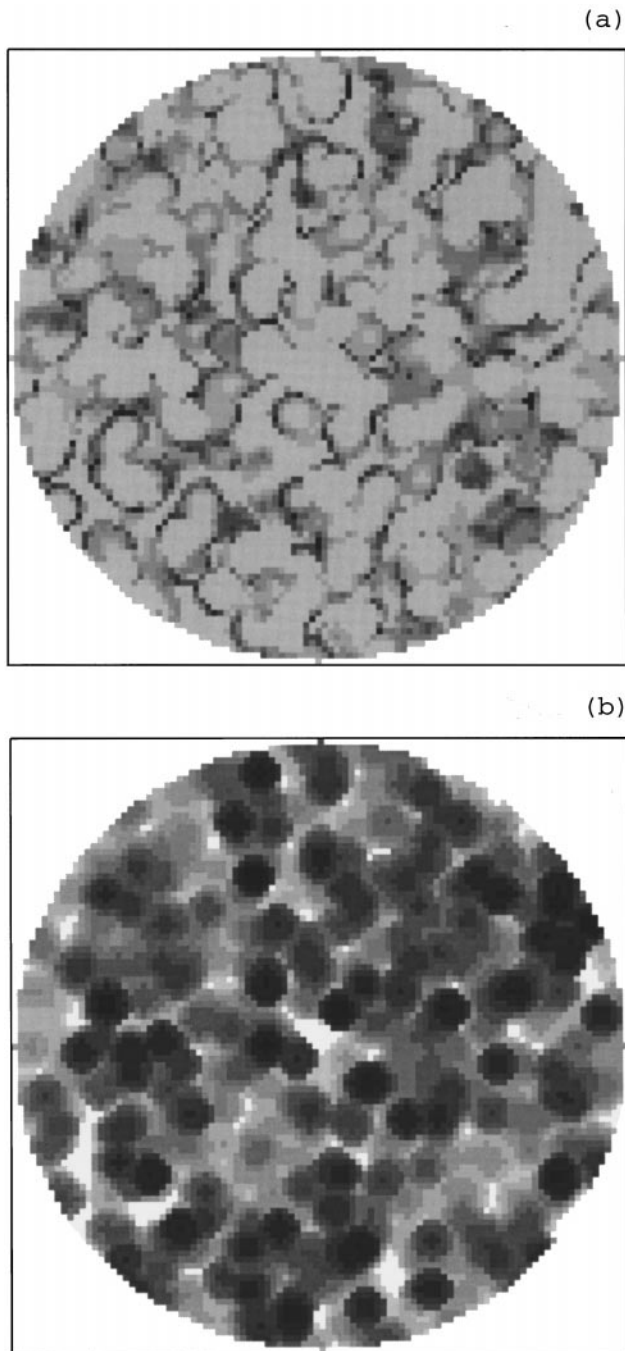


FIG. 38. Patterns of clone size (a) and corresponding field values (b) that result from a two-dimensional lattice map model of shape space. Illustrated is the solution to Eq. (5.4) after 500 iterations.

set of antigens involves parts of the pattern remaining relatively invariant for long periods. Patterns do change on a slow time scale due to the influx of new cells and perturbations by antigens. Whether these low-dimensional models can usefully represent the changing immune repertoire remains to be seen.

The effect of changing the dimensionality  $d$  of the network was studied by Stauffer and Weisbuch (1992). Bit-string models correspond to large- $d$  networks, while 1- or 2- $d$  networks have a small dimension with respect

to the dimension required for a valid mean-field approximation. The shape-space model of Perelson and Oster (1979) suggested that the immune system operates with a shape space of an intermediate value of  $d$  between 5 and 10. By systematic studies of three-state cellular lattices with  $d$  varying from 1 to 10, Stauffer was able to observe that small- $d$  lattices ( $d < 4$ ) were always ordered, thus having localized attractors, while large- $d$  lattices exhibited a chaotic regime when the initial disorder was above a given threshold.

## VI. DISCUSSION

Immunology developed over the past 200 years as a branch of medicine originally aimed at preventing infectious disease through vaccination. Because of these beginnings immunology through most of the 19th and 20th centuries has been dominated by physicians and has been taught in medical schools, usually in departments of pathology or departments of immunology and microbiology. First slowly at the beginnings of the 20th century, with the interests of chemists in immunological reactions, and with accelerating pace in the last decade with cell and molecular biologists taking increasing interest in immunology, the field has become one of basic science. The newest group of scientists to take an active interest in the field are theoreticians, trained in physics and mathematics. The Nobel Laureate Jerne, for example, had undergraduate training in physics. An era is thus beginning in immunology in which theory is playing a part in the intellectual development of the field. We feel that, as in other areas in which systems are complex, theory and techniques of theoretical physics have an important contribution to make towards increasing our understanding of the phenomena of immunology.

Theories in immunology have taken two forms: verbal or nonmathematical and mathematical. Nonmathematical theories have been pioneered by experimental immunologists, such as MacFarlane Burnet, the inventor of clonal selection theory, and Neils Jerne, the inventor of idiotypic network theory. These theories, while not originally formulated in a quantitative way, have been developed into quantitative theories (see Secs. II and IV). The other class of theories have been formulated mathematically. For example, the model of Percus, Percus, and Perelson (1993), which predict the size of epitopes (Sec. II.C), the models of receptor cross-linking (Sec. III.A), and affinity maturation (Sec. III.C) are all of this form. Both classes of models are important and have made contributions to the field of immunology.

One area in which mathematical models will probably grow in importance is in the study of global behavior of the immune system. Cellular and molecular biologists and immunologists have achieved great success in isolating and even in understanding many of the molecules and cells of the immune system. However, their reductionist techniques fail when one asks questions about the behavior of large collections of cells and molecules. For example, what controls the total number of lymphocytes in the body or what determines the level of serum im-

munoglobulin are questions that have not yet been answered. Models have the potential of showing how local interactions among cells and molecules can generate the global coordinated behavior that characterizes many immune phenomena. The model of De Boer and Perelson (1991), discussed in Sec. IV.G, illustrated how control of the total serum antibody level could be attained as a consequence of a log-bell-shaped activation function for cells in a network.

Dynamics is an area well appreciated by physicists but one in which little work is being done in immunology. Because of difficulties in collecting data from one animal at many time points, dynamic experiments are rarely done, and when they are done they rarely have data taken at more than a few time points. Thus questions about whether immune systems operate at steady state, whether they oscillate, whether they are chaotic, etc. are difficult to answer. It is hoped that through modeling we can demonstrate the power of dynamic analyses to the experimental community and perhaps generate the motivation for carrying out both difficult and expensive dynamic experiments.

Lee Segel has said that one of the hallmarks of a complex system is that it is a system that cannot be described by a single model (Segel, 1995). This point has been well illustrated in this article. Different individuals and different groups have explored fundamentally different models of the same phenomena. For example, Weisbuch and co-workers have pursued immune network models that have localized attractors and that can account for some of the most basic phenomena in immunology—immunity and tolerance. Perelson, on the other hand, in addition to pursuing localized attractor models, has also investigated models that operate in a chaotic regime and that are typically characterized by nonlocal percolative behavior. In these models he has shown that, although individual clones or small sets of clones may act chaotically, when averages are taken over large populations the immune system behavior appears regular and controlled. Insufficient data exist at the level of single clones to distinguish between these classes of models and thus at this stage in the development of a field of quantitative immunology both classes of models are being studied.

Mathematical modeling in immunology is a field still in its infancy. The payoffs for developing successful models will be increased understanding of the operation of the immune system, the generation of new ideas, and new experiments to test them, as well as the eventual possibility of conducting immunological experiments *in machina* rather than *in vitro* or *in vivo* (Celada and Seiden, 1992, 1996). The models described above already contain insights into how clonal selection works, how affinity maturation occurs, how immunological networks may be involved in immune memory and how networks may be responsible for controlling the serum level of immunoglobulin. The challenge in immunology, as in brain research, is to understand a system of enormous complexity. One can only hope that the principles and ideas being developed in complex systems, nonlin-

ear science, and the tools of computer simulation will help unravel the remaining mysteries.

## ACKNOWLEDGMENTS

Portions of this work were performed under the auspices of the U.S. Department of Energy. The work was supported by NIH Grants RR06555 and AI28433, by Inserm grant 879002, by NATO CRG 900998, and the Santa Fe Institute through a grant from the Joseph P. and Jeanne M. Sullivan Foundation. The Laboratoire de Physique Statistique de l'ENS is associated with CNRS (URA 1306). Much of the work reported here was done in collaboration with Rob De Boer, Avidan Neumann, and Lee Segel. We thank the Santa Fe Institute's program in Theoretical Immunology for facilitating these interactions. We also thank B. Sulzer and D. Sherrington for their careful comments on a draft of this manuscript, and B. Goldstein for help with the illustrations.

## REFERENCES

- Agur, Z., G. Mazor, and I. Meilijson, 1991, Proc. R. Soc. London, Ser. B **245**, 147–150.
- Agur, Z., G. Mazor, and I. Meilijson, 1992, in *Theoretical and Experimental Insights into Immunology*, edited by A. S. Perelson and G. Weisbuch (Springer, Berlin), pp. 323–332.
- Ajitkumar, P., S. S. Geler, K. V. Kesari, Borriello, M. Nakagawa, J. A. Bluestone, M. A. Saper, D. C. Wiley, and S. G. Nathenson, 1988, Cell **54**, 47–56.
- Amit, A. G., R. A. Mariuzza, S. E. V. Phillips, and R. J. Poljak, 1986, Science **233**, 747–753.
- Anderson, R. W., A. Neumann, and A. S. Perelson, 1993, Bull. Math. Biol. **55**, 1091–1131.
- Atlan, H., and I. R. Cohen, 1985, *Theories of Immune Networks* (Springer, New York).
- Atlan, H., and I. R. Cohen, 1992, in *Theoretical and Experimental Insights into Immunology*, edited by A. S. Perelson and G. Weisbuch (Springer, Berlin), pp. 379–395.
- Batt, B. C., and D. S. Kompala, 1990, J. Theor. Biol. **142**, 317–340.
- Behn, U., K. Lippert, C. Möller, J. L. van Hemmen, and B. Sulzer, 1993, in *Phase Transitions: Physics, Mathematics, and Biology*, edited by R. Kotecky (World Scientific, Singapore), pp. 27–34.
- Behn, U., J. L. van Hemmen, and B. Sulzer, 1992, in *Theoretical and Experimental Insight into Immunology*, edited by A. S. Perelson and G. Weisbuch (Springer, Berlin), pp. 249–260.
- Behn, U., J. L. van Hemmen, and B. Sulzer, 1993, J. Theor. Biol. **165**, 1–25.
- Bell, G. I., 1970, J. Theor. Biol. **29**, 191–232.
- Bell, G. I., 1971, J. Theor. Biol. **33**, 339–378.
- Bell, G. I., A. S. Perelson, and G. Pimbley, Jr., 1978, Eds., *Theoretical Immunology* (Dekker, NY).
- Berek, C., A. Berger, and M. Apel, 1991, Cell **67**, 1121–1129.
- Berek, C., and C. Milstein, 1988, Immunol. Rev. **105**, 5–26.
- Bersini, H., and V. Calenbuhr, 1995, Chaos Solitons Fractals **5**, 1533–1540.
- Binion, S. B., and L. S. Rodkey, 1982, J. Exp. Med. **156**, 860–82.

- Boutet de Monvel, J. H., and O. C. Martin, 1995, *Bull. Math. Biol.* **57**, 109–136.
- Brass, A., R. K. Grencis, and K. J. Else, 1994, *J. Theor. Biol.* **166**, 189–200.
- Bruni, C., G. Doria, G. Koch, and R. Strom, 1979, Eds., *Systems Theory in Immunology* (Springer, New York/Berlin).
- Burnet, F. M., 1959, *The Clonal Selection Theory of Acquired Immunity* (Vanderbilt University, Nashville, TN)
- Calenbuhr, V., H. Bersini, J. Stewart, and F. J. Varela, 1995, *J. Theor. Biol.* **177**, 199–213.
- Cancro, M. P., W. Gerhard, and N. R. Klinman, 1978, *J. Exp. Med.* **147**, 776–786.
- Carneiro, J., A. Coutinho, J. Faro, and J. Stewart, 1996, *J. Theor. Biol.* **182**, 513–529.
- Carneiro, J., A. Coutinho, and J. Stewart, 1996, *J. Theor. Biol.* **182**, 531–547.
- Celada, F., 1971, *Prog. Allergy* **14**, 223–267.
- Celada, F., 1992, in *Theoretical and Experimental Insights into Immunology*, edited by A. S. Perelson and G. Weisbuch (Springer, Berlin), pp. 3–13.
- Celada, F., and P. E. Seiden, 1992, *Immunol. Today* **13**, 56–62.
- Celada, F., and P. E. Seiden, 1996, *Eur. J. Immunol.* **26**, 1350–1358.
- Chowdhury, D., and D. Stauffer, 1992, *Physica A* **186**, 61–81.
- Chu, G., 1978, *J. Immunol.* **120**, 1261–1267.
- Cohen, I. R., 1986, *Immunol. Rev.* **94**, 5–21.
- Colman, P. M., W. G. Laver, J. N. Varghese, A. Baker, P. A. Tulloch, G. M. Air, and R. G. Webster, 1987, *Nature (London)* **326**, 358–363.
- Cosenza, H., 1976, *Eur. J. Immunol.* **6**, 114–116.
- Coutinho, A., 1989, *Immunol. Rev.* **110**, 63–87.
- Coutinho, A., and M. Kazatchkine, 1994, *Autoimmunity, Physiology and Disease* (Wiley, New York).
- Cronin, J., 1987, *Mathematical Aspects of the Hodgkin-Huxley Neural Theory* (Cambridge University, Cambridge, England).
- Cyglar, M., D. R. Rose, and D. R. Bundle, 1991, *Science* **253**, 442–445.
- Dasgupta, S. 1992, *Physica A* **189**, 403–410.
- Davies, K. A., V. Hird, S. Stewart, G. B. Sivolapenko, P. Jose, A. A. Epenetos, and M. Walport, 1990, *J. Immunol.* **144**, 4613–4620.
- Davis, M. M., and P. J. Bjorkman, 1988, *Nature (London)* **334**, 395–402.
- De Boer, R. J., 1983, GRIND: Great Integrator Differential Equations. Bioinformatics Group, University of Utrecht, The Netherlands.
- De Boer, R. J., 1988, in *Theoretical Immunology, Part Two*, edited by A. S. Perelson (Addison-Wesley, Redwood City, CA), p. 265.
- De Boer, R. J., 1989, in *Theories of Immune Networks*, edited by H. Atlan and I. R. Cohen (Springer, Berlin), pp. 26–37.
- De Boer, R. J., and M. C. Boerlijst, 1994, *Proc. Natl. Acad. Sci. USA* **94**, 544–548.
- De Boer, R. J., M. C. Boerlijst, B. Sulzer, and A. S. Perelson, 1996, *Bull. Math. Biol.* **58**, 285–312.
- De Boer, R. J., and P. Hogeweg, 1989a, *Bull. Math. Biol.* **51**, 517.
- De Boer, R. J., and P. Hogeweg, 1989b, *Bull. Math. Biol.* **51**, 223–246.
- De Boer, R. J., and P. Hogeweg, 1989c, *Bull. Math. Biol.* **51**, 381–408.
- De Boer, R. J., P. Hogeweg, and A. S. Perelson, 1992, in *Theoretical and Experimental Insights into Immunology*, edited by A. S. Perelson and G. Weisbuch (Springer, Berlin), pp. 223–247.
- De Boer, R. J., I. G. Kevrekidis, and A. S. Perelson, 1990, *Chem. Eng. Sci.* **45**, 2375–2382.
- De Boer, R. J., and A. S. Perelson, 1991, *J. Theor. Biol.* **149**, 381–424.
- De Boer, R. J., and A. S. Perelson, 1993, *Proc. R. Soc. London, Ser. A* **55**, 781–816.
- De Boer, R. J., and A. S. Perelson, 1994, *J. Theor. Biol.* **169**, 375–390.
- De Boer, R. J., and A. S. Perelson, 1995, *J. Theor. Biol.* **175**, 567–576.
- De Boer, R. J., A. S. Perelson, and I. G. Kevrekidis, 1993a, *Bull. Math. Biol.* **55**, 745–780.
- De Boer, R. J., A. S. Perelson, and I. G. Kevrekidis, 1993b, *Bull. Math. Biol.* **55**, 781–816.
- De Boer, R., L. A. Segel, and A. S. Perelson, 1992, *J. Theor. Biol.* **155**, 295–333.
- De Boer, R., J. D. van der Laan, and P. Hogeweg, 1993, in *Thinking About Biology*, edited by F. J. Varela and W. D. Stein (Addison-Wesley, Reading, MA), pp. 231–252.
- DeLisi, C., 1980, *Math. Biosci.* **52**, 159–184.
- DeLisi, C., 1981, *Nature (London)* **289**, 322–323.
- DeLisi, C., 1983, *Annu. Rev. Biophys. Bioeng.* **12**, 117–138.
- DeLisi, C., and J. R. J. Hiernaux, 1982, *Regulation of Immune Response Dynamics*, Vols. I and II (CRC, Boca Raton, FL).
- DeLisi, C., and F. W. Wiegel, 1983, *J. Theor. Biol.* **102**, 307–322.
- Dembo, M., and B. Goldstein, 1978, *J. Immunol.* **121**, 345–353.
- Dembo, M., and B. Goldstein, 1980, *Cell* **22**, 59–67.
- Detours, V., H. Bersini, J. Stewart, and F. Varela, 1994, *J. Theor. Biol.* **170**, 401–414.
- Detours, V., B. Sulzer, and A. S. Perelson, 1996, *J. Theor. Biol.* **183**, 409–416.
- Dintzis, R. Z., B. Vogelstein, and H. M. Dintzis, 1982, *Proc. Natl. Acad. Sci. USA* **79**, 884–888.
- Dolezal, J., and T. Hrabá, 1994, *Folia Biologica (Praha)* **40**, 193–199.
- Dower, S. K., J. A. Titus, and D. M. Segal, 1984, in *Cell Surface Dynamics*, edited by A. S. Perelson, C. DeLisi, and F. Wiegel (Dekker, NY), pp. 277–328.
- Du Pasquier, L., 1973, *Curr. Top. Microbiol. Immunol.* **61**, 37–88.
- Du Pasquier, L., and J. Haimovitch, 1976, *Immunogenetics* **3**, 381.
- Eichmann, K., 1978, *Adv. Immunol.* **26**, 195–254.
- Eichmann, K., and K. Rajewsky, 1975, *Eur. J. Immunol.* **5**, 661–666.
- Eisen, H., 1980, *Immunology*, 2nd ed. (Harper and Row, NY).
- Eisenfeld, J., and C. DeLisi, 1985, in *Mathematics and Computers in Biomedical Applications*, edited by J. Eisenfeld and C. DeLisi (Elsevier, Amsterdam), pp. 39–53.
- Eisenfeld, J., and P. Prueitt, 1988, in *Theoretical Immunology, Part One*, edited by A. S. Perelson (Addison-Wesley, Redwood, CA), pp. 223–255.
- Essunger, P., and A. S. Perelson, 1994, *J. Theor. Biol.* **170**, 367–391.
- Farmer, J. D., S. A. Kaufman, N. H. Packard, and A. S. Perelson, 1987, *Ann. (N.Y.) Acad. Sci.* **504**, 118–130.
- Farmer, J. D., N. H. Packard, and A. S. Perelson, 1986, *Physica D* **22**, 187–204.

- Feller, W., 1968, *An Introduction to Probability Theory and its Applications*, Vol. 1, 3rd ed. (Wiley, NY), pp. 323–326.
- Fishman, M. A., and A. S. Perelson, 1993, *J. Theor. Biol.* **160**, 311–342.
- Fishman, M. A., and A. S. Perelson, 1994, *J. Theor. Biol.* **170**, 25–56.
- Fishman, M. A., and A. S. Perelson, 1995, *J. Theor. Biol.* **173**, 241–262.
- Forrest, S., B. Javornik, R. E. Smith, and A. S. Perelson, 1993, *Evolutionary Computation* **1**, 191–211.
- Freitas, A., O. Burlen, and A. Coutinho, 1988, *J. Immunol.* **140**, 4097–4102.
- Frost, S. D. W., and A. R. McLean, 1994a, *J. Acquir. Immune Defic. Syndr.* **7**, 236–244.
- Frost, S. D. W., and A. R. McLean, 1994b, *AIDS* **8**, 323–332.
- Goldstein, B., and A. S. Perelson, 1984, *Biophys. J.* **45**, 1109–1123.
- Goldstein, B., D. Jones, I. G. Kevrekidis, and A. S. Perelson, 1992, *Int. Immunol.* **4**, 23–32.
- Gunther, N., and G. W. Hoffmann, 1982, *J. Theor. Biol.* **94**, 815–855.
- Hardt, D. A., A. L. Wang, L. L. Pawlak, and A. Nisonoff, 1972, *J. Exp. Med.* **135**, 1293–1300.
- Hertz, J., A. Krogh, and R. G. Palmer, 1991, *Introduction to the Theory of Neural Computation* (Addison-Wesley, Redwood City, CA).
- Herzenberg, L. A., S. J. Black, and L. A. Herzenberg, 1980, *Eur. J. Immunol.* **10**, 1–11.
- Hiernaux, J., 1977, *Immunochem.* **14**, 733–739.
- Ho, D. D., A. U. Neumann, A. S. Perelson, W. Chen, J. M. Leonard, and M. Markowitz, 1995, *Nature (London)* **373**, 123–126.
- Hodgkin, A. L., and A. F. Huxley, 1952, *J. Physiol. (London)* **117**, 500–544.
- Hoffmann, G. W., 1975, *Eur. J. Immunol.* **5**, 638–647.
- Hoffmann, G. W., 1979, *Lect. Notes Biomath.* **32**, 239–257.
- Hoffmann, G. W., 1980, *Contemp. Top. Immunol.* **11**, 185–226.
- Hoffmann, G. W., T. A. Kion, R. B. Forsyth, K. G. Soga, and A. Cooper-Willis, 1988, in *Theoretical Immunology, Part Two*, edited by A. S. Perelson (Addison-Wesley, Redwood, CA), pp. 291–315.
- Hoffmann, G. W., J. G. Levy, and G. T. Nepon, Eds., 1986, *Paradoxes in Immunology* (CRC, Boca Raton, FL).
- Holmberg, D., Å. Andersson, L. Carlson, and S. Forsgen, 1989, *Immunol. Rev.* **110**, 89–103.
- Holmberg, D., S. Forsgen, F. Ivars, and A. Coutinho, 1984, *Eur. J. Immunol.* **14**, 435–441.
- Holmberg, D., G. Wennerstrom, L. Andrade, and A. Coutinho, 1986, *Eur. J. Immunol.* **16**, 82–87.
- Hraba, T., and J. Dolezal, 1989, *Folia Biologica (Praha)* **35**, 156–163.
- Hraba, T., and J. Dolezal, 1994, *Folia Biologica (Praha)* **40**, 103–111.
- Hraba, T., J. Dolezal, and S. Celikovský, 1990, *Immunobiol.* **181**, 108–118.
- Inman, J. K., 1978, in *Theoretical Immunology*, edited by G. I. Bell, A. S. Perelson, and G. H. Pimbley, Jr. (Dekker, NY), pp. 243–278.
- Jerne, N. K., 1974, *Ann. Immunol. (Inst. Pasteur)* **125** C, 373–389.
- Kang, C.-Y., and H. Kohler, 1986a, *Ann. (N.Y.) Acad. Sci.* **475**, 114–122.
- Kang, C.-Y., and H. Kohler, 1986b, *J. Exp. Med.* **163**, 787–796.
- Kauffman, S. A., E. D. Weinberger, and A. S. Perelson, 1988, in *Theoretical Immunology, Part One, SFI Studies in the Sciences of Complexity*, edited by A. S. Perelson (Addison-Wesley, Redwood City, CA), pp. 349–382.
- Kaufman, M., 1988, in *Theoretical Immunology, Part One*, edited by A. S. Perelson (Addison-Wesley, Redwood City, CA), pp. 199–222.
- Kaufman, M., F. Andris, and O. Leo, 1992, in *Theoretical and Experimental Insights into Immunology*, edited by A. S. Perelson and G. Weisbuch (Springer, Berlin), pp. 93–115.
- Kaufman, M., and R. Thomas, 1987, *J. Theor. Biol.* **129**, 141–162.
- Kaufman, M., J. Urbain, and R. Thomas, 1985, *J. Theor. Biol.* **114**, 527–561.
- Kearney, J. F., and M. Vakil, 1986, *Immunol. Rev.* **94**, 39–50.
- Kearney, J. F., M. Vakil, and N. Nicholson, 1987, in *Evolution and Vertebrate Immunity: The Antigen Receptor and MHC Gene Families*, edited by G. Kelsoe and D. Schulze (University of Texas, Austin, TX), pp. 373–389.
- Kepler, T. B., and A. S. Perelson, 1993a, *Immunol. Today* **14**, 412–415.
- Kepler, T. B., and A. S. Perelson, 1993b, *J. Theor. Biol.* **164**, 37–64.
- Kepler, T. B., and A. S. Perelson, 1995, *Proc. Natl. Acad. Sci. USA* **92**, 8219–8223.
- Kevrekidis, I. G., A. D. Zecha, and A. S. Perelson, 1988, in *Theoretical Immunology, Part One*, edited by A. S. Perelson (Addison-Wesley, Redwood City, CA), pp. 167–197.
- Kirschner, D. E., and A. S. Perelson, 1995, in *Mathematical Population Dynamics: Analysis of Heterogeneity and the Theory of Epidemics*, edited by O. Arino, D. E. Axelrod, M. Kimmel, and M. Langlais (Wuerz Publishing, Winnipeg, Canada), pp. 295–310.
- King, R. B., 1988, in *Theoretical Immunology, Part One*, edited by A. S. Perelson (Addison-Wesley, Redwood City, CA), pp. 257–272.
- Klinman, N. R., and J. L. Press, 1975, *Transplant. Rev.* **24**, 41–83.
- Kürten, K. E., 1992, in *Theoretical and Experimental Insights into Immunology*, edited by A. S. Perelson and G. Weisbuch (Springer, Berlin), pp. 163–170.
- Kuznetsov, V. A., I. A. Makalkin, M. A. Taylor, and A. S. Perelson, 1994, *Bull. Math. Biol.* **56**, 295–321.
- Lefèvre, O., and G. Parisi, 1993, *Networks* **4**, 39–65.
- Liu, Y.-J., G. D. Johnson, J. Gordon, and I. C. M. MacLennan, 1992, *Immunol. Today* **13**, 17–21.
- Lundkvist, I., A. Coutinho, F. Varela, and D. Holmberg, 1989, *Proc. Natl. Acad. Sci. USA* **86**, 5074–5078.
- Mackay, C. R., 1993, *Adv. Immunol.* **53**, 217–265.
- Macken, C. A., P. Hagan, and A. S. Perelson, 1991, *SIAM (Soc. Ind. Appl. Math.) J. Appl. Math.* **51**, 799–827.
- Macken, C. A., and A. S. Perelson, 1984, *J. Immunol.* **132**, 1614–1624.
- Macken, C. A., and A. S. Perelson, 1985a, *Branching Processes Applied to Cell Surface Aggregation Phenomena*, Lecture Notes in Biomathematics Vol. 51 (Springer, Berlin).
- Macken, C. A., and A. S. Perelson, 1985b, *Acta Applicandae Mathematicae* **4**, 157–200.
- Macken, C. A., and A. S. Perelson, 1986, *IMA J. Math. Appl. Med. Biol.* **3**, 71–97.
- Macken, C. A., and A. S. Perelson, 1989, *Proc. Natl. Acad. Sci. USA* **86**, 6191–6195.

- Macken, C. A., and A. S. Perelson, 1991, in *Evolution on Rugged Landscapes: Proteins, RNA and the Immune System*, edited by A. S. Perelson and S. A. Kauffman, SFI Studies in the Sciences of Complexity Vol. 9 (Addison-Wesley, Redwood City, CA), pp. 93–118.
- Macken, C. A., and A. S. Perelson, 1995, Proc. Natl. Acad. Sci. USA **92**, 9657–9661.
- Marchuk, G. I., 1983, *Mathematical Models in Immunology* (Springer, New York)
- Marchuk, G. I., and L. N. Belykh, Eds., 1983, *Mathematical Modeling in Immunology and Medicine* (North-Holland, Amsterdam).
- McLean, A. R., 1992, in *Theoretical and Experimental Insights into Immunology*, edited by A. S. Perelson and G. Weisbuch (Springer, Berlin), pp. 149–162.
- McLean, A. R., 1992, Trends Microbiol. **1**, 9–13.
- McLean, A. R., and T. B. L. Kirkwood, 1990, J. Theor. Biol. **147**, 177–230.
- McLean, A. R., and M. A. Nowak, 1992, J. Theor. Biol. **155**, 69–102.
- Merrill, S. J., 1982, Math. Biosci. **62**, 219–236.
- Merrill, S. J. 1989, in *Mathematical and Statistical Approaches to AIDS Epidemiology*, edited by C. Castillo-Chavez, Lecture Notes in Biomath. Vol. 83 (Springer, NY), 371–385.
- Merrill, S. J., R. J. De Boer, and A. S. Perelson, 1994, Rocky Mt. J. Math. **24**, 213–231.
- Merrill, S. J., and S. Sathananthan, 1986, Math. Biosci. **80**, 223–238.
- Mezard, M., G. Parisi, and M. Virasoro, 1988, *Spin Glass Theory and Beyond* (World Scientific, Singapore).
- Michie, C. A., A. McLean, C. Alcock, and P. C. L. Beverley, 1992, Nature (London) **360**, 264–265.
- Möller, G., 1988, Scand. J. Immunol. **27**, 247–250.
- Morel, B. F., M. A. Burke, J. Kalagnanam, S. A. McCarthy, D. J. Tweedy, and P. A. Morel, 1996, Bull. Math. Biol. **58**, 569–594.
- Morel, B. F., J. Kalagnanam, and P. A. Morel, 1992, in *Theoretical and Experimental Insights into Immunology*, edited by A. S. Perelson and G. Weisbuch (Springer, Berlin), pp. 171–189.
- Mosier, D., and H. Sieburg, 1994, Immunol. Today **15**, 332–339.
- Nelson, G. W., and A. S. Perelson, 1992, J. AIDS **5**, 82–93.
- Nelson, G. W., and A. S. Perelson, 1995, Math. Biosci. **125**, 127–153.
- Neumann, A., and G. Weisbuch, 1992a, Bull. Math. Biol. **54**, 21–44.
- Neumann, A., and G. Weisbuch, 1992b, Bull. Math. Biol. **54**, 699–726.
- Nowak, M. A., 1992, J. Theor. Biol. **155**, 1–20.
- Nowak, M. A., R. M. Anderson, A. R. McLean, T. F. W. Wolfes, J. Goudsmit, and R. M. May, 1991, Science **254**, 963–969.
- Nowak, M. A., and R. M. May, 1991, Math. Biosci. **106**, 1–21.
- Nowak, M. A., and R. M. May, 1992, J. Theor. Biol. **159**, 329–342.
- Nowak, M. A., and R. M. May, 1993, AIDS **7** (Suppl. 1), S3–S18.
- Nowak, M. A., R. M. May, and R. M. Anderson, 1990, AIDS **4**, 1095–1103.
- Nowak, M. A., and A. R. McLean, 1991, Proc. R. Soc. London, Ser. B **246**, 141–146.
- Ohno, S., 1991, Proc. Natl. Acad. Sci. USA **88**, 3065–3068.
- Oprea, M., and A. S. Perelson, 1997, J. Immunol. **158**, 5155–5162.
- Pandey, R. B., 1991, Physica A **179**, 442–470.
- Pandey, R. B., and D. Stauffer, 1990, J. Stat. Phys. **61**, 235–240.
- Parisi, G., 1988, in *Chaos and Complexity*, edited by R. Livi, S. Ruffo, S. Ciliberto, and M. Buiatti (World Scientific, Singapore), 394–401.
- Parisi, G., 1990, Proc. Natl. Acad. Sci. USA **87**, 429–433.
- Percus, J. K., O. E. Percus, and A. S. Perelson, 1992, in *Theoretical and Experimental Insights into Immunology*, edited by A. S. Perelson and G. Weisbuch (Springer, Berlin), pp. 63–70.
- Percus, J. K., O. E. Percus, and A. S. Perelson, 1993, Proc. Natl. Acad. Sci. USA **90**, 1691–1695.
- Perelson, A. S., 1981, Math. Biosci. **51**, 1–39.
- Perelson, A. S., 1984, in *Cell Surface Dynamics: Concepts and Models*, edited by A. S. Perelson, C. DeLisi and F. W. Wiegel (Dekker, NY), pp. 223–276.
- Perelson, A. S., 1986, in *Paradoxes in Immunology*, edited by G. W. Hoffmann, J. G. Levy, and G. T. Nepom (CRC Boca Raton, Florida), pp. 199–214.
- Perelson, A. S., 1988, Ed., *Theoretical Immunology, Parts One and Two*, SFI Studies in the Sciences of Complexity (Addison-Wesley, Redwood City, CA).
- Perelson, A. S., 1989a, in *Cell to Cell Signalling: From Experiments to Theoretical Models*, edited by A. Goldbeter (Academic, NY), pp. 261–272.
- Perelson, A. S., 1989b, Immunol. Rev. **110**, 5–36.
- Perelson, A. S., 1989c, in *Mathematical and Statistical Approaches to AIDS Epidemiology*, edited by C. Castillo-Chavez, Lecture Notes in Biomath. Vol. 83 (Springer, NY), pp. 350–370.
- Perelson, A. S., 1990, in *1989 Lectures in Complex Systems*, SFI Studies in the Sciences of Complexity, Lect. Vol. II, edited by E. Jen (Addison-Wesley, Redwood City, CA), pp. 465–99.
- Perelson, A. S., 1992, in *Theory and Control of Dynamical Systems: Applications to Systems in Biology*, edited by S. I. Andersson, A. E. Andersson, and U. Ottoson (World Scientific, Singapore), pp. 200–230.
- Perelson, A. S., 1994, in *Complexity: Metaphors, Models and Reality*, edited by G. Cowan, D. Pines, and D. Meltzer (Addison-Wesley, Reading, MA), pp. 185–197.
- Perelson, A. S., and G. I. Bell, 1982, J. Immunol. **129**, 2796–2801.
- Perelson, A. S., and C. DeLisi, 1980, Math. Biosci. **48**, 71–110.
- Perelson, A. S., and B. Goldstein, 1992, in *Theoretical and Experimental Insights into Immunology*, edited by A. S. Perelson and G. Weisbuch (Springer, Berlin), pp. 117–148.
- Perelson, A. S., B. Goldstein, and S. Rocklin, 1980, J. Math. Biol. **10**, 209–256.
- Perelson, A. S., R. Hightower, and S. Forrest, 1996, Res. Immunol. **147**, 202–208.
- Perelson, A. S., and S. A. Kauffman, 1991, Eds., *Evolution on Rugged Landscapes: Proteins, RNA and the Immune System* (Addison-Wesley, Redwood City, CA).
- Perelson, A. S., D. E. Kirschner, and R. De Boer, 1993, Math. Biosci. **114**, 81–125.
- Perelson, A. S., and C. A. Macken, 1984, Math. Biosci. **70**, 161–194.
- Perelson, A. S., C. A. Macken, E. A. Grimm, L. S. Roos, and B. Bonavida, 1984, J. Immunol. **132**, 2190–2198.
- Perelson, A. S., M. Mirmirani, and G. F. Oster, 1976, J. Math. Biol. **3**, 325–367.
- Perelson, A. S., M. Mirmirani, and G. F. Oster, 1978, J. Math. Biol. **5**, 213–256.

- Perelson, A. S., A. U. Neumann, M. Markowitz, J. M. Leonard, and D. D. Ho, 1996, *Science* **271**, 1582–1586.
- Perelson, A. S., and G. F. Oster, 1979, *J. Theor. Biol.* **81**, 645–670.
- Perelson, A. S., and G. Weisbuch, 1992a, *Bull. Math. Biol.* **54**, 649–672.
- Perelson, A. S., and G. Weisbuch, 1992b, Eds., *Theoretical and Experimental Insights into Immunology* (Springer, Berlin).
- Perelson, A. S., and F. W. Wiegel, 1979, *J. Theor. Biol.* **79**, 317–332.
- Pierre, D. M., D. Goldman, Y. Bar-Yam, and A. S. Perelson, 1997, *J. Theor. Biol.* **186**, 159–171.
- Posner, R. G., C. Wofsy, and B. Goldstein, 1995, *Math. Biosci.* **126**, 171–190.
- Príkrylová, D., M. Jílek, and J. Waniewski, 1992, *Mathematical Modeling of the Immune Response* (Springer, New York).
- Richter, P. H., 1975, *Eur. J. Immunol.* **5**, 350–354.
- Richter, P. H., 1978, in *Theoretical Immunology*, edited by G. I. Bell, A. S. Perelson, and G. H. Pimbley, Jr. (Dekker, NY), pp. 539–569.
- Rodkey, L. S., and F. L. Adler, 1983, *J. Exp. Med.* **157**, 1920–1931.
- Rose, R., and A. S. Perelson, 1994, in *Frontiers of Mathematical Biology*, edited by S. Levin, Springer Lecture Notes in Biomath. No. 100 (Springer, Berlin), pp. 159–172.
- Schwartz, R. H., 1989, *Cell* **57**, 1073–1081.
- Schweitzer, A. N., J. Swinton, and R. M. Anderson, 1992, in *Theoretical and Experimental Insights into Immunology*, edited by A. S. Perelson and G. Weisbuch (Springer, Berlin), pp. 191–202.
- Segel, L. A., 1995, *Complexity* **2(2)**, 18–25.
- Segel, L. A., and E. Jäger, 1994, *Bull. Math. Biol.* **56**, 687–721.
- Segel, L. A., and A. S. Perelson, 1988, in *Theoretical Immunology, Part Two*, SFI Studies in the Sciences of Complexity, edited by A. S. Perelson (Addison-Wesley, Redwood City, CA), pp. 321–343.
- Segel, L. A., and A. S. Perelson, 1989a, *Immunol. Lett.* **22**, 91–100.
- Segel, L. A., and A. S. Perelson, 1989b, In *Cell to Cell Signaling: From Experiments to Theoretical Models*, edited by A. Goldbeter (Academic, NY), pp. 273–283.
- Segel, L. A., and A. S. Perelson, 1989c, in *Theories of Immune Networks*, edited by H. Atlan and I. R. Cohen (Springer, Berlin), pp. 63–70.
- Segel, L. A., and A. S. Perelson, 1990, *SIAM (Soc. Ind. Appl. Math.) J. Appl. Math.* **50**, 91–107.
- Seiden, P. E., and F. Celada, 1992, *J. Theor. Biol.* **158**, 329–357.
- Sheriff, S., E. W. Silverton, E. A. Padlan, G. H. Cohen, S. J. Smith-Gill, B. C. Finzel, and D. R. Davies, 1987, *Proc. Natl. Acad. Sci. USA* **84**, 8075–8079.
- Shoenfeld, Y., and E. Moses, 1990, *FASEB J.* **4**, 2646–2651.
- Siskind, G. W., and B. Benacerraf, 1969, *Adv. Immunol.* **10**, 1–50.
- Stadler, P. F., P. Schuster, and A. S. Perelson, 1994, *J. Math. Biol.* **33**, 111–137.
- Stauffer, D., and M. Sahimi, 1994, *J. Theor. Biol.* **166**, 289–297.
- Stauffer, D., and G. Weisbuch, 1992, *Physica A* **180**, 42–52.
- Stewart, J., and F. J. Varela, 1989, *Immun. Rev.* **110** (1989), 37–61.
- Stewart, J., and F. J. Varela, 1990, *J. Theor. Biol.* **144**, 103–115.
- Stewart, J., and F. J. Varela, 1991, *J. Theor. Biol.* **153**, 477–498.
- Sulzer, B., R. J. De Boer, and A. S. Perelson, 1996, *Biophys. J.* **70**, 1154–1168.
- Sulzer, B., and A. S. Perelson, 1996, *Math. Biosci.* **135**, 147–185.
- Sulzer, B., J. L. van Hemmen, and U. Behn, 1994, *Bull. Math. Biol.* **56**, 1009–1040.
- Sulzer, J. L. van Hemmen, A. U. Neumann, and U. Behn, 1993, *Bull. Math. Biol.* **55**, 1133–1182.
- Takemori, T., and K. Rajewsky, 1984, *Immunol. Rev.* **79**, 103.
- Tew, J. G., and T. E. Mandel, 1979, *Immunology* **37**, 69–76.
- Tew, J. G., R. P. Phipps, and T. E. Mandel, 1980, *Immunol. Rev.* **53**, 175–211.
- Uspensky, J. V., 1937, *Introduction to Mathematical Probability* (McGraw-Hill, New York), pp. 77–84.
- Vakil, M., H. Sauter, C. Paige, and J. F. Kearney, 1986, *Eur. J. Immunol.* **16**, 1159–1165.
- Varela, F. J., A. Anderson, G. Dietrich, A. Sundblad, D. Holmberg, M. Kazatchkine, and A. Coutinho, 1991, *Proc. Natl. Acad. Sci. USA* **88**, 5917–5921.
- Varela, F., and A. Coutinho, 1991, *Immunol. Today* **159**, 159–166.
- Varela, F., A. Coutinho, B. Dupire, and N. M. Vaz, 1988, in *Theoretical Immunology, Part Two*, edited by A. S. Perelson (Addison-Wesley, Redwood City, CA), pp. 359–375.
- Vogelstein, B., R. Z. Dintzis, and H. M. Dintzis, 1982, *Proc. Natl. Acad. Sci. USA* **79**, 395–399.
- von Boehmer, H., 1991, *Sci. Am. (Int. Ed.)*, 74–81.
- Wei, X., S. K. Ghosh, M. E. Taylor, V. A. Johnson, V. A. Emimi, P. Deutsch, J. D. Lifson, S. Bonhoeffer, M. A. Nowak, B. H. Hahn, M. S. Saag, and G. M. Shaw, 1995, *Nature (London)* **373**, 117–122.
- Weinand, R., 1991, in *Molecular Evolution on Rugged Landscapes: Proteins, RNA and the Immune System*, edited by A. S. Perelson and S. A. Kauffman (Addison-Wesley, Redwood City, CA), pp. 215–236.
- Weisbuch, G., 1990a, *Complex Systems Dynamics* (Addison-Wesley, Redwood City, CA).
- Weisbuch, G., 1990b, *J. Theor. Biol.* **143**, 507–522.
- Weisbuch, G., and H. Atlan, 1988a, *J. Phys. A* **21**, L189–L192.
- Weisbuch, G., and H. Atlan, 1988b, in *Theories of Immune Networks*, edited by H. Atlan and I. R. Cohen (Springer, Berlin), pp. 53–62.
- Weisbuch, G., R. De Boer, and A. S. Perelson, 1990, *J. Theor. Biol.* **146**, 483–499.
- Weisbuch, G., and M. Oprea, 1994, *Bull. Math. Biol.* **56**, 899–921.
- Weisbuch, G., and A. S. Perelson, 1991, in *Molecular Evolution on Rugged Landscapes: Proteins, RNA and the Immune System*, edited by A. S. Perelson and S. A. Kauffman (Addison-Wesley, Redwood City, CA), pp. 189–205.
- Wiegel, F. W., and A. S. Perelson, 1981, *J. Theor. Biol.* **88**, 533–568.
- Zöller, M., and M. Achtnich, 1991, *Scand. J. Immunol.* **33**, 15–24.